Non-invasive imaging of estrogen receptor-coregulator interaction by luciferase fragment complementation.

Madryn Lake

Imperial College London
Department of Surgery and Cancer

A thesis submitted for the degree of
Doctor of Philosophy of Imperial College London

Declaration

I declare that the work described in this thesis is my own and that the work of others is appropriately referenced.

Abstract

Breast cancer is the most common cancer in the UK and approximately 1 in 8 women will be affected by the disease. Estrogen regulates breast cancer growth through the action of the estrogen receptors ERα and ERβ. Antiestrogens, in particular tamoxifen, have contributed greatly to the reduction in breast cancer mortality. Tamoxifen is a tissue selective antiestrogen; it is antiestrogenic in the breast but estrogenic in other tissues, thereby enabling it to promote the beneficial effects of estrogen, such as maintaining bone density. However, like estrogen, tamoxifen also promotes endometrial cancer, so there is an impetus for the development of novel tissue selective ERα ligands.

Regulation of gene expression by the estrogen receptors requires the ligand-regulated recruitment of transcription coregulator proteins. In breast cancer ERα-coactivator interactions are associated with tumour progression while ERα-corepressor interactions are associated with receptor antagonism and a therapeutic block of ERα signalling.

This thesis details the development of a luciferase fragment complementation assay to image the interaction of ERα with the coactivator AIB1 and corepressor SMRT. It is hoped that elucidation of these interactions will enable a greater appreciation of the tissue selective actions of ERα ligands and aid in the screening of novel ERα antagonists.

By means of complimentary luciferase fragment fusion proteins, it is shown that ligand dependent ERα-coregulator interaction can be imaged *in vitro* and *in vivo*. ERα and AIB1 luciferase fusion proteins indicate an E2 induced increase in luciferase fragment complementation which is modulated by antiestrogens. The complementation observed correlates with ERα transcriptional activity and the specificity has been further validated by ERα fusion protein mutants. Consistent with the notion that the ERα-SMRT interaction is characteristic of ERα antagonism, ERα and SMRT fusion proteins show increased luciferase fragment complementation with antiestrogens compared with estrogen.

Acknowledgements

I would like to sincerely thank Professors Eric Aboagye and Simak Ali for all their help, advice and guidance throughout the last 4 years. I would also particularly like to thank Simak for his thorough and timely proof-reading during preparation of this thesis.

Table of contents

Chapter 1 Introduction.....18

1.1 Breast cancer.....19

1.2 Estrogen.....20

1.3 Estrogen receptors.....20

1.4 Estrogen signalling.....23

1.4.1 Genomic signalling.....24

1.4.2 Non genomic signalling.....24

1.4.3 Transcription Regulation by ERα.....25

1.4.3.1 AIB1.....26

1.4.3.2 Transcription repression by ERα.....29

1.5 Estrogen signalling as a therapeutic target.....30

1.5.1 SERMs.....31

1.5.1.1 SERM mode of action.....32

1.6 Molecular imaging.....34

1.7 Bioluminescence imaging.....35

1.7.1 Luciferase.....39

1.8 Imaging protein-protein interactions.....40

1.8.1 Luciferase fragment complementation assay.....40

1.9 Imaging ER activity.....47

1.10 Thesis synopsis.....48

Chapter 2 Materials and Methods.....50

2.1 Chemicals, enzymes and reagents.....51

2.2 Plasmids.....51

2.3 Polymerase chain reaction (PCR) 51
2.4 Agarose gel electrophoresis 52
2.5 DNA ligations and bacterial transformation 52
2.6 Construction of luciferase-fragment reporter plasmids 52
2.7 Cell lines and culturing 56
2.8 Preparation of cell lysates 56
2.9 Cell growth assays 57
2.10 Cell transfection 57
2.11 Luciferase assays 59
2.12 *In vivo* imaging 60
2.13 Antibodies 61
2.14 Immunoblotting 62
2.15 Immunofluorescence 63
2.16 Statistical analysis 64
Chapter 3 Results 65
3.1 Characterisation of MELN cell line 66
3.2 Characterisation of NLuc-FRB and FKBP12-CLuc 71
3.3 ERα-coregulator split-luciferase assay feasibility study 74
3.4 Truncated ER-LBD-AIB-RID split-luciferase assay 82
3.5 Full length ERα-AIB1 split-luciferase assay 104
3.6 Truncated ER-LBD/AIB-RID split-luciferase reporters and the tissue specific actions of ERα ligands 110
3.6.1 MCF7 stable cell lines 110
3.6.2 U2OS stable cell lines 117
3.6.3 Reporting of the tissue specific agonist actions of OHT 124

3.7 SMRT split-luciferase assay 128

Chapter 4 Discussion 137

4.1 Conclusions and Future Directions 149

Chapter 5 References 153

Table of figures

Figure 1.1 - Structure of human ERα. 22

Figure 1.2 - ER signalling. 27

Figure 1.3 - IVIS imaging system. 37

Figure 1.4 - Luciferase fragment complementation assay. 45

Figure 3.1 - E2 response of MELN cells. 67

Figure 3.2 - Modulation of MELN E2 response by OHT and ICI. 68

Figure 3.3 - *In vivo* bioluminescence imaging of MELN tumours. 70

Figure 3.4 - pcDNA-NLuc-FRB and pcDNA-FKBP12-CLuc. 72

Figure 3.5 - FRB-FKBP12 mediated luciferase fragment complementation. 73

Figure 3.6 - Cloning strategy. 75

Figure 3.7 - Initial assessment of NLuc-AIB-RID, ER-LBD-CLuc and ER-CLuc. 77

Figure 3.8 - Specificity of rapamycin and E2 induced luciferase fragment complementation. 79

Figure 3.9 - Immunofluorescence of NLuc-AIB-RID, ER-LBD-CLuc, ER-CLuc and endogenous ERα and AIB1 80

Figure 3.10 - Influence of spacer insertion on NLuc-AIB-RID/ER-LBD-CLuc complementation. 83

Figure 3.11 - NLuc-ER-LBD/AIB-RID-CLuc complementation and the impact of spacer insertion. 85

Figure 3.12 - E2 response of ER-LBD/AIB-RID split-luciferase constructs. 87

Figure 3.13 - Y537S and L539/40A ER-LBD split-luciferase constructs. 89

Figure 3.14 - Modulation of ER-LBD/AIB-RID split-luciferase E2 response by OHT and ICI. 91

Figure 3.15 - Expression of ER-LBD and AIB-RID fusion proteins in E2, OHT and ICI treated cells. 92
Figure 3.16 - Time-course of E2 response in ER-LBD/AIB-RID split-luciferase transfected and MELN cells..... 93
Figure 3.17 - Minute time-course of E2 response in ER-LBD/AIB-RID split-luciferase constructs. 95
Figure 3.18 - Time-course of E2 signal ablation in ER-LBD/AIB-RID split-luciferase transfected and MELN cells..... 96
Figure 3.19 - Minute time-course of E2 signal ablation in ER-LBD/AIB-RID split-luciferase constructs. 98
Figure 3.20– *In vivo* modulation of ER-LBD/AIB-RID split-luciferases by E2 and ICI. 100
Figure 3.21– *In vivo* modulation of ER-LBD/AIB-RID split-luciferase transfected and MELN cells by E2 and OHT. 102
Figure 3.22 - Ratio transfections of full length ER/AIB split-luciferase reporters.... 105
Figure 3.23 - Immunofluorescence of full length ER/AIB split-luciferase reporters. 107
Figure 3.24 - U2OS NLuc-SS-AIB/ER-SS-CLuc stable cell lines. 109
Figure 3.25 - E2 response of MCF7 NLuc-ER-LBD/AIB-RID-SS-CLuc stable cell lines. 111
Figure 3.26 - E2 response of MCF7 NLuc-ER-LBD/AIB-RID-SS-CLuc #1 and #4. 113
Figure 3.27 – Modulation of MCF7 NLuc-ER-LBD/AIB-RID-SS-CLuc #1 and #4 E2 response by OHT and ICI. 114

Figure 3.28 - Signal dynamics of MCF7 NLuc-ER-LBD/AIB-RID-SS-CLuc #1 and #4.....116
Figure 3.29 - E2 response of U2OS stable cell lines. 118
Figure 3.30 - Western blot of fusion proteins in U2OS stable cell lines. 119
Figure 3.31 - Modulation of E2 response in U2OS stable cell lines by OHT and ICI. 121
Figure 3.32 – Time-course of luciferase signal in U2OS stable cell lines.....122
Figure 3.33 - Titration of OHT and ICI on U2OS stable cell lines. 125
Figure 3.34 - Transient transfection of ER-LBD/AIB-RID split-luciferase constructs into Ishikawa cells.....127
Figure 3.35 - Initial assessment of SMRT-RID constructs.....129
Figure 3.36 - Immunofluorescence of SMRT-RID constructs. 132
Figure 3.37 - Ligand titration on SMRT-RID constructs. 134

Table of tables

Table 1.1 – Comparison of molecular imaging modalities……36

Table 2.1 – Oligonucleotides used for construction of split-luciferase constructs…53

List of abbreviations

Å	angstrom
AEBSF	4-(2-Aminoethyl)benzenesulfonyl fluoride
AF1	activation function 1
AF2	activation function 2
AIB1	amplified in breast cancer 1
AIB-RID	AIB1 nuclear receptor interaction domain
AP1	activator protein 1
APS	ammonium persulfate
ATP	adenosine triphosphate
BCA	bicinchoninic acid
BLI	bioluminescence imaging
bp	base pair
BRET	bioluminescence resonance energy transfer
BSA	bovine serum albumin
cAMP	cyclic adenosine monophosphate
CBP	CREB binding protein
CCD	charge coupled device
ChIP	chromatin immunoprecipitation
CLuc	C terminal luciferase fragment
CoIP	coimmunoprecipitation
CREB	cAMP response element binding
DAPI	4',6-diamidino-2-phenylindole

DBD	DNA binding domain
DMEM	Dulbecco's modified Eagle's medium
DMSO	dimethyl sulfoxide
DNA	deoxyribonucleic acid
dNTP	deoxyribonucleotide triphosphates
DRIP	vitamin D receptor interacting protein
DTT	dithiothreitol
E.coli	*Escherichia coli*
E2	17-β-estradiol
EDTA	ethylendiaminetetraaceticacid
EGFP	green fluorescent protein
EGFR	epidermal growth factor receptor
ER	estrogen receptor
ERE	estrogen response element
ER-LBD	estrogen receptor ligand binding domain
FCS	foetal calf serum
FDG	fluorodeoxyglucose
FKBP12	FK506 binding protein 1A
FRB	FKBP12-rapamycin binding domain of mammalian target of mTOR
FRET	fluorescence resonance energy transfer
H&E	haematoxylin and eosin
HAT	histone acetyltransferase
HDAC	histone deacetlyase
HER2	human epidermal growth factor receptor 2
HRP	horse radish peroxidase

HRT	hormone replacement therapy
ICI	ICI 182, 780; fulvestrant
Ig	immunoglobulin
IGF-IR	insulin-like growth factor receptor I
IP	immunprecipitation
IVC	individual ventilated cage
Kb	kilobase
Kd	dissociation constant
KDa	kilodalton
LB	luria broth
LBD	ligand binding domain
MAPK	mitogen activated protein kinase
MELN	MCF7-ERE-luciferase cell line
mg	milligram
ml	millilitre
mM	millimolar
MRI	magnetic resonance imaging
mRNA	messenger RNA
mTOR	mammalian target of rapamycin
NCoR	nuclear receptor corepressor
ng	nanogram
nl	nanolitre
NLuc	N terminal luciferase fragment
nM	nanomolar
OHT	4-hydroxytamoxifen

PAGE	polyacrylamide gel electrophoresis
PBS	phosphate buffered saline
PBS-T	0.1% tween 20/phosphate buffered saline
PBS-Tx	0.1% triton X/phosphate buffered saline
pCAF	p300/CBP associated factor
PCR	polymerase chain reaction
PET	positron emission tomography
PI3K	phosphoinositide 3-kinase
pM	picomolar
PPI	peptidyl-propyl isomerase
RIPA	radioimmunoprecipitation assay
RNA	ribonucleic acid
ROI	region of interest
S	Gly-Gly-Gly-Gly-Ser flexible spacer
SDS	sodium dodecyl sulphate
SERM	selective estrogen receptor modulator
SMRT	silencing mediator of retinoic acid and thyroid hormone receptors
SMRT-RID	SMRT nuclear receptor interaction domain
SOB	super optimal broth
SP1	specificity protein 1
SRB	sulforhodamine B
SRC	steroid receptor coactivator
SS	2 copies of Gly-Gly-Gly-Gly-Ser flexible spacer
TBE	tris borate EDTA buffer
TCA	tricholoacetic acid

TEMED	tetramethylenthylenediamine
TRAP	thyroid hormone receptor associated proteins
tris	tris(hydroxymethyl)aminomethane
U	enzyme units
V	vehicle
µg	microgram
µl	microlitre
µM	micromolar

Chapter 1 Introduction

1.1 Breast cancer

Breast cancer is the most common cancer in the UK and it is estimated that 1 in 8 women will be affected by the disease during their lifetime (CRUK, 2011a). Globally, breast cancer is the most common cause of female cancer death (Ferlay J, 2010). Breast cancer incidence is the highest in developed western countries and the incidence increases as countries become more developed. An individual's risk of breast cancer increases if they move from a low-risk to a high-risk country (Ziegler et al., 1993). This indicates that lifestyle plays an important role in the development of breast cancer. Identified factors associated with increased breast cancer incidence include an early menarche or late menopause, having few or no children, having children later in life, not breastfeeding, and the use of exogenous hormones such as the contraceptive pill or hormone replace therapy (HRT), as well as diet related increases, including alcohol consumption and obesity (CRUK, 2011b). The incidence of breast cancer has steadily increased in the UK over the last 30 years: 75 women per 100,000 were diagnosed with the disease in 1979, which increased to 124 women per 100,000 in 2008 (CRUK, 2011a, Hery et al., 2008). Although incidence has increased, patient survival rates have also greatly improved: the 5 year survival rate for women diagnosed between 1971 and 1975 was 52%, but for women diagnosed between 2001 and 2006 the 5 year survival rate was 82%. The breast cancer screening program and improved treatment options are thought to be responsible for the trend towards increased survival among breast cancer patients (CRUK, 2011c, Ferlay J, 2010)

1.2 Estrogen

Estrogens are steroid sex hormones that promote cellular proliferation and survival. They are required for the development and maintenance of normal sexual and reproductive function, in addition to performing a range of more homeostatic functions in the cardiovascular, musculoskeletal, immune and central nervous systems (Huang and Kaley, 2004, Riggs et al., 2002, Heldring et al., 2007). In females, there are 3 major types of estrogen, estrone, estradiol and estriol, which are all synthesised from androgens by the aromatase enzyme. 17β-estradiol (E2) is the dominant estrogen from menarche to menopause; estrone and estriol are associated with the menopause and pregnancy, respectively.

Removal of the ovaries has been recognised as being an effective treatment for breast cancer since 1896, however, it was not appreciated that this was due to the production of estrogen by the ovaries for another 40 years (Jensen and Jordan, 2003). The link between estrogen exposure and breast cancer risk has been extensively demonstrated by epidemiological studies and is supported by *in vitro* and *in vivo* preclinical work which shows estrogen is capable of transforming breast epithelial cells and increases the incidence and growth of breast cancer in rodents (Clemons and Goss, 2001, Henderson and Feigelson, 2000, Henderson et al., 1982, Jensen and Jordan, 2003, Russo et al., 2006).

1.3 Estrogen receptors

Estrogens signal through the estrogen receptor (ER), of which there are two types, ERα and ERβ (Enmark and Gustafsson, 1999). Both ERs are members of the nuclear

hormone receptor superfamily, which includes receptors for other steroidal and non-steroidal hormones such as progestins, glucocorticoids, thyroid hormones, retinoids, androgens and vitamin D, as well as various orphan receptors which have no known ligand (Mangelsdorf et al., 1995).

The ERs proteins share the conserved structure common to the majority of nuclear receptors (Figure 1.1). They have two regions required for transcription activation, activation functions AF1 and AF2; AF1 is contained within the amino terminal A/B region and can act in a ligand-independent manner when isolated from the ligand binding domain (LBD), while AF2 is located in the carboxy terminal E/F region and is intrinsic to the LBD (Tora et al., 1989b, Lees et al., 1989). Estrogens and antiestrogens bind to the LBD, located in region E. DNA binding is mediated by a near central DNA binding domain (DBD; region C), consisting of two zinc finger motifs. A "hinge" region (region D) is involved in nuclear localisation and interaction with heat shock protein complexes (Kumar et al., 1987). The DBD is highly conserved between ERα and ERβ, and the receptors bind to the same consensus deoxyribonucleic acid (DNA) sequences with similar affinities (Enmark et al., 1997). ERα and ERβ also bind to E2, and the antiestrogens 4-hydroxytamoxifen (OHT) and ICI 182, 780 (ICI) with similar affinities. However, selective synthetic ligands for ERα and ERβ have been identified. In reporter gene assays, ERα and ERβ show differential transcription activation with the differences in activity likely to be due for the greater part to the low amino acid sequence homology between the two receptors (Kuiper et al., 1997).

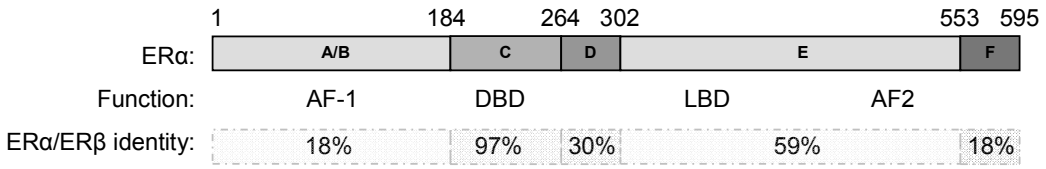

Figure 1.1 - Structure of human ERα. Cloning of ERα from different species highlighted regions of differing amino acid sequence homologies across the length of the protein, resulting in the naming of regions A-F (Krust et al 1986). Subsequent deletional analysis linked these regions with specific activities. ERα shares the conserved nuclear receptor structure consisting of an amino terminal ligand independent activation function (AF1; A/B), a DNA binding domain (DBD; C), a hinge region (D) and a ligand dependent activation function (AF2; E/F), which incorporates the ligand binding domain (LBD). The numbers show the amino acid position that represents the start and end of the different domains. Amino acid sequence identity in the different domains for human ERα and ERβ is also shown (Enmark et al., 1997).

ERα and ERβ are believed to have distinct and non-redundant roles, and this is supported by their differing expression patterns and ligand specificities (Mosselman et al., 1996, Pearce and Jordan, 2004, Kuiper et al., 1997). Indeed, it has been reported that at some promoters ERα and ERβ are capable of producing opposing responses (Liu et al., 2002). Although ERβ is expressed in normal and malignant breast tissue, current evidence suggests that it is principally ERα, rather than ERβ, that is responsible for the estrogen associated pathology of breast cancer, and will be the focus of the remainder of this report (Hartman et al., 2009, Anderson, 2002).

1.4 Estrogen signalling

ERα is a transcription factor whose activity is regulated by phosphorylation, methylation, acetylation, sumoylation and ubiquitination (Le Romancer et al., 2011). In the classical ligand dependent signalling pathway, ligand binding to the ER stimulates a conformational change in the receptor that results in heat-shock protein dissociation and receptor homodimerisation, or heterodimerisation with ERβ (Kumar and Chambon, 1988, Pace et al., 1997). Depending on the specific post-translational modifications induced by the ligand, the receptor is then able to alter the transcription of the cell. The most widely studied post-translational modification of ERα is phosphorylation, which enables ERα to influence cellular transcription in a ligand-dependent and ligand-independent manner (Chen et al., 2002). Phosphoylation of ERα, particularly at serines -104, -106, -118 and -167, is associated with transcriptional activation of the receptor (Ali et al., 1993, Chen et al., 2002, Thomas et al., 2008). Ligand independent ERα phosphorylation and signalling is associated with activation of intracellular signalling cascades, such as the mitogen activated protein

kinase (MAPK) pathway which is particularly associated with growth factor signalling (Cenni and Picard, 1999, El-Tanani and Green, 1997, Chen et al., 2002).

1.4.1 Genomic signalling

Once activated, ERα is able to affect cellular transcription in a number of different ways (Figure 1.2). The canonical mechanisms through which estrogen regulates gene expression is through ER binding as a dimer to a 13 base pair (bp) palindromic estrogen response element (ERE), first identified in the *Xenopus* vitellogenin A2 gene and having the consensus sequence GGTCANNNTGACC, where N represents any nucleotide (Klein-Hitpass et al., 1986). However, ERα is also able to regulate the expression of genes which do not contain an ERE by interaction with other transcription factors, particularly activator protein 1 (AP-1) and specificity protein 1 (Sp-1) (Saville et al., 2000, Kushner et al., 2000). Indeed, chromatin immunoprecipitation (ChIP) in U2OS cells has suggested that as few as 11% of E2 regulated genes contain an ERE (Levy et al., 2008).

1.4.2 Non genomic signalling

In addition to nuclear ER, accumulating evidence suggests the existence of a plasma membrane ER, which mediates changes in intracellular signalling within a few minutes of estrogen addition; too rapid to be attributed to transcription dependent ER actions. Membrane initiated ER signalling results in activation of the MAPK/ERK and phosphoinositide 3-kinase (PI3K)/AKT pathways, which is thought to occur, at least in part, through activation of insulin-like growth factor receptor I (IGF-IR), epidermal growth factor receptor (EGFR) and human epidermal growth factor

receptor 2 (HER2) (Song et al., 2006, Song et al., 2007, Song et al., 2002, Razandi et al., 2003, Shou et al., 2004). As this aspect is not a feature of the work reported in the thesis, I will not describe these activities any further, although it is noteworthy that activation of intracellular kinases could affect the genomic actions of ERα through phosphorylation of ERα and its cofactors (Font de Mora and Brown, 2000, Shou et al., 2004).

1.4.3 Transcription Regulation by ERα

Chromatin bound ERα is able to stimulate or block the transcription of estrogen responsive genes by recruitment of coactivator or corepressor proteins, which is thought to be primarily determined by the specific receptor conformation induced by ligand binding. Crystallographic studies of the ER-LBD have revealed that agonist and antagonist ligands produce distinct receptor conformations which promote or occlude coactivator binding. The ER-LBD is a wedge shaped structure composed of antiparallel α-helices; in the agonist bound receptor, the carboxy helix 12 folds over the ligand binding cavity to reveal a hydrophobic groove which is the interaction surface for coactivator proteins. When bound by antagonists such as tamoxifen or raloxifene, helix 12 is displaced and the hydrophobic groove is not formed, thereby preventing coactivator interaction (Shiau et al., 1998, Brzozowski et al., 1997).

ERα-mediated transcription activation has been shown to be associated with the recruitment of a range of coactivator proteins such as the DRIP/TRAP (vitamin D receptor interacting protein/thyroid hormone receptor associated proteins) complex, p300, CBP (cyclic adenosine monophosphate (cAMP) response element binding (CREB) binding protein), pCAF (p300/CBP associated factor) and steroid receptor

coactivators (SRC) -1, -2, and -3. These proteins primarily interact with the ER-LBD through the conserved coactivator nuclear receptor recognition sequence: LXXLL, where L is leucine and X is any amino acid (Torchia et al., 1997, Heery et al., 1997). However, non-LXXLL coactivator-ERα AF1 interactions have also been reported which are believed to be required for AF1 activity and synergism with the AF2 (Webb et al., 1998). Coactivator proteins are able to promote transcription by modifying the chromatin structure and acting as a scaffold for the recruitment of additional proteins as part of transcritption complex assembly. In particular, a number of coactivator proteins have been shown to possess intrinsic histone acetyltransferase (HAT) activity; histone acetylation has been shown to be associated with increased gene transcription (Glass and Rosenfeld, 2000). ChIP experiments have shown that the recruitment of ERα, coactivators and ribonucleic acid (RNA) polymerase II to estrogen responsive promoters occurs in a dynamic process with cycles of association and disassociation which last approximately 60 minutes (Shang et al., 2000).

1.4.3.1 AIB1

Amplified in breast cancer 1 (AIB1, also referred to as SRC3 and NCoA3) is a member of the p160 family of nuclear receptor transcriptional coactivators, which also includes SRC1 (NCoA1) and SRC2 (TIF2, GRIP1, NCoA2). The p160 family of coactivators are able to bind to nuclear receptors, including ERα, and recruit additional coactivator proteins and components of the transcriptional machinery to the promoter. In addition to their functioning as adaptors between nuclear receptors and other coactivator proteins, SRC1 and AIB1 also possess intrinsic HAT activity

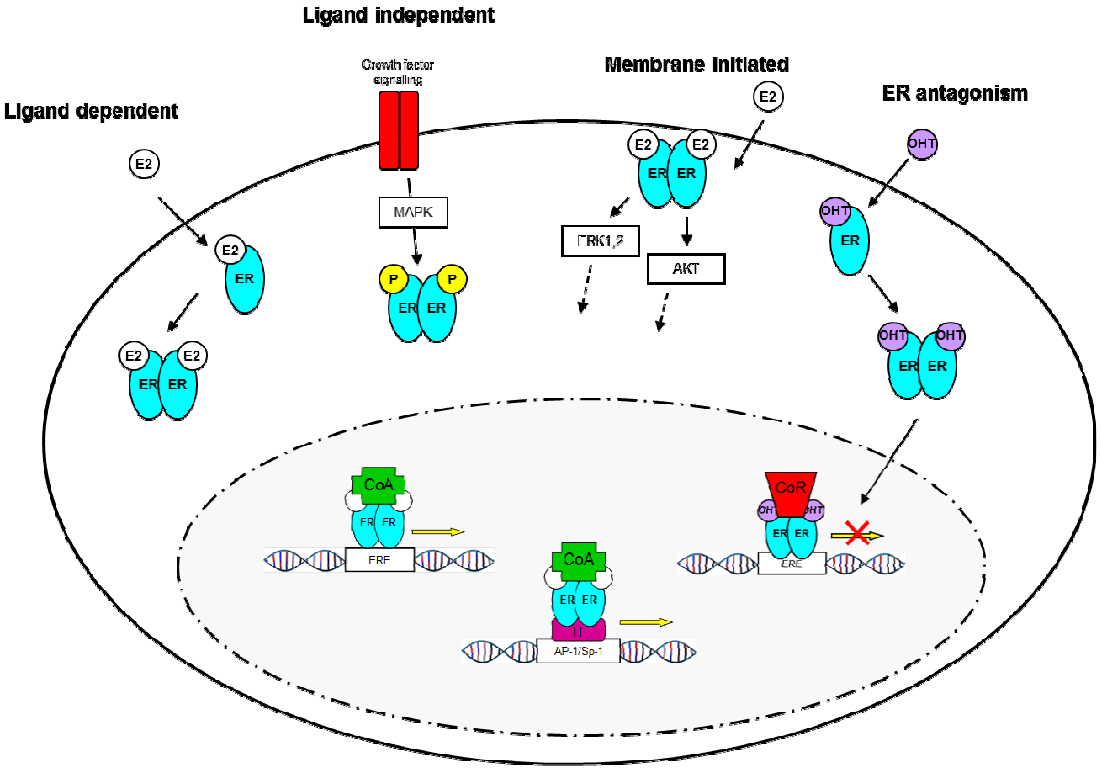

Figure 1.2 - ER signalling. The ER can stimulate transcription from promoters containing an estrogen response element (ERE) or through tethering to other transcription factors (TF), such as AP-1 and Sp-1 regulated gene promoters. Estrogen signalling can be stimulated in a ligand dependent and ligand independent manner by estrogen (E2) and growth factor signalling, respectively. E2 binding to the ER also stimulates rapid non-genomic membrane initiated ER signalling, which is associated with the activation of the AKT and ERK1/2 signalling pathways. ER antagonists, such as 4-hydroxytamoxifen (OHT), can repress ER transcriptional activity from ERE and AP1 or SP1 site containing promoters by promoting corepressor (CoR) rather than coactivator (CoA) recruitment. Figure adapted from (Le Romancer et al., 2011)

and can modify the chromatin directly (Wu et al., 2005, Klinge, 2000, Chen et al., 1997, Spencer et al., 1997).

AIB1 was originally identified from screening of breast cancer cell lines to identify genes associated with regions of amplification in breast cancer cell lines. Several studies have subsequently investigated AIB1 amplification and expression in normal and malignant tissues. Although there inconsistencies regarding the degree of amplification and overexpression in tumour samples, increased AIB1 does appear to be associated with a malignant phenotype; amplification of the AIB1 gene has been reported in 2-10% of breast tumours and over-expression has been reported in as many as 64% of breast tumours (Anzick et al., 1997, Bouras et al., 2001, Kirkegaard et al., 2007, Murphy et al., 2000, Iwase et al., 2003). A causal role for high AIB1 expression in breast cancer is supported by the high incidence of mammary tumours in transgenic mice which over-express AIB1 (Torres-Arzayus et al., 2004). *In vitro* analysis indicates that AIB1 is a critical factor in ERα signalling: AIB1 interacts with ERα in an E2 dependent manner and can stimulate a dose dependent increase in ERα signalling. Depletion of endogenous AIB1 has shown that it is a rate limiting factor for ERα transcription and estrogen dependent growth (Anzick et al., 1997, Li et al., 1997, List et al., 2001, Shang and Brown, 2002). *In vitro* analyses have also shown that the activity and stability of AIB1 is regulated by a 'phosphorylation code'; different combinations of the 9 identified phosphorylation sites spread across AIB1 are phosphorylated in response to different stimuli, and the precise residues phosphorylated determine the transcription factors to which AIB1 is recruited and AIB1 turn-over (Wu et al., 2007, Wu et al., 2004, Gojis et al., 2010).

Clinically, high expression of AIB1 in breast tumours is associated with a poor response to tamoxifen, particularly in HER2 over-expressing tumours (Osborne et al., 2003). Laboratory studies have suggested that this could be a consequence of increased birdirectional cross-talk between the ER and EGFR/HER2 pathways in these cells; in breast cancer cells which express high levels of AIB1 and HER2 it has been shown that OHT acts as an agonist in an EGFR/HER2 dependent manner. The critical interaction between ER/AIB1 and the EGFR/HER2 pathways in tamoxifen resistance is further supported by an *in vivo* model which indicates that the acquisition of tamoxifen resistance is associated with increased EGFR and HER2 expression and signalling. A recent study has indicated that combining OHT treatment with an EGFR inhibitor may be beneficial for some patients (Osborne et al., 2011, Schiff et al., 2003, Massarweh et al., 2008).

1.4.3.2 Transcription repression by ERα

In contrast to ER agonists, ER antagonists induce a receptor conformation which promotes the recruitment of corepressor proteins. The nuclear receptor corepressor (NCoR) and silencing mediator of retinoic acid and thyroid hormone receptors (SMRT) proteins were originally identified by their ability to interact with unliganded nuclear receptors (Horlein et al., 1995, Chen and Evans, 1995). The structurally similar proteins have since been shown to interact with steroid hormone receptors, including ERα, to mediate the repressive effects of receptor antagonists (Lavinsky et al., 1998, Zhang et al., 1998, Chen et al., 1996, Ordentlich et al., 1999). Corepressors interact with the hormone binding domain of ERα and other nuclear receptors through conserved CoRNR ('corner') boxes within the carboxy terminus of the proteins. The CoRNR boxes have the amino acid sequence (I/L)XX(I/V)I , where X is any amino

acid (Hu and Lazar, 1999, Nagy et al., 1999, Webb et al., 2000). Both corepressor proteins function as a bridge between nuclear receptors and proteins with histone deacetlyase (HDAC) activity. Histone deacetylation results in a more condensed chromatin structure and has been shown to be associated with gene repression (Hu and Lazar, 1999, Klinge, 2000). In addition to being regulated by changes in the nuclear receptor, NCoR and SMRT interactions are also affected by phosphorylation of the corepressors. However, although NCoR and SMRT appear to be structurally and functionally very similar, the proteins are phosphorylated in response to different cellular signalling pathways (Jonas and Privalsky, 2004, Privalsky, 2004, Hermanson et al., 2002, Jepsen and Rosenfeld, 2002). Phosphorylation of NCoR and SMRT can enhance or inhibit binding to nuclear receptors.

Both NCoR and SMRT interact with ERα in the presence of the antiestrogens OHT and raloxifene. The importance of NCoR and SMRT in determining the agonist/antagonist actions of OHT are supported by experiments showing that silencing of the corepressors can ablate the growth repressive effects of OHT and overexpression of SMRT can reduce some of the agonist actions of OHT (Keeton and Brown, 2005, Shang and Brown, 2002, Smith et al., 1997, Lavinsky et al., 1998).

1.5 Estrogen signalling as a therapeutic target

Approximately two thirds of all breast tumours express ERα and the growth of 50-70% of these can be arrested by inhibiting estrogen signalling (Clark et al., 1984). An interruption of estrogen signalling has been achieved through various methods, including blocking estrogen binding to its receptor, down regulating the receptor and inhibiting the synthesis of estrogen. However, because of the range of effects which

estrogen exerts in tissues other than the breast and uterus, a complete withdrawal of estrogen can be associated with a range of negative side effects, most notably menopausal symptoms, joint problems and a loss of bone density (Lintermans et al., 2011, Scott et al., 2011).

1.5.1 SERMs

Selective estrogen receptor modulators (SERMs) are compounds that are able to agonise or antagonise estrogen signalling in different contexts. Their mixed agonist/antagonist actions offer the potential to block the negative effects of estrogen in the breast and uterus while maintaining its positive influence in the bones and cardiovascular system.

Tamoxifen, one of the first clinically applicable SERMs, has been used to successfully treat breast cancer for over 20 years (Lewis and Jordan, 2005). Approximately half of all $ER\alpha^{+}$ breast cancer patients respond favourably to tamoxifen, and when used as an adjuvant, tamoxifen almost halves the annual likelihood of disease recurrence and prolongs a patient's overall disease free survival (EBCTCG, 1992, EBCTCG, 1998, Osborne, 1998). In high-risk patients, tamoxifen has also been used as a chemopreventive agent and can reduce breast cancer incidence by up to 50% (Fisher et al., 1998, Cuzick et al., 2003). Tamoxifen is particularly attractive as a breast cancer therapy because, in addition to blocking estrogen action in the breast, its use increases bone mineral density and reduces cholesterol; as such, tamoxifen use is associated with a reduction in osteoporotic fractures and cardiovascular deaths (Costantino et al., 1997, Fisher et al., 2005, Kristensen et al., 1994, Rutqvist and Mattsson, 1993, Love et al., 1992). However, although tamoxifen

blocks the negative actions of estrogen in the breast and promotes estrogenic action to maintain bone density, it is not the ideal SERM; long term tamoxifen use is associated with an increased risk of endometrial cancer because it acts as a partial agonist in the uterus (Lewis and Jordan, 2005, Jordan et al., 1987, Turner et al., 1987, Love et al., 1992, Shang and Brown, 2002, Fisher et al., 1994, Fornander et al., 1989). Tamoxifen use is also associated with other negative side effects such as hot flushes. Raloxifene is a SERM used for the prevention and treatment of osteoporosis which has been identified as being associated with a reduced risk of breast cancer. In the Study of Tamoxifen and Raloxifene (STAR) trial, tamoxifen and raloxifene were compared for breast cancer prevention, and it was shown that both drugs provide bone-protective and lipid-lowering effects but the increased incidence of endometrial cancer observed with tamoxifen was reduced with raloxifene. However, raloxifene was also less effective than tamoxifen at reducing the incidence of breast cancer (Vogel et al., 2006). Because of these limitations, there continues to be much interest in the development of novel SERMs and antiestrogens for the treatment of breast cancer and other estrogen associated diseases such as osteoporosis (Papoutsi et al., 2007, Yadav et al., 2011).

1.5.1.1 SERM mode of action

The mechanism through which SERMs are able to exert E2 agonist and antagonist properties in different contexts is not fully understood, although it has been shown that it depends on the N terminal AF1 region of ERα and is promoter and cell context specific (Katzenellenbogen et al., 2000, Berry et al., 1990, Tzukerman et al., 1994). The transcriptional activity of ERα at different gene promoters is determined by the recruitment of coactivator or corepressor proteins, which was classically thought to

depend upon the specific receptor conformation induced by different ligands. However, this clearly does not account for the actions of SERMs, where a single ligand can act as an ERα agonist and antagonist in different cell types. For example, OHT is an ERα antagonist in breast cancer cells but a mild agonist in endometrial cells; the agonist and antagonist actions of OHT in breast and endometrial cell has been shown to correlate with the recruitment of coactivator and corepressor proteins, respectively (Shang and Brown, 2002). The ability of OHT bound ERα to recruit different coregulators in different contexts is attributed to tissue specific epigenetic factors such as the relative and absolute expression levels of ERα and its coregulators, tissue specific post-translational modifications of proteins, including ERα and its coregulators, and the promoter context (Osborne et al., 2003, Shang and Brown, 2002, Green and Carroll, 2007, Wu et al., 2005). The pivotal role that coactivator and corepressor proteins play in the tissue specific actions of SERMs has been demonstrated with knock-down and overexpression studies. In one study it was shown that the agonist actions of OHT in endometrial cell lines is dependent on relatively high expression levels of SRC1: knock down of SRC1 in endometrial cells ablates OHT stimulated gene expression and overexpression of SRC1 in breast cancer cells results in OHT stimulated gene expression similar to that seen in endometrial cells (Shang and Brown, 2002). Similarly, knock-down of nuclear receptor corepressors can enhance the agonist actions of OHT (Smith et al., 1997, Lavinsky et al., 1998, Keeton and Brown, 2005). It has also been proposed that changes in coregulator expression levels could, at least in part, be responsible for the development of endocrine resistance (Schiff et al., 2003).

Nuclear receptors are attractive drug targets for a range of different disease states and the central role that coactivator and corepressor interactions play in determining nuclear receptor activity has led several groups to develop methods to measure nuclear receptor-coregulator interactions (Llopis et al., 2000, Zhou et al., 1998, Jankevics et al., 2005, Sladek, 2003, Iannone et al., 2004, Bai and Giguere, 2003, Awais et al., 2007, Hultman et al., 2005, Stafslien et al., 2007).

1.6 Molecular imaging

Molecular imaging has been defined as "the visualization, characterization, and measurement of biological processes at molecular and cellular levels in humans and other living systems" (Mankoff, 2007). This has been achieved through numerous strategies, including labelled antibodies and receptor ligands, activated enzyme substrates and transcriptional reporters. Clinically, molecular imaging enables a greater depth of understanding than anatomical imaging alone, and is of particular use for the personalisation of medical treatments.

Within the field of cancer biology there are numerous applications of molecular imaging; molecular imaging can be used to identify tumours and distant metastases and can also be used to characterize the tumour to determine the best treatment strategy. Similarly, a focus on the intracellular processes rather than external morphology allows molecular imaging to identify the response to treatment sooner than a reduction in tumour size could be observed (Kelloff et al., 2005). Preclinically, molecular imaging in small animal models is used extensively in assessing the value of pharmaceutical targets and the efficacy of compounds which target them.

Positron emission tomography (PET) is perhaps the most widely used molecular imaging modality in clinical oncology. [^{18}F]fluorodeoxyglucose (FDG), a glucose analogue, can be used as a marker of tumour growth to diagnose, stage and investigate treatment response. PET has many advantages as an imaging technique; it allows good resolution, quantitative 3D imaging of superficial and deep tissues in clinical and preclinical applications (Table 1.1). However, PET imaging is also very expensive, relatively slow and requires the use of radioactive isotopes. Magnetic resonance imaging (MRI) and ultrasound imaging are other clinically applicable imaging techniques, which both produce high resolution images, however their strengths currently lie in anatomical imaging with limited molecular imaging probes and applications.

1.7 Bioluminescence imaging

Bioluminescence imaging (BLI) is an optical imaging technique that can be used for *in vitro* and *in vivo* visualization of biological processes. It relies upon modification of cells or organisms to express a luciferase enzyme, which produces light as a by-product of substrate catalysis. The requirement for luciferase expression prohibits its use in humans, however, as a preclinical tool it has many advantages.

BLI in small animals is conducted using a cooled charge coupled device (CCD) camera. Mice are injected with the enzyme substrate intraperitoneally, anaesthetised, and then placed in a light tight imaging chamber with a CCD camera above (Figure 1.3). Two images

Table 1.1 - Comparison of molecular imaging modalities. Adapted from (Massoud and Gambhir, 2003)

	PET	**MRI**	**Ultrasound**	**Fluorescence**	**BLI**
Contrast agent	Radiolabelled probe	None or paramagnetic contrast agent	None or microbubble contrast agent	Fluorophore tagged probe	Genetically modified to express luciferase enzyme
Sensitivity	+++	+	++	++	+++
Spatial resolution	1-2mm	25-100µm	50-500µm	3-5mm*	3-5mm*
Temporal resolution	++	+	+++	+++	+++
Clinical application	✓	✓	✓	✓	×
Cost	£££	£££	£	£	£
Quantitative	+++	++	+	++	++
Throughput	+	+	++	+++	+++
Deep imaging	+++	+++	++	+	+

* Depth dependent, decreases as a function of signal origin depth
PET; positron emission tomography
MRI; magnetic resonance imaging
BLI; bioluminescence imaging

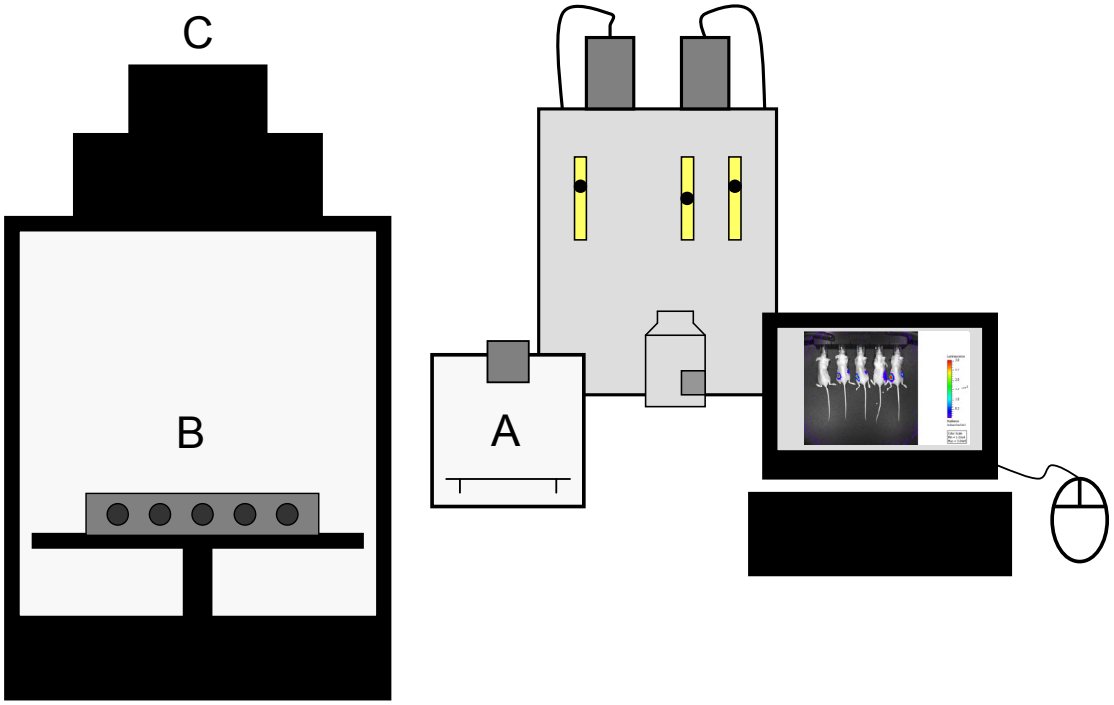

Figure 1.3 - IVIS imaging system. Mice are anaesthetised in the anaesthetic induction box (A) prior to transfer to the 37°C imaging chamber (B). The sample stage is height adjustable and has an anaesthetic manifold for up to 5 subjects. Photon emission from subjects is captured using the cooled CCD camera (C).

are acquired; a grey scale photographic image and a bioluminescence image. The acquisition time for the bioluminescence image depends on the signal strength but ranges from seconds to minutes. The photonic signal emitted from the sample is captured by the CCD camera and converted into an electrical signal, thereby allowing emission from a given area to be quantified. The quantified bioluminescence signal data is then superimposed over the grey scale image using a pseudo-colour intensity scale. Photon emission is proportional to amounts of luciferase protein over several orders of magnitude, which enables signal quantification over a broad range.

As a method for small animal imaging, BLI is generally preferred to fluorescence imaging. This is principally because BLI is associated with a very low background signal, which makes the technique very sensitive and capable of detecting low intensity signals (Troy et al., 2004). Although fluorescence probes usually emit much more light, the requirement for an exogenous light source and tissue autofluorescence produce a high background signal, which reduces the sensitivity of the technique and limits its potential for *in vivo* imaging.

Non-invasive BLI can be performed on the same subjects on multiple occasions, which enables longitudinal studies with animals acting as their own controls. Repeat imaging can reduce the number of animals required for each experiment and also reduce data variability, which can further reduce the number of animals required for each experiment. Repeated fluorescence imaging can be more problematic because of fluorophore photobleaching.

As an imaging modality, BLI lends itself to high throughput applications. Using the IVIS imaging system, up to 5 mice can be imaged at the same time with acquisition times of a few minutes. The imaging procedure is also relatively low cost; once the imaging equipment has been purchased, the only reagents required for scanning are the anaesthetic and enzyme substrate, which cost a few pounds per mouse. Experimentation costs are also reduced if fewer animals are used for each experiment.

1.7.1 Luciferase

Bioluminescent light production is dependent on luciferase enzymes. Luciferases have been isolated from many different organisms, including bacteria, insects and a range of marine organisms (Hastings, 1996). All luciferases are oxygenases and require oxygen to oxidate their substrate luciferin (S) to form an excited-state product (P*) which decays to ground state (P) emitting light (hv).

$$S + O_2 \rightarrow P^* \rightarrow P + hv$$

Although all luciferases are oxygenases, the diversity of enzyme and substrate structure suggests that the ability to emit light evolved more than once (Hastings, 1983) .

Whilst luciferase genes have been identified in many species, the luciferase enzyme from the North American firefly *Photinus pyralis* is the most widely used for *in vivo* imaging. Firefly luciferase is a 62 kilodalton (KDa), 550 amino acid protein which consists of a large N-terminal domain and a smaller C-terminal domain joined by a flexible hinge region (de Wet et al., 1985, de Wet et al., 1987, Conti et al., 1996).

Firefly luciferase catalyses the conversion of its substrate D-luciferin to oxyluciferin using oxygen and adenosine triphosphate (ATP), emitting a broad spectrum of light with a peak of approximately 610nm at 37°C (Zhao et al., 2005). This emission spectrum is particularly favourable for *in vivo* imaging because light absorption by tissue elements, particularly haemoglobin and water, is greatest in the blue-green spectrum and is less at wavelengths above 600nm (Zhao et al., 2005, Weissleder and Ntziachristos, 2003). In addition to its favourable emission spectrum, firefly luciferase is also well suited to *in vivo* imaging because the signal it emits is relatively bright and stable and the substrate D-luciferin has good bioavailability (Bhaumik and Gambhir, 2002, Luker and Luker, 2008).

Firefly luciferase has been widely used for imaging biological systems. The ATP dependence of the enzyme has lent itself to use in ATP detection assays, but it has also been used to monitor cell fate, gene expression, enzymatic activity and messenger RNA (mRNA) stability (Ciana et al., 2003, Neufeld et al., 1975, Caceres et al., 2003, Hickson et al., 2010, Laguette et al., 2011). More recently split-luciferase assays have been used to study protein-protein interactions and protein conformations.

1.8 Imaging protein-protein interactions

Protein-protein interactions are fundamental to most cellular processes and can produce numerous outcomes. As such, the study of protein-protein interactions is important in biological sciences. As far as reasonably possible, it is desirable to study

protein-protein interactions in living cells and in living subjects: with the aim that the interactions observed are true representations of the endogenous scenario.

Interaction networks and novel interaction partners can be investigated using techniques such as affinity chromatography, affinity blotting and yeast-two hybrid or other library based methods. Using these techniques, the protein of interest in used as a bait to identify interacting proteins for further analysis. These assays can be performed to a greater or lesser degree in a native cellular environment, but can be associated with a high number of false positives and negatives (von Mering et al., 2002).

Coimmunoprecipitation (CoIP), a mainstay molecular biology technique, is widely used to investigate protein-protein interactions and can be applied to the study of interactions between endogenous proteins. It can be used to identify novel interaction partners, verify interacting proteins identified by other methods, and investigate the factors which affect the interaction of two or more proteins. CoIP depends upon antibody specificity and can be associated with a relatively high background signal, which can limit its use to the investigation of relatively high affinity interactions between abundant proteins (Berggard et al., 2007). CoIP also requires individual sample preparation for each interaction snapshot and is not readily applicable to imaging dynamic interactions or interaction kinetics in an *in vivo* context.

Fluorescence resonance energy transfer (FRET) is the gold standard for imaging interaction dynamics between two proteins of interest. FRET occurs between two fluorophores when the emission spectrum of the donor fluorophore overlaps the

excitation spectrum of the acceptor fluorophore; this has been applied to the study of protein-protein interactions by tagging interacting proteins with appropriate donor and acceptor fluorophores (Fernandez and Berlin, 1976). The acceptor:donor fluorescence ratio increases when proteins are within 100 angstroms (Å) of each other, allowing the fluorescence ratio to be used as a molecular ruler (Stryer and Haugland, 1967). The discovery and cloning of genetically encoded fluorescent proteins has enabled FRET to be applied to imaging protein-protein interaction kinetics in live cells (Prasher et al., 1992, Shimomura et al., 1962, Day et al., 2001, Demarco et al., 2006, Llopis et al., 2000, Sun et al., 2011). However, because of the limitations associated with fluorescence imaging in animal models, namely low sensitivity, FRET is not well suited to *in vivo* imaging. Bioluminescence resonance energy transfer (BRET), where a bioluminescent light source is used to excite the acceptor fluorophore, which excludes the requirement for an external light source, is an adaptation of FRET which offers the potential to investigate protein-protein interactions in living subjects. However, at present the method is still in its infancy and suitable donor and acceptor proteins for *in vivo* imaging are still being developed in proof of principle experiments (De and Gambhir, 2005, De et al., 2009, Dragulescu-Andrasi et al., 2011).

Perhaps the most effective method for imaging protein-protein interactions in living subjects is the split reporter assay, in particular those using luciferases and thymidine kinase (Bhaumik and Gambhir, 2002, Massoud et al., 2010, Paulmurugan et al., 2002). These split reporter assays are a development of ubiquitin, β-galactosidase and dihydrofolate reductase protein fragment complementation assays, which have previously been used to image protein-protein interactions (Johnsson and Varshavsky,

1994, Pelletier et al., 1998, Rossi et al., 1997, Paulmurugan et al., 2002). As previously discussed, PET imaging (using thymidine kinase split reporter assays) provides highly resolved, 3D, deep tissue imaging, but it is relatively expensive, slow and dangerous. Firefly and *Renilla* luciferases are the predominant luciferases which have been used for imaging protein-protein interactions in living subjects. Because of its emission spectrum, substrate bioavailability and robust signal, firefly luciferase is the preferred luciferase for imaging *in vivo* (Zhao et al., 2005).

1.8.1 Luciferase fragment complementation assay

The basis of the luciferase fragment complementation assay is that the enzyme can be split into two subunits, the N-terminal and C-terminal luciferase fragments (NLuc and CLuc, respectively). Individually these fragments are absent of activity, but when they are brought into close proximity they are able to complement and enzymatic activity is restored. In order to image protein-protein interactions the NLuc and CLuc fragments are fused in frame with two interacting proteins of interest; when the proteins interact, the luciferase fragments are brought into close proximity and complement so the interaction can be imaged by the restoration of luciferase activity (Figure 1.4). The luciferase fragments used should not self-complement, and so in the absence of interaction between the two proteins of interest, minimal luciferase activity should be observed. Firefly, *Renilla, Gaussia* and click beetle luciferases have all been used to image protein-protein interactions using such an assay (Villalobos et al., 2010, Paulmurugan et al., 2004, Luker et al., 2004, Remy and Michnick, 2006). The optimal location to split firefly luciferase for complementation assays has been found to be in the region of the flexible hinge between the N- and C-terminal protein domains (Luker et al., 2004, Paulmurugan and Gambhir, 2007). The specific

luciferase fragments used and their position within the fusion protein has been shown to significantly alter the luciferase activity observed in the presence and absence of the interaction inducer; luciferase fragments which spontaneously complement have also been identified (Paulmurugan and Gambhir, 2007).

Firefly luciferase protein complementation has been applied to the detection of a range of biological processes *in vivo*, including ligand-induced CXCR4 and EGFR activation, AKT activation and apoptosis (Li et al., 2008, Luker et al., 2008, Zhang et al., 2007, Coppola et al., 2008). It has also been successfully employed to detect protein-protein interactions in plants (Chen et al., 2008). More recently, red and green click beetle luciferases have been used to image interactions between three proteins (Villalobos et al., 2010).

In studying protein-protein interactions, it is desirable to use a method which is capable of indicating interaction kinetics. In cellular systems, different time-course

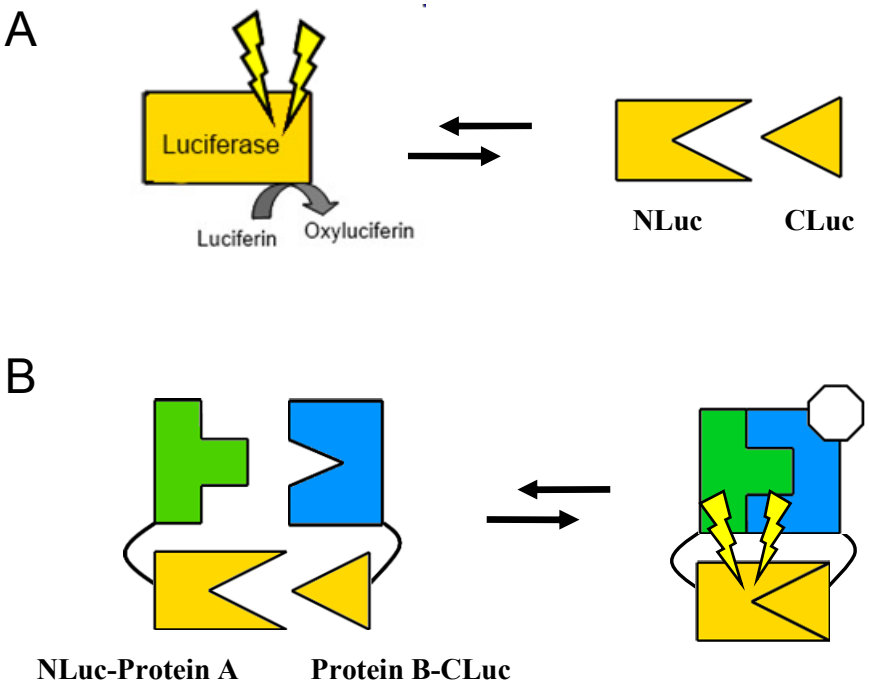

Figure 1.4 - Luciferase fragment complementation assay. (A) The luciferase enzyme can be split into two enzymatically inactive subunits, NLuc and CLuc, which can complement when brought into close proximity. (B) By fusing NLuc and CLuc to Protein-A and Protein-B, the interaction between Protein-A and Protein-B can be detected by the emission of light in the presence of the substrate luciferin.

studies have indicated that split-luciferase proteins require ligand or interaction-inducer incubations in the range of minutes to hours in order to reach a plateau in luciferase fragment complementation. It has been argued that the range of different incubations required are a reflection of the time frame of the specific processes being monitored or membrane permeability to ligand, rather than complementation between the luciferase fragments being the rate limiting step; in cell free systems or cell lysates, a signal plateau is reached within 1-2 minutes (Luker et al., 2004, Taneoka et al., 2009, Luker et al., 2008, Luker et al., 2009, Yang et al., 2009, Villalobos et al., 2010).

In addition to being able to detect the kinetics of protein-protein interactions, the ability to image interaction dynamics is also desirable. In principle, protein fragment complementation assays should be reversible because the restored reporter activity only depends on protein folding and not covalent modification of the luciferase fragments, although green and yellow fluorescent protein complementation assays have been demonstrated to be irreversible (Hu et al., 2002, Magliery et al., 2005). However, the available evidence suggests that this is not the case for luciferase fragment complementation assays; to date, *Gaussia, Renilla* and click beetle luciferase fragment complementation assay have all been shown to be reversible in nature (Villalobos et al., 2010, Stefan et al., 2007, Remy and Michnick, 2006). Depending on the system being studied, reduced complementation between luciferase fragments was observed in seconds to minutes in these studies.

1.9 Imaging ER activity

Given the central role that ERα plays in the development and progression of breast cancer and its use as a therapeutic target, various methods to image ER activity have been developed by different groups. These broadly fall into two categories; transcriptional reporters and ER-coregulator interaction assays.

The central role that ER coactivators and corepressors play in determining the activity of ER has been exploited as a mechanism for imaging ER activity. Using a range of fluorescence based techniques, the association of the full length ERα, ERα-LBD or ERβ with coactivator LXXLL peptides or the receptor interaction domains (RID) have been imaged. These assays have been used to determine the pharmacology of novel ERα ligands and the specific coactivator preferences of ERα and ERβ relative to other nuclear receptors (Liu et al., 2003, Zhou et al., 1998, Llopis et al., 2000, Bai and Giguere, 2003, Dong et al., 2006, Iannone et al., 2004, Jankevics et al., 2005, Weatherman et al., 2002). Because of the limitations of fluorescence for *in vivo* imaging, these studies have all been conducted with purified proteins or in cultured cells.

In vivo and *ex vivo* imaging of ER activity has been achieved with transcriptional reporters. Transgenic ERE-luciferase reporter mice have been developed to image time and tissue dependent ER transcription in response to different ligands (Ciana et al., 2001, Ciana et al., 2003, Della Torre et al., 2011, Lemmen et al., 2004). Using these mice, it has been shown that the magnitude and time-frame of ERE activity in response E2 is different in different tissues. ERE-green fluorescent protein (GFP) and ERE-β-galactosidase transgenic mice have also been developed for *ex vivo* analysis of

ligand specific ER activation in different tissues (Toda et al., 2004, Nagel et al., 2001). In order to specifically appreciate transcriptional activation mediated by ERα, rather than the combined actions of ERα and ERβ from the classic ERE, an ERα activity indicator model mouse has recently been developed. A bacterial artificial chromosome has been used to achieve endogenous expression levels of an ERα protein in which the DBD has been replaced with the Gal4 DBD. This enables ERα specific expression of GFP in different tissues in response to ligand, although to date this reporter has only been used in proof-of-principle experiments (Han et al., 2009).

1.10 Thesis synopsis

The aim of this project was to develop a luciferase fragment complementation assay that would allow non-invasive *in vivo* imaging of the interactions between ERα and key transcriptional coregulator proteins. It was hoped that the development of such a method would allow imaging of the tissue-selective activities of agonist and antagonist bound ERα. As the split-luciferase method provides the most sensitive method for *in vivo* imaging of protein-protein interactions (see above), I decided to generate constructs based on the split-luciferase constructs described by Professor S Gambhir (Paulmurugan and Gambhir, 2007). AIB1 and SMRT were chosen as an ERα coactivator and a corepressor, respectively, as these proteins are known to have important roles in regulation of agonist and antagonist bound ERα activities. To perform such studies *in vivo*, I first generated a series of ERα-coregulator split-luciferase constructs and characterised their activities *in vitro* before imaging selected constructs *in vivo*. The results of these studies are presented, and the value of such an approach for imaging ERα-coregulator interactions *in vivo* and as a means of developing an understanding of the tissue-specific action of ERα agonists and

antagonists are discussed, together with a discussion of possible future direction.

Chapter 2 Materials and Methods

2.1 Chemicals, enzymes and reagents

Unless otherwise stated, all chemicals and reagents were obtained from Sigma Aldrich (Gillingham, UK). *BamHI*, *NheI*, *XhoI* and *KpnI* restriction enzymes, deoxyribonucleotide triphosphates (dNTPs), high fidelity PCR enzyme mix, FastAP™ thermosensitive alkaline phosphatase, T4 DNA ligase, and protein and DNA size markers for electrophoresis were all purchased from Fermentas Life Sciences (St Leon-Rot, Germany).

2.2 Plasmids

pcDNA-NLuc-FKBP12-rapamycin binding protein (FRB) and pcDNA-FK506 binding protein 1A (FKBP12)-CLuc were a gift from Professor S. Gambhir at Stanford University. The coding sequences for ERα, AIB1 and SMRT were obtained from the plasmids pSG5-HEG0 (Tora et al., 1989a), (Tora et al., 1989a), pcDNA-AIB1 (Anzick et al., 1997) and pCMX-SMRT (Chen and Evans, 1995), respectively. *Renilla* luciferase was from the pRLTK vector (Promega, Southampton, UK).

2.3 Polymerase chain reaction (PCR)

Sequences for cloning were amplified by PCR. Each reaction contained 0.5ng DNA template, 1μM of each primer, 200nM dNTP and 2.5U of high fidelity enzyme mix in 1 x high fidelity PCR buffer. PCR was performed for 35 cycles of 94°C for 1 minute, 60°C for 1 minute and 72°C for 3 minutes, with a final elongation step at 72°C for 10 minutes. PCR products were column purified using the QIAquick PCR Purification Kit (Qiagen, Crawley, UK) immediately after the PCR in order to avoid degradation of the amplified product.

2.4 Agarose gel electrophoresis

Nucleic acids were separated by 0.5-1.5% agarose gel electrophoresis in 1 x TBE buffer (90mM tris(hydroxymethyl)aminomethane (tris), 90mM boric acid, 20mM ethylendiaminetetraaceticacid (EDTA)). Incorporated into the gel for nucleic acid staining was either 0.003% ethidium bromide or 1 x SYBR® Nucleic Acid Gel Stain (Invitrogen, Paisley, UK).

2.5 DNA ligations and bacterial transformation

25ng ligations were performed with a 1:1 and 3:1 molar ratio of insert:vector with 5 enzyme units (U) T4 DNA ligase in 1 x ligase buffer overnight at room temperature. 50µl of DH5α *Escherichia coli* (*E.coli;* Invitrogen) were transformed with 10ng of ligation product by placing on ice for 30 minutes prior to heat shock at 42°C for 30 seconds followed by 2 minutes on ice. The bacteria were then allowed to recover by the addition of 1ml Super Optimal Broth (SOB; Invitrogen) and incubation at 37°C for 1 hour before plating on Luria broth (LB)-agar plates, containing 100µg/ml ampicillin. Plates were incubated at 37°C overnight. Individual colonies from the plates were expanded in 3ml of LB overnight and plasmid DNA was prepared from the cultures using the GeneJET™ Plasmid Miniprep Kit (Fermentas). Plasmid DNAs were screened for the presence of an insert by restriction enzyme digestion and confirmed by sequencing.

2.6 Construction of luciferase-fragment reporter plasmids

The ERα, AIB1 and SMRT split-luciferase reporter constructs were generated through modification of pcDNA-NLuc-FRB (pcDNA-*Nhe1*-Firefly luciferase amino acids 1-

398 – *BamHI* – FRB – *XhoI)* and pcDNA-FKBP12-CLuc (pcDNA-*Nhe1*- FKBP12– *BamH1* – Firefly luciferase 394-550 – *XhoI).*

To prepare the backbones, FRB and FKBP12 were excised; pcDNA-NLuc-FRB was digested with *BamHI* and *XhoI* in 1 x *BamHI* buffer using a 2-fold excess of *XhoI* and pcDNA-FKBP12-CLuc was digested with *NheI* and *XhoI* in 1 x Tango buffer (Fermentas). Digests were performed at 37°C for 2 hours. The enzymes were heat inactivated at 65°C for 15 minutes prior to agarose gel electrophoresis of the digest products. Fragments of the appropriate size (approximately 6.5 and 5.9 kilo-base pair (Kb) for pcDNA-NLuc and pcDNA-CLuc respectively) were excised and purified from the gels using the QIAquick Gel Extraction Kit (Qiagen). Because FRB and FKBP12 are both relatively small (approximately 300bp each), the excised fragments may be contaminated with linearised vectors, resulting from incomplete restriction enzyme digestion. So, to prevent re-ligation of partially digested vectors, 5' phosphates were removed using a thermosensitive alkaline phosphatase for 10 minutes at 37°C. The alkaline phosphatase was heat inactivated at 75°C for 15 minutes prior to ligation reactions.

To replace FRB and FKBP12, full length or "interaction domains" of ERα, AIB1 and SMRT were PCR amplified for cloning into the pcDNA-NLuc or pcDNA-CLuc backbones. The primers used for the PCR reactions had restriction enzyme sites engineered into them and transcription start/stop codons inserted/removed as appropriate (Table 2.1). Prior to ligation, the column purified PCR products were digested and gel purified as described for the backbones.

Ligations between pcDNA-NLuc and pcDNA-CLuc and the inserts were performed and the constructs sequenced for verification. 25ng ligations were performed with a 1:1 and 1:3 molar ratio of vector to insert in 10µl volume. Reactions were incubated overnight at room temperature.

To generate the G_4S flexible spacer, oligonucleotides having the sequences 5'-GATCCGGTGGAGGCGGTTCAGGCGGAGGTGGCAGCGGTACCC-3' and 5'-GATCGGGTACCGCTGCCACCTCCGCCTGAACCGCCTCCACCG-3' were heated in a 1:1 molar ratio in annealing buffer (10mM tris, 50mM NaCl, 1nM EDTA, pH 8.0) to 80°C in a water bath for 10 minutes, then allowed to cool slowly overnight. To insert, plasmids were digested between the luciferase-fragment and fusion protein with *BamHI,* gel purified and then ligated with the insert. Insertion of the spacer introduced a *KpnI* restriction enzyme site, which was used to screen for positives. The number of spacers inserted and their orientation was determined by sequencing.

Mutant ERα constructs were generated using the QuickChange Site-Directed Mutagenesis kit (Agilent Technologies, Edinburgh, UK). The primers used were 5'-TGGTGCCCCTCTATGACGCGGCGCTGGAGATGCTGGACG-3', 5' CGTCCAGCATCTCCAGCGCCGCGTCATAGAGGGGCACCA-3' for the L539A/L540A mutants and 5'-AAGAACGTGGTGCCCCTCTCTGACCTGCTG-3' and 5'-CAGCAGGTCAGAGAGGGGCACCACGTTCTT-3' for the Y537S mutants.

Table 2.1 - Oligonucleotides used for construction of split-luciferase constructs. Primer sequences which complement the template (and are used for primer annealing) are shown in capital letters. Lower case denotes sequences not present in the gene of interest. Restriction enzyme sites are in bold. "-" in the primer sequence denotes a deleted base relative to the gene sequence.

Split-luciferase construct (pcDNA-)	PCR product (Protein: amino acids)	Primer sequence (5'-3')
NLuc-ER	ERα:	F - agatc**ggatcc**ACCCTCCACACCAAAGCATCTGGG
	4-595	R - tgatc**ctcgag**TCAGACTGTGGCAGGGAAACCCTCTGCC
NLuc-ER-LBD	ERα:	F - agatc**ggatcc**TCTGCTGGAGACATGAGAGCTGCC
	282-595	R - tgatc**ctcgag**TCAGACTGTGGCAGGGAAACCCTCTGCC
ER-CLuc	ERα:	F - agatc**gctagc**ATGACCATGACCCTCCACACCAAAGC
	1-595	R - tgatc**ggaTCC**GACTGTGGCAGGGAAACCCTCTGCCTCCCCCGT
ER-LBD-CLuc	ERα:	F - agatc**gctagc**atGTCTGCTGGAGACATGAGAGCTGCC
	282-595	R - tgatc**ggaTCC**GACTGTGGCAGGGAAACCCTCTGCCTCCCCCGT
NLuc-AIB1	AIB1:	F -agatc**GGATCC**-CTGGCCAGTGATTCACGAAAAC
	11-1424	R - tgatc**ctcgag**tcaGCAGTATTTCTGATCAGGACC
NLuc-AIB-RID	AIB1:	F - agatc**ggatcc**GTGGAGAGTTCAATGTGTCAGTC
	580-839	R - cagac**ctcgag**ctaCAAACCCAGAGAATTAGTTCCTT
AIB1-CLuc	AIB1:	F - agatc**gctagc**aTGGCCAGTGATTCACGAAAACGCAAATTGCC
	12-1424	R - tgatc**ggatcc**GCAGTATTTCTGATCAGGACCCATAGG
AIB-RID-CLuc	AIB1:	F - agatc**gctagc**atgGTGGAGAGTTCAATGTGTCAGTC
	580-839	R - tgatc**ggatcc**CAAACCCAGAGAATTAGTTCCTTG
NLuc-SMRT-RID	SMRT:	F - agatc**ggatcc**ACCCCTGCGAAGAACCTCGCAC
	1988-2462	R - tgatc**ctcgag**TCACTCGCTGTCGGAGAG
SMRT-RID-CLuc	SMRT:	F - agatc**gctagc**catgACCCCTGCGAAGAACCTCGCACCTC
	1988-2462	R - tgatc**ggatcc**CTCGCTGTCGGAGAG

2.7 Cell lines and culturing

All cell culture reagents were obtained from Invitrogen unless otherwise stated. 293H (human embryonic kidney; Invitrogen), Ishikawa (endometrial adenocarcinoma; Sigma-Aldrich), U2OS (osteosarcoma; ATCC, Teddington, UK), MCF7 (breast adenocarcinoma; ATCC) and MELN (MCF7-ERE- Luciferase; (Balaguer et al., 2001)) cells were all routinely maintained at 37°C in a 5% CO_2 atmosphere, in Dulbecco's modified Eagle's medium (DMEM) supplemented with 2mM L-glutamine, 10% foetal calf serum (FCS; Lonza, Slough, UK), 100U/ml penicillin, 100ug/ml streptomycin and 1ug/ml Fungizone™ antimycotic.

Prior to estrogen induction experiments, cells were grown for a minimum of 3 days in phenol red-free DMEM supplemented with 2mM L-glutamine and 5% double charcoal and T70 dextran-coated charcoal-stripped FCS (Interlink UK, Birmingham, UK) and were maintained in the charcoal-stripped medium for the duration of the assay. E2, OHT, raloxifene hydrochloride and ICI 182,780 (Tocris Bioscience, Bristol, UK) were solubilised in ethanol. Rapamycin (Merck, Hoddesdon, UK) was solubilised in dimethyl sulfoxide (DMSO).

2.8 Preparation of cell lysates

Whole cell lysates were prepared using radioimmunoprecipitation assay (RIPA) buffer (50mM Tris-HCl pH7.2, 150mM NaCl, 1% NP40, 1% sodium deoxycholate, 0.1% sodium dodecyl sulphate (SDS)) with 1 x protease inhibitor cocktail (final concentration 1mM 4-(2-Aminoethyl)benzenesulfonyl fluoride hydrochloride (AEBSF.HCl), 800nM aprotinin, 50µM bestatin, 15µM E-64, 5µM EDTA, 20µM

leupeptin, 10μM pepstatin A; Thermo Scientific, Loughborough, UK). Culture medium was poured or aspirated from the tissue culture vessel and cells were washed twice in ice-cold phosphate buffered saline (PBS) on ice. Lysis buffer was added to the cells and a cell scrapper was used to detach and collect the cells. The cells were then transferred to a tube, agitated by vortexing, and kept on ice for 30 minutes with 3 additional vortexes at 10 minute intervals. Cell debris was then cleared from the lysates by centrifugation at 16,000xg for 10 minutes at 4°C and the supernatant was transferred to a new tube and stored at -80°C. Protein concentration was determined using a bicinchoninic acid (BCA) protein assay (Thermo Scientific).

2.9 Cell growth assays

A sulforhodamine B (SRB) assay was used to assay cell growth and cytotoxicity in 96 well plates. Cells were fixed for 1 hour at 4°C after addition of 50μl of ice-cold 50% tricholoacetic acid (TCA) onto 200μl growth medium. Plates were then thoroughly rinsed under a running tap and plates were dried. Adhered cell were stained with 0.4% SRB in 1% acetic acid for 30 minutes, after which unincorporated dye was removed by rinsing in 1% acetic acid. After drying, bound dye was solubilised by adding 200μl of 10mM Tris to wells and absorbance was measured at 565nm.

2.10 Cell transfection

Details specified are based upon transfection in a 96 well plate format, quantities were scaled up for transfections in 6 well and 10cm plates (33- and 200-fold respectively). One day prior to transfection, cells were plated at 70-80% confluency in antibiotic-

free media. The following day, the cells in each well were transfected with 200ng plasmid and 0.6µl Lipofectamine 2000 transfection reagent (Invitrogen) using DMEM supplemented with 2mM L-glutamine. For luciferase assays, 50ng of pRLTK was transfected with the experimental plasmids in order to normalize data with regard to transfection efficiency. 6 hours post-transfection, the transfection mixture was removed and replaced with fresh media, containing estrogen, antiestrogens or rapamycin, as appropriate. An equal volume of the solvent was added to vehicle controls.

For stable cell line generation, Lipofectamine LTX transfection reagent (Invitrogen) was used according to the manufacturer's instructions. Cells were seeded to 80% confluency in 6 well plates and transfected the following day using 5µg plasmid DNA. To increase yield a range of transfection conditions were routinely used; reactions were performed using 10µl and 20µl of Lipofectamine LTX with 2.5µl or 7.5µl of Plus Reagent. After 6 hours, media were changed. The following day, cells were passaged into 15cm tissue culture plates and selective antibiotics, 4µg/ml puromycin and 500µg/ml G418 as appropriate, were added the following day to select for stable integrants. SRB assays had been carried out to determine the lowest concentration of these antibiotics at which all cells die in the absence of transfection with the plasmids encoding the resistance genes. Selective antibiotic containing media was replenished every 4-5 days until colonies formed, usually 2-3 weeks. Colonies were picked using 3mm cloning discs, propagated and screened for luciferase activity +/- E2.

2.11 Luciferase assays

In vitro luciferase assays were performed in clear-bottom black 96 well plates (Corning Incorporated, Amsterdam, The Netherlands). Luciferase activity was quantified using a Topcount:NXT luminescence counter (PerkinElmer, Buckinghamshire, UK) or IVIS 100 (Caliper Life Sciences, Runcorn, UK).

For transiently transfected cells, firefly and *Renilla* luciferase activity was quantified using the Dual Glo® Luciferase Assay System (Promega) approximately 48 hours post transfection. Medium was poured/tapped from the wells and 60µl of 1:1 phenol red-free DMEM:Luciferase Reagent was added to the wells 10 minutes before determination of firefly luciferase activity. 30µl of Stop and Glo reagent was subsequently added to the wells and *Renilla* luciferase activity was obtained 10 minutes later. Firefly luciferase readings were normalised to the *Renilla* luciferase transfection efficiency control.

For stably transfected cell lines, luciferase activity was measured in live cells approximately 48 hours after treatment by the addition of 200µg/ml D-luciferin potassium salt in PBS (Gold Biotechnology, Missouri, USA). Where stipulated, the luciferase activity measured was normalised to total protein; after quantification of luciferase activity, cells were washed twice in PBS and 25µl of RIPA buffer was added to wells before freezing at -80°C. Plates were subsequently defrosted for 1 hour at room temperature with shaking and the protein content was determined using a BCA protein assay (Thermo Scientific).

2.12 *In vivo* imaging

All animals were housed in individually ventilated cages (IVC) within the CBS facilities at Imperial College. Procedures and humane end points were defined and adhered to according to the project license and Home Office regulations.

Prior to implantation, cells were washed twice in PBS, counted with a haemocytometer and resuspended in PBS. 100µl of cell suspension containing 1-10x10^6 cells was injected subcutaneously into the flank or scruff of 4-6 week old female nu/nu BALB/c mice (Harlan, Bicester, UK) anaesthetised with isoflurane (Abbot Laboratories, Maidenhead, UK).

Where tumours were allowed to develop, the volume was calculated from tumour caliper measurements using the ellipsoid volume formula $\pi/6$ x (tumour length(mm) x tumour width(mm) x tumour breadth(mm)) (Tomayko and Reynolds, 1989)

Estrogen and tamoxifen were administered to mice through slow release pellets; 0.72mg/60 day 17β-estadiol, 5mg/60 day tamoxifen or 60 day placebo pellets (Innovative Research of America, Florida, USA) were implanted into isoflurane anaesthetized mice either simultaneous to cell injection or 5 days prior. A small incision was made approximately 1.5cm from the desired pellet location and a subcutaneous pocket was formed by carefully separating the skin from the muscle layer. The pellet was placed 1.5cm into the pocket (to prevent expulsion) and the skin either side of the incision was joined with the absorbable suture Vicryl (Ethicon, Edinburgh, UK). 1.64µg/ml Metacam® (Boehringer Bracknell, UK) was added to drinking water for 48 hours following surgery as additional pain relief. Mice were

treated with 5mg of ICI 182,780 by subcutaneous administration of 100µl of the breast cancer approved drug Faslodex (AstraZeneca, London, UK). Peanut oil was administered as a placebo for fulvestrant.

All *in vivo* imaging was conducted using the IVIS 100 (Caliper Life Sciences). Mice were injected intraperitoneally with 150mg/kg D-luciferin potassium salt (Gold Biotechnology)/100µl sterile PBS. Approximately 10 minutes later, mice were aneasthetised with isoflurane and placed into the imaging chamber. Images were acquired using a CCD camera until a signal plateau was reached. Photon emission was quantified using the Living Image Software (Caliper Life Sciences); regions of interest (ROI) of a standard area were placed over cell populations and the total photons/second (flux) were quantified and used for data analysis after subtraction of background ROI values.

For analysis, tumours were excised after sacrifice of the animals, washed in PBS and fixed in 4% formaldehyde. Tissues were embedded, sectioned and stained with haematoxylin and eosin (H&E) by the Hammersmith Hospital Histopathology department.

2.13 Antibodies

Mouse anti-AIB1 (BD611105) and mouse anti-SMRT (BD611387) were purchased from Becton Dickinson and Company (Oxford, UK). Rabbit anti-AIB1 (sc9119), rabbit anti-SMRT (sc20778), mouse anti-ERα (sc8002), rabbit anti-ERα (sc543), mouse anti-firefly luciferase (sc57603) and rabbit anti-firefly luciferase (sc32896) were purchased from Santa Cruz Biotechnology (Heidelberg, Germany). Mouse anti-

β-actin was purchased from Abcam (ab6276; Cambridge, UK). Goat anti-rabbit immunoglobulins (Ig)/horse radish peroxidase (HRP; P0448) and goat anti-mouse Ig/HRP (P0447) were purchased from Dako (Ely, UK). Alexa Fluor® 594 goat anti-rabbit IgG (A11012), Alexa Fluor® 594 goat anti-mouse IgG (A11005), Alexa Fluor® 488 goat anti-rabbit IgG (A11008), Alexa Fluor® 488 goat anti-mouse IgG (A11001), rabbit IgG isotype control (10500C) and mouse IgG isotype control (10400C) antibodies were purchased from Invitrogen.

2.14 Immunoblotting

2 x loading buffer (125nM tris, 4% SDS, 0.2% bromophenol blue, 200mM dithiothreitol (DTT), 20% glycerol, pH6.8) was added to an equal volume of protein lysates and the samples were boiled for 5 minutes and resolved by SDS-polyacrylamide gel electrophoresis (SDS-PAGE). 1.5mm thick 8x10cm mini-gels were cast using the Mighty Small 4-gel Caster (GE Healthcare, Little Chalfort, UK). Gels were cast with a 5% stacking gel (5% acrylamide (Protogel, National Diagnostics, East Riding, UK), 125mM Tris, 0.1% SDS, pH6.8) and 8% or 10% resolving gel (8 or 10% acrylamide, 375mM Tris, 0.1% SDS, pH8.8). The stacking and resolving gels were polymerised with 1:100 10% ammonium persulfate (APS) and 1:1000 tetramethylenthylenediamine (TEMED). Electrophoresis was performed in an SE250 Electrophoresis Unit (Hoefer Incorporated, Fisher Scientific, Loughborough, UK) with a 25mM Tris, 190mM glycine, 0.1% SDS, pH8.3 running buffer.

Following separation by electrophoresis, proteins were transferred to Hybond™ ECL nitrocellulose membrane (GE Healthcare) in a 20% methanol, 25mM Tris, 38mM

glycine, pH8.3 buffer using the Mini Trans-Blot Electrophoretic Transfer Cell (Bio-Rad, Hemel Hempstead, UK). Membranes were blocked for 1 hour in blocking buffer (5% milk powder, 0.1% Tween 20-PBS (PBS-T)) before incubation with primary antibody diluted in blocking buffer overnight at 4°C. For AIB1 detection, rabbit anti-AIB1 antibody was diluted 1:4000. For ERα blotting, mouse anti-ERα antibody was diluted 1:1000. As a loading control, all membranes were blotted for β-actin with a mouse anti-β-actin antibody diluted 1:100,000. Membranes were washed 3 times in PBS-T prior to incubation with secondary antibody (goat anti-mouse/rabbit Ig/HRP) diluted 1:2000 in blocking buffer for 1 hour at room temperature. Membranes were finally washed 3 more times in PBS-T, incubated with SuperSignal West Pico or Femto Chemiluminescent Substrate (Thermo Scientific) and used to exposure of Amersham Hyperfilm ECL (GE Healthcare).

2.15 Immunofluorescence

Cells were plated in chamber slides (Corning Incorporated) prior to transfection and/or treatment. 24 hours after plating or treatment, cells were washed twice in ice-cold PBS and fixed with 4% formaldehyde for 15 minutes at 37°C. Cells were subsequently washed 3 times in PBS, permeabilised with 0.1% Triton-X-PBS (PBS-Tx) for 10 minutes and then blocked with 1% bovine serum albumin (BSA)-PBS-Tx for 1 hour. Cells were incubated with primary antibodies diluted 1:150 in 1%BSA-PBS-Tx for 1 hour. Primary antibody was removed with 3 washes in PBS-Tx before incubation with secondary antibodies diluted 1:400 in 1%BSA-PBS-Tx for 1 hour at room temperature. Cells were finally washed 3 times in PBS-Tx and mounted with Prolong® Gold antifade with DAPI (4',6-diamidino-2-phenylindole; Invitrogen).

2.16 Statistical analysis

All statistical analysis was performed using Prism 5.01 (Graphpad Software, California, USA). An unpaired t-test was used to compare results +/- treatment and an analysis of variance (ANOVA) was used to compare larger data sets. Bonferroni or Dunnett's multiple comparison post tests were used to compare all results or results relative to vehicle, respectively.

Chapter 3 Results

3.1 Characterisation of MELN cell line

The capacity to image estrogen receptor activity is an important tool for the development of novel estrogen receptor modulators. The MELN cell line is an ERα transcriptional reporter. It is an MCF7 cell line which has been stably transfected with an estrogen responsive promoter driving transcription of the firefly luciferase reporter gene (ERE-Luciferase, (Balaguer et al., 2001)). I chose to use the MELN cell line as a control for the split luciferase constructs developed during this project. For this reason, an initial characterization of the cell line was performed.

Incubation of the MELN cell line with E2 produced a dose dependent increase in luciferase activity (Figure 3.1A). Peak luciferase activity was observed at concentrations of 10^{-8}M, although near maximal activity was obtained at a concentration of 10^{-11}M E2. The luciferase activity observed with E2 was greater with longer E2 incubations (Figure 3.1B), with luciferase activity being near maximal at 8 hours. The antiestrogens OHT (Figure 3.2A) and ICI (Figure 3.2B) inhibited luciferase activity observed with 10^{-9}M E2. With both antiestrogens, partial inhibition was observed in the presence of 10^{-8}M antiestrogen and near complete inhibition was observed at 10^{-7}M and above. The luciferase activity observed with higher concentrations of the antiestrogens was well below that observed with vehicle treatment.

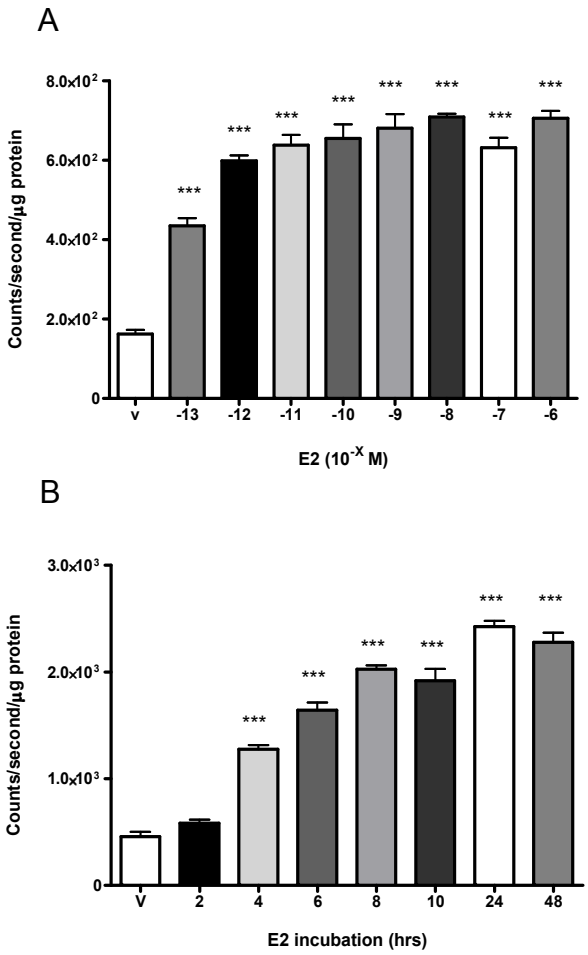

Figure 3.1 - E2 response of MELN cells. $1.5x10^4$ MELN cells were treated with vehicle (ethanol) or increasing concentrations of E2 for 48 hours (A) or 10^{-6}M E2 for increasing periods of time (B) prior to quantification of luciferase activity. Mean luciferase activities (n = 3) are shown, normalized to total protein. Error bars represent the standard errors of the mean (SEM). The ANOVA test was used to determine statistical significance relative to vehicle treatment (***, $p \leq 0.001$).

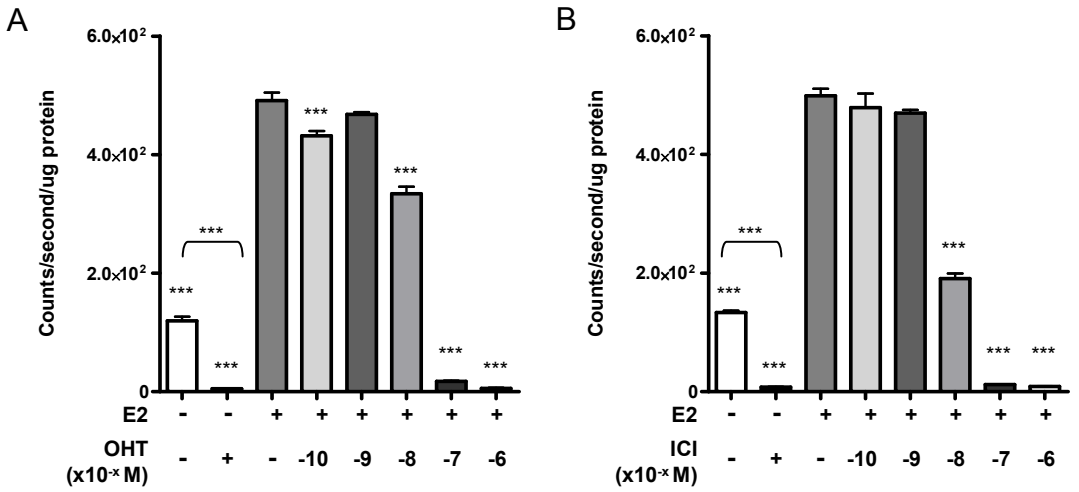

Figure 3.2 - Modulation of MELN E2 response by OHT and ICI. $1.5x10^4$ MELN cells were treated with vehicle (ethanol) or 10^{-9}M E2 and different concentrations of OHT (A) or ICI (B) for 48 hours. Mean luciferase activities (n = 3) are shown, normalized to total protein. Error bars represent the standard errors of the mean (SEM). The ANOVA test was used to determine statistical significance relative to the E2 treatment (***, $p \leq 0.001$.).

In order to assess the tumourgenicity of the MELN cell line and determine if *in vivo* tumour imaging was possible, $1x10^7$ cells were injected subcutaneously into the flank of 6 nude mice. E2 pellets were implanted into the opposing flank at the same time as cell inoculation, since MCF7 cells require estrogen for their growth. Tumour development was monitored by calliper measurements and by imaging the luciferase activity every 7 days (Figure 3.3). Tumours developed in 4 of the 6 mice inoculated. Half of the tumour bearing mice developed palpable tumours within 2 weeks but tumour development was much slower in the other 2 mice. Regardless of tumour size, luciferase activity was detectable in all 4 mice at all imaging time points. Luciferase activity generally increased as tumour volume increased, although at later time points the luciferase activity in the larger tumours decreased even though the tumour volume continued to increase; a moderate decrease in luciferase activity was observed in mouse #4, but the luciferase activity in mouse #3 showed a significant decline so that the activity observed on day 42 was similar to that observed on day 7. This reduction in signal could be caused by a necrotic core and reduced blood flow (and consequently substrate delivery) in the larger tumours. Upon sacrifice, H&E staining showed that there was significantly more necrosis in the larger tumours of mice #3 and #4. Dissection also revealed that a cyst-like sac had formed around the E2 pellet in mouse #3.

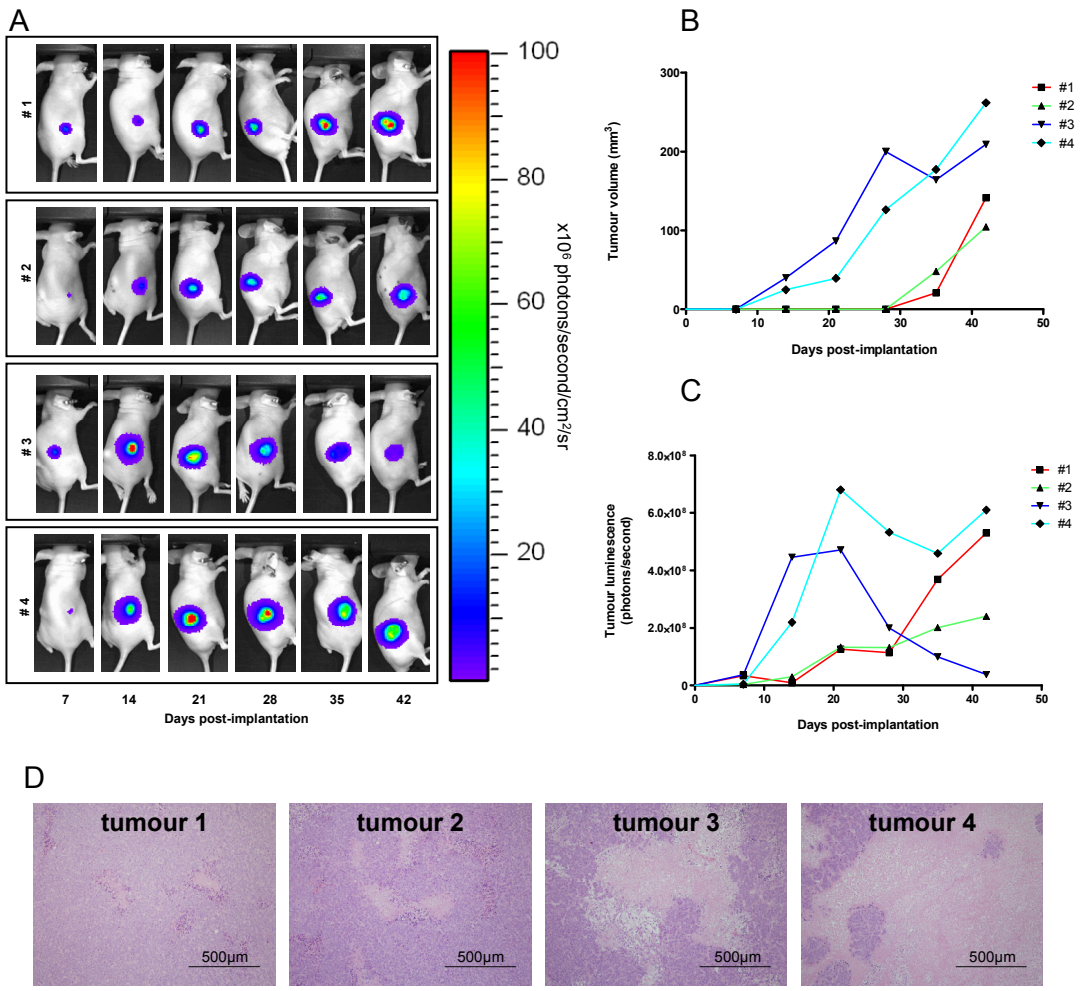

Figure 3.3 - *In vivo* bioluminescence imaging of MELN tumours. $1x10^7$ MELN cells were subcutaneously injected in to the right flank of mice at the same time as E2 pellet implantation in the opposing flank. Tumour development was monitored for 6 weeks by quantifying luminescence with the IVIS 100 (A and C) and by calliper measurements of tumours (B). (D) Representative H&E staining of each tumour is shown.

3.2 Characterisation of NLuc-FRB and FKBP12-CLuc

At the start of the project, I was kindly given a pair of split-luciferase vectors by Professor Sanjiv Gambhir at Stanford University. The plasmids encode FK506 binding protein 1A (FKBP12) and the FKBP12-rapamycin binding (FRB) domain of mammalian target of mTOR fused to N- and C-terminal fragments, respectively, of firefly luciferase (Figure 3.4). FKBP12 and FRB exhibit a strong interaction in the presence of rapamycin; this interaction should bring the N- and C-terminal portions of firefly luciferase into close proximity to allow firefly luciferase reconstitution. Hence, the restored firefly luciferase activity allows appreciation and imaging of protein-protein interaction. The aim of my project was to modify the NLuc-FRB/FKBP12-CLuc split-luciferase to generate an ERα-coregulator interaction assay.

In order to test the FRB-FKBP12 mediated luciferase fragment complementation the constructs were transfected into 293 cells individually and together and the cells were treated with vehicle or $4x10^{-7}$M rapamycin (Figure 3.5). Transfection of the constructs individually showed no luciferase activity in the presence of the substrate luciferin, consistent with the assertion that the luciferase fragments have no enzymatic activity on their own. When the cells were co-transfected with the two constructs, luciferase activity could be detected in the presence and absence of the interaction inducer rapamycin. However, the luciferase activity was stimulated approximately 16-fold in the presence of rapamycin.

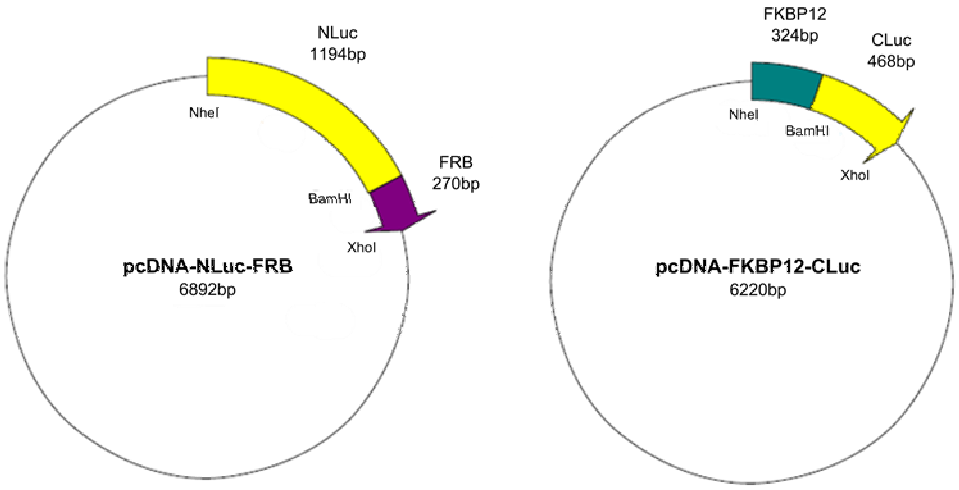

Figure 3.4 - pcDNA-NLuc-FRB and pcDNA-FKBP12-CLuc. The NLuc fragment is 1194 bp in length and encodes amino acids 1-398 of firefly luciferase and is in frame with a 270 bp fragment encoding the 90 amino acid FRB, to give the fusion protein NLuc-FRB. NLuc-FRB is flanked in pcDNA-NLuc-FRB by a 5' *Nhe* I site and a 3' *Xho* I site. There is a *Bam*HI site between the NLuc and FRB coding regions. The CLuc fragment is 468 bp in length and encodes amino acids 395-550 of firefly luciferase. It is cloned in frame with the 324 bp region encoding the 108 amino acids of FKBP12. The fusion construct is flanked by a 5' *Nhe* I site and a 3' *Xho* I site and there is a *Bam*HI site at the boundary of the FKBP12 and CLuc fragments.

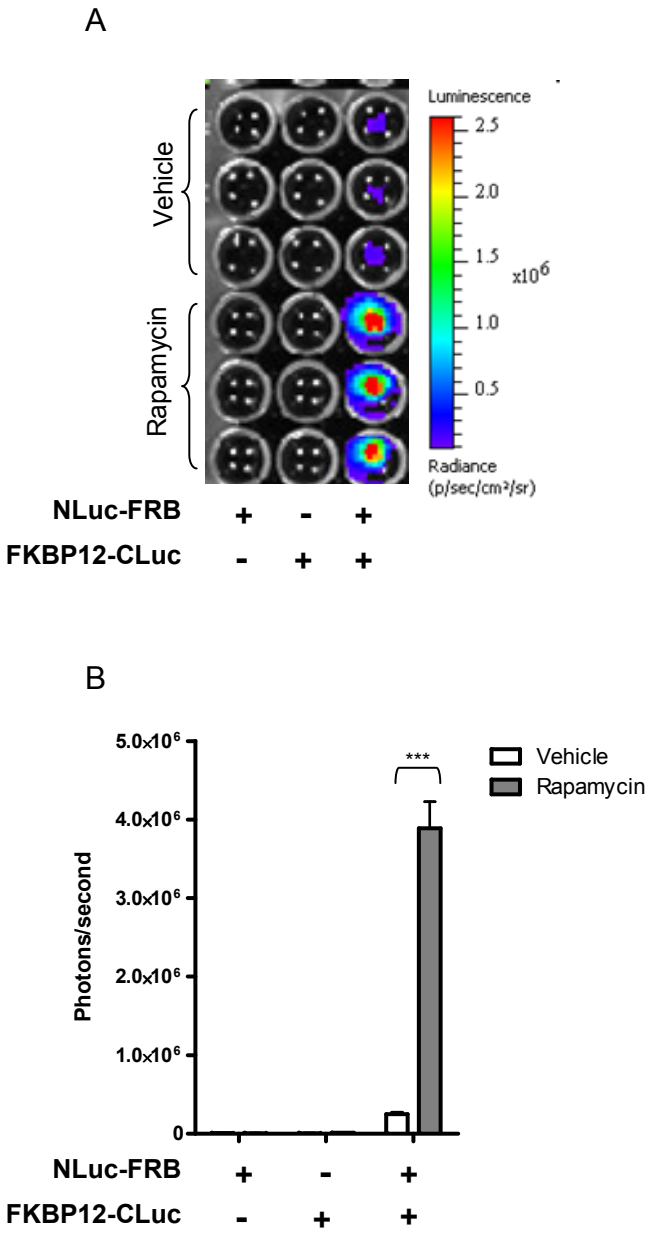

Figure 3.5 - FRB-FKBP12 mediated luciferase fragment complementation. $4x10^4$ 293H cells were transfected with 200ng NLuc-FRB, FKBP12-CLuc or NLuc-FRB and FKBP12-CLuc, as indicated. Cells were treated with vehicle (DMSO) or $4x10^{-7}$M rapamycin for 24 hours prior to quantification of luciferase activity in live cells using the IVIS 100. (A) Captured image. (B) data quantified from ROI measurements showing mean luciferase activities (n = 3). Error bars represent the standard errors of the mean (SEM). A t-test was used to determine statistical significance relative to vehicle treatment (***, $p \leq 0.001$).

3.3 ERα-coregulator split-luciferase assay feasibility study

Having confirmed that the rapamycin-stimulated interaction of FRB and FKBP12 allows the functional reconstitution of split firefly luciferase, I wanted to establish whether luciferase fragment complementation could be used to assay ERα-coregulator interactions. ERα-coregulator interactions are transient and are therefore likely to be considerably weaker than the strong FKBP12-rapamycin-FRB interaction (Banaszynski et al., 2005).

I chose to initially focus on the interaction between ERα and the coactivator AIB1. In order to determine whether it was possible to use split-luciferase complementation to examine ERα-coactivator interactions, the FKBP12 fragment was excised from FKBP12-CLuc and replaced with the ERα ligand binding domain (ER-LBD-CLuc) or full-length ERα (ERα-CLuc) coding sequences. Similarly, the FRB sequences in NLuc-FRB were replaced with the AIB1 nuclear receptor interaction domain (NLuc-AIB-RID), encoded within amino acids 580-839 of human AIB1 (Figure 3.6). As previously discussed the ERα-LBD and AIB-RID fragments have previously been used to demonstrate nuclear receptor-cofactor interactions in fluorescence-based *in vitro* assays (Bramlett et al., 2001, Chang et al., 1999, Kraichely et al., 2000, Liu et al., 2003, Ozers et al., 2005, Zhou et al., 1998).

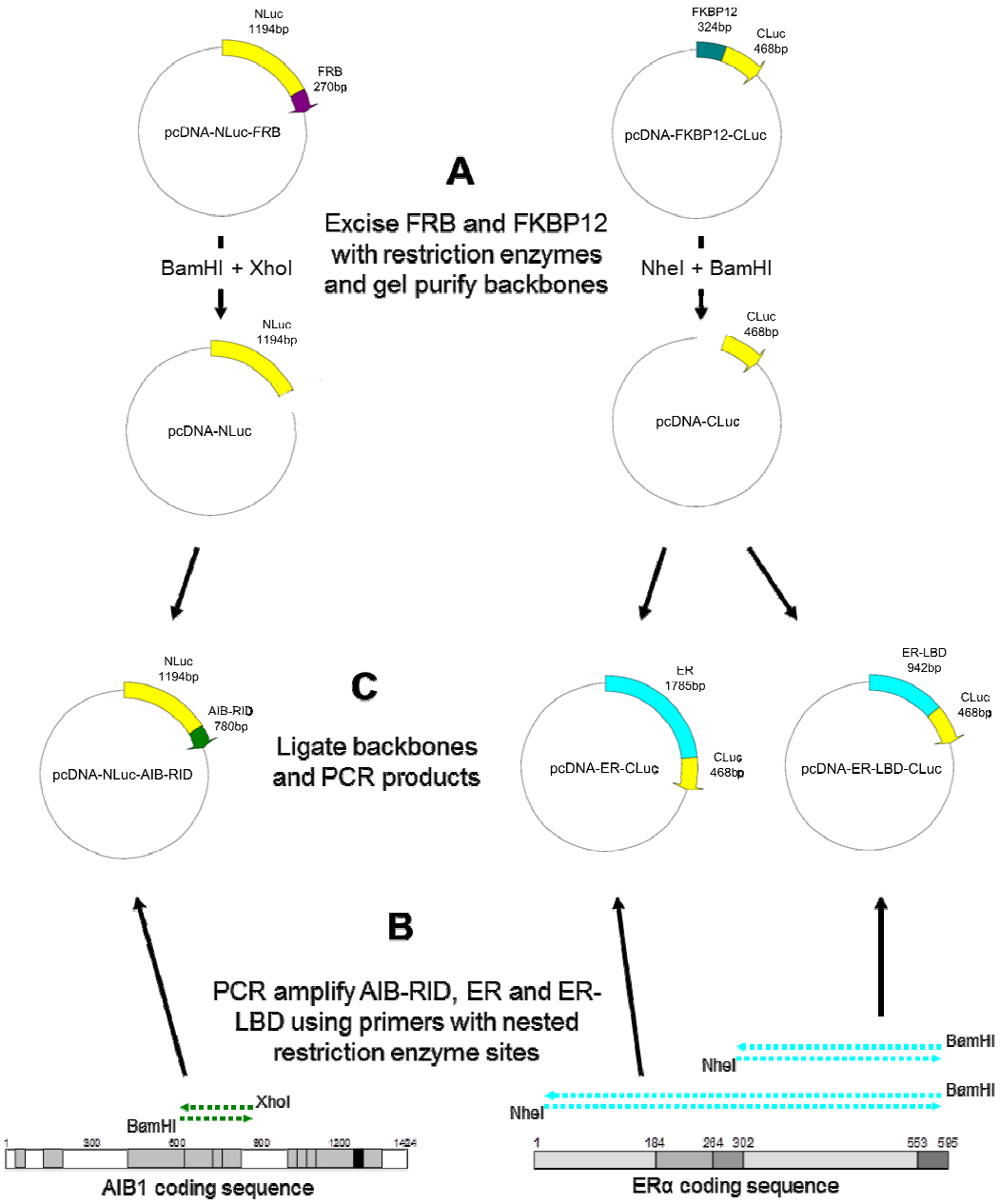

Figure 3.6 - Cloning strategy. (A) FRB and FKBP12 were excised from the appropriate split-luciferase plasmids by restriction enzyme digestion and the backbones were gel purified. (B) The AIB-RID, ER and ER-LBD coding fragments were PCR amplified using primers with appropriate restriction enzyme sites engineered into them. (C) Ligations were performed between the NLuc backbone and AIB-RID PCR product and the CLuc backbone and ER and ER-LBD PCR products.

At this stage, I did not try to produce a full length AIB1 because I wanted to be sure that the assay was capable of detecting transcription factor-coactivator interaction before attempting to express the full-length 160 KDa AIB1 as a fusion with NLuc.

To test for functional reconstitution of NLuc and CLuc through the interaction of ERα and the AIB1 RID, 293H cells were co-transfected with NLuc-AIB-RID together with ER-LBD-CLuc or ER-CLuc, and the cells were treated with 10^{-6}M E2 or vehicle. NLuc-FRB/FKBP12-CLuc plasmids +/- rapamycin were also transfected for comparison (Figure 3.7). As described above, a 15-fold increase in luciferase complementation was observed for NLuc-FRB/FKBP12-CLuc transfected cells treated with rapamycin. Interestingly, cotransfection of NLuc-AIB-RID and ER-LBD-CLuc yielded luciferase activity that was about 30% of the activity obtained for NLuc-FRB/FKBP12-CLuc, suggestive of a strong interaction between the ER-LBD and AIB1. Addition of E2 stimulated the interaction, although there was only a 2-fold stimulation.

By contrast, there was very low luciferase activity in the case of the full length ER-CLuc and NLuc-AIB-RID in the absence of E2. E2 treatment of the NLuc-AIB-RID/ER-CLuc transfected cells did produce a small increase in luciferase activity, but the signal was very low, less than that observed in vehicle treated NLuc-FRB/FKBP12-CLuc transfected cells, suggesting poor interaction between full-length ERα and the AIB-RID or poor transfection or expression of ER-CLuc.

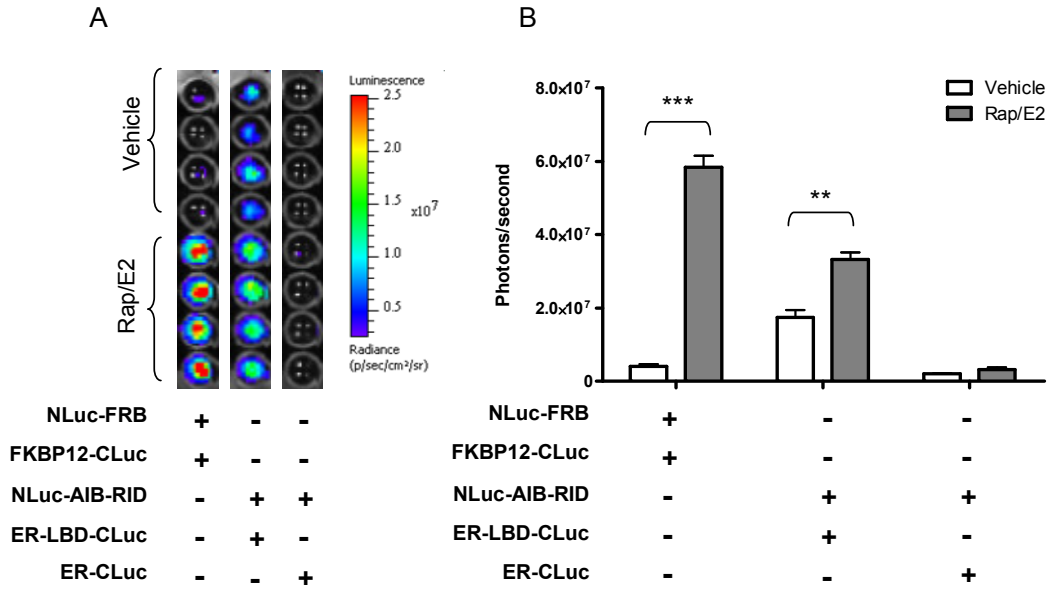

Figure 3.7 - Initial assessment of NLuc-AIB-RID, ER-LBD-CLuc and ER-CLuc. $4x10^4$ 293H cells were transfected with 200ng NLuc-FRB, FKBP12-CLuc, NLuc-AIB-RID, ER-LBD-CLuc and ER-CLuc, as indicated. Cells were treated with vehicle (DMSO), $4x10^{-7}$M rapamycin (NLuc-FRB/FKBP12-CLuc) or 10^{-6}M E2 (NLuc-AIB-RID/ER-LBD-CLuc and NLuc-AIB-RID/ER-CLuc) for 24 hours prior to quantification of luciferase activity in live cells using the IVIS 100. (A) Captured image (B) data quantified from ROI measurements showing mean luciferase activities (n = 3). Error bars represent the standard errors of the mean (SEM). A t-test was used to determine statistical significance (***, $p \leq 0.001$, **, $p \leq 0.01$).

To control for the specificity of the observed increases in luciferase activity for the ER and AIB1 fragments, cells were transfected with NLuc-FRB/ER-LBD-CLuc or NLuc-AIB-RID/FKBP12-CLuc and treated with rapamycin or E2 (Figure 3.8). This experiment was only performed with NLuc-AIB-RID and ER-LBD-CLuc because of the low signal and E2 induction observed with the ER-CLuc constructs.

Treatment of the NLuc-FRB/FKBP12-CLuc transfected cells with rapamycin and NLuc-AIB-RID/ER-LBD-CLuc transfected cells with E2 resulted in similar stimulation of luciferase activity as before. As expected, cells co-transfected with NLuc-FRB/ER-LBD-CLuc showed very little luciferase activity with vehicle, rapamycin or E2 treatment. However, the cells transfected with NLuc-AIB-RID/FKBP12-CLuc showed moderate luciferase activity in the presence of vehicle, rapamycin and DMSO. Furthermore, the activity observed in the NLuc-AIB-RID/FKBP12-CLuc transfected cells appeared to be modulated by ligand treatment; the activity observed with rapamycin was approximately 40% of that observed with DMSO.

Taken together, these findings indicate that it is possible to use the luciferase complementation assay to detect ERα-coregulator interactions, although the magnitude of the complementation, as well as ligand-independent interaction might reduce the utility of such an assay. In order to determine the reasons for the low complementation observed in NLuc-AIB-RID/ER-CLuc transfections, an immunocytochemical analysis of co-transfected 293 cells was performed to determine their cellular localisation (Figure 3.9).

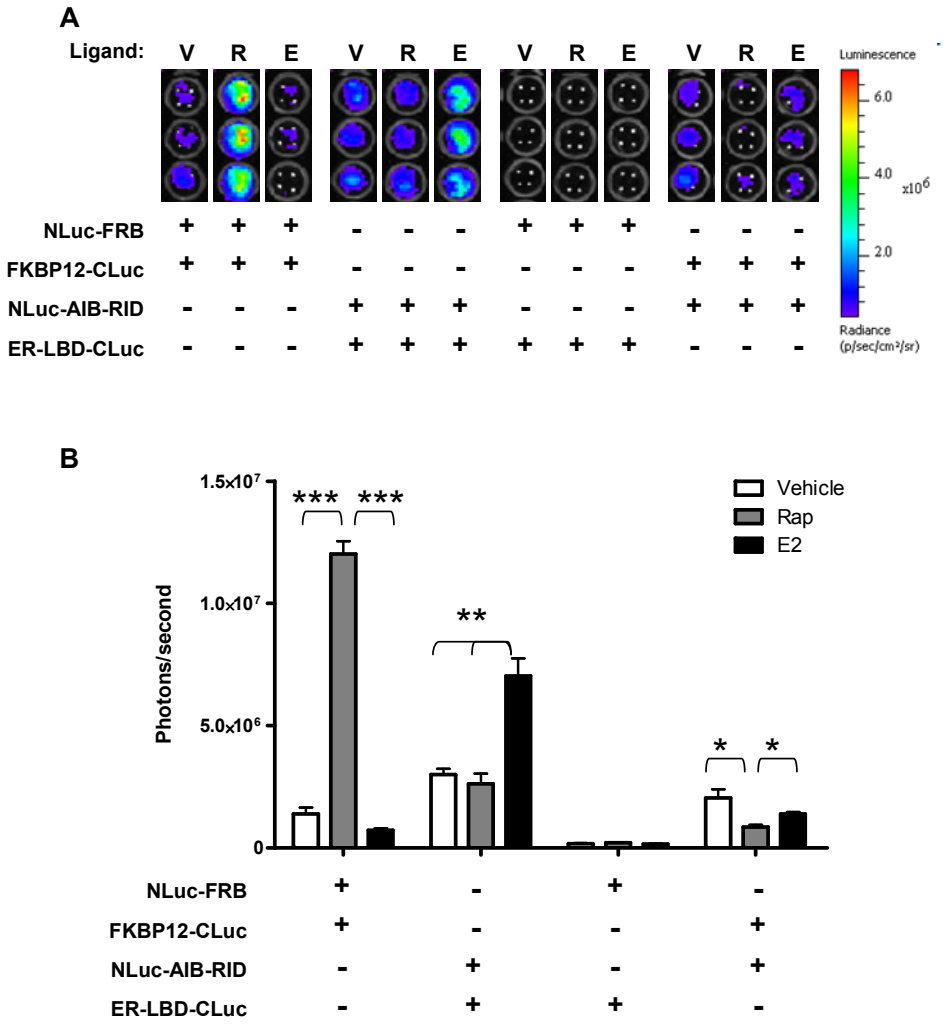

Figure 3.8 - Specificity of rapamycin and E2 induced luciferase fragment complementation. $4x10^4$ 293H cells were transfected with 200ng NLuc-FRB, FKBP12-CLuc, NLuc-AIB-RID, as indicated. Cells were treated with vehicle (DMSO; V), $4x10^{-7}$M rapamycin (R) or 10^{-6}M E2 (E) for 24 hours prior to quantification of luciferase activity in live cells using the IVIS 100. (A) Captured image. (B) Data quantified from ROI measurements showing mean luciferase activities (n = 3). Error bars represent the standard errors of the mean (SEM). The ANOVA test was used to determine statistical significance (***, $p \leq 0.001$, **, $p \leq 0.01$, *, $p \leq 0.05$).

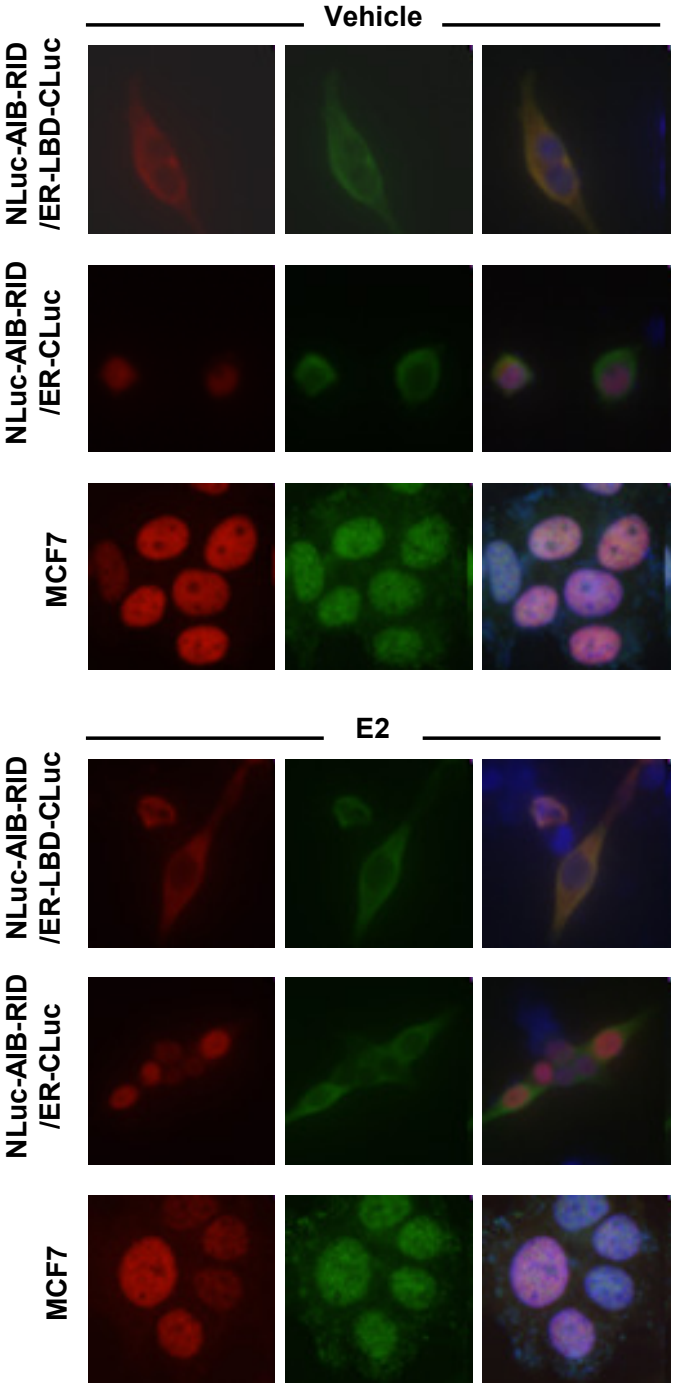

Figure 3.9 - Immunofluorescence of NLuc-AIB-RID, ER-LBD-CLuc, ER-CLuc and endogenous ERα and AIB1. $4x10^4$ 293 cells were seeded in chamber slides prior to transfection with NLuc-AIB-RID/ER-LBD-CLuc or NLuc-AIB-RID/ER-CLuc. Cells were treated with vehicle or 10^{-6}M E2 for 24 hours prior to staining with mouse-anti-ERα/Alexa Fluor 594 antibodies and rabbit anti-AIB1/Alexa Fluor 488 antibodies. Slides were mounted with Prolong Gold Antifade with DAPI. Photographs show ERα (red), AIB1 (green) and a merged image with DAPI stained nuclei (blue). Also shown is the immunofluorescence staining of endogenous ERα and AIB1 in MCF7 cells.

In MCF7 cells, the endogenous ERα and AIB1 are nuclear in both vehicle and E2 treated populations (Figure 3.9). Immunofluorescence staining for ERα and AIB1 in NLuc-AIB-RID/ER-LBD-CLuc transfected cells showed that the luciferase fusion proteins were cytoplasmic in the presence or absence of E2. Although this is different from the localisation of the endogenous proteins, the luciferase fusion proteins are in the same cellular compartment and complementation is therefore possible. However, the ER-CLuc fusion protein, in which the full length ERα is fused to CLuc, was nuclear, thus providing an explanation for the lack of luciferase complementation observed between nuclear ER-CLuc and cytoplasmic NLuc-AIB-RID (Figure 3.9).

Following the immunocytochemical analysis of the fusion protein localization, I chose to continue to develop the truncated AIB-RID and ER-LBD split-luciferase assay while investigating the possibility of producing a full length ERα and AIB1 split-luciferase assay in parallel.

3.4 Truncated ER-LBD-AIB-RID split-luciferase assay

Having established that ER-LBD and AIB-RID luciferase fragment fusion proteins could be used to detect ERα-AIB1 interaction, it was desirable to optimise the assay to maximise its sensitivity. Insertion of a flexible spacer between fusion proteins has previously been proposed to enhance native folding of fusion protein fragments by increasing the distance between, and therefore reducing any steric hindrance between, moieties (Newton et al., 1996, Arai et al., 2001, Arai et al., 2004) To determine whether a flexible spacer would enhance the NLuc-AIB-RID and ER-LBD-CLuc split-luciferase assay, the constructs were modified to include 1 or 2 copies of a glycine rich flexible spacer (Figure 3.10A). The spacer was made of an oligonucleotide encoding 2 repeats of a Gly-Gly-Gly-Gly-Ser sequence and was inserted into the *Bam*HI site between the fusion proteins. Glycine and serine rich flexible spacers have been frequently used to separate fusion proteins in luciferase fragment complementation assays (Kim et al., 2007a, Luker et al., 2004, Stefan et al., 2007, Paulmurugan and Gambhir, 2003).

As shown above, NLuc-AIB-RID and ER-LBD-CLuc interaction was stimulated by the addition of 10^{-6}M E2 (Figure 3.10B). No stimulation was observed with 10^{-9}M E2. The addition of glycine spacers into ER-LBD-CLuc did not greatly influence interaction with NLuc-AIB-RID. Neither did a single glycine spacer in NLuc-AIB-RID aid interaction. However, a double spacer between the NLuc and AIB-RID protein fusions considerably improved complementation, even in the presence of 10^{-9}M E2. The greatest activity was observed with NLuc-SS-AIB-RID and ER-LBD-SS-CLuc.

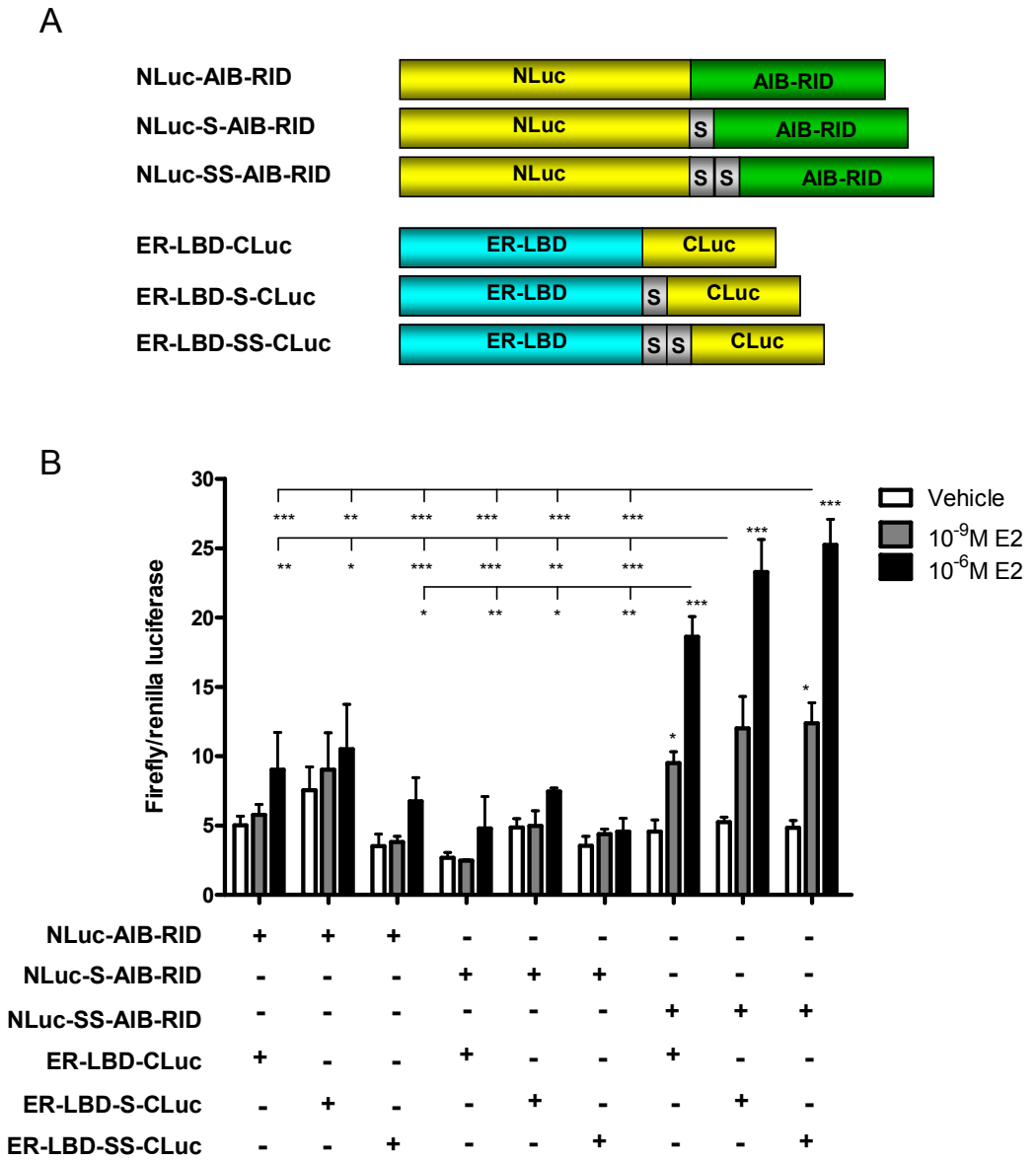

Figure 3.10 - Influence of spacer insertion on NLuc-AIB-RID/ER-LBD-CLuc complementation. NLuc-AIB-RID and ER-LBD-CLuc were modified to contain one (S) or two (SS) copies of a glycine rich flexible spacer (A). (B) $4x10^4$ 293 cells were transfected with 50ng *Renilla* luciferase and 150ng of NLuc-(S/SS)-AIB-RID/ER-LBD-(S/SS)-CLuc as indicated. Cells were treated with vehicle (ethanol; V), 10^{-9}M or 10^{-6}M E2 for 48 hours prior to quantification of luciferase activities. Mean firefly luciferase activities (n = 3) normalized to *Renilla* luciferase activities are shown. Error bars represent the standard errors of the mean (SEM). The ANOVA test was used to determine statistical significance. Asterisks above columns indicate differences +/- E2 are significant, asterisks on horizontal bars indicate that mean of 10^{-6}M E2 treated cells is significantly different (***, $p \leq 0.001$, **, $p \leq 0.01$, *, $p \leq 0.05$).

To further optimize the ER-LBD/AIB-RID split-luciferase assay, the impact of altering the protein-luciferase fragment fusions was investigated. Previous studies have indicated that the relative orientation of protein fragments within a fusion can have a significant impact on reporter fragment complementation (Paulmurugan and Gambhir, 2007). Accordingly, NLuc-ER-LBD and AIB-RID-CLuc fusion protein constructs were generated and 1 or 2 copies of the glycine rich flexible spacer were inserted between the fusions (Figure 3.11A).

Transfection of 293 cells indicated that altering the orientation of the fusion proteins had a major impact on the E2 stimulated luciferase fragment complementation; incubation of cells transfected with NLuc-ER-LBD/AIB-RID-CLuc led to a 9-fold stimulation in luciferase activity in the presence of 10^{-6}M E2 (Figure 3.11). The sensitivity of the split-luciferase assay to the lower 10^{-9}M E2 was also much greater in this orientation. NLuc-ER-LBD/AIB-RID-CLuc transfected cells treated with 10^{-9}M E2 showed a 6-fold increase in activity, which was 75% of the maximum signal observed with this construct pair.

Of note, the signal intensity in NLuc-(S/SS)-ER-LBD/AIB-RID-(S/SS)-CLuc transfected cells was 10-fold less than in NLuc-(S/SS)-AIB-RID/ER-LBD-(S/SS)-CLuc transfections (Figure 3.11B versus Figure 3.10B).

Insertion of flexible spacers into NLuc-ER-LBD did not greatly influence the complementation observed with vehicle or E2. However, inserting one or two copies of the flexible spacer into AID-RID-CLuc increased the complementation observed

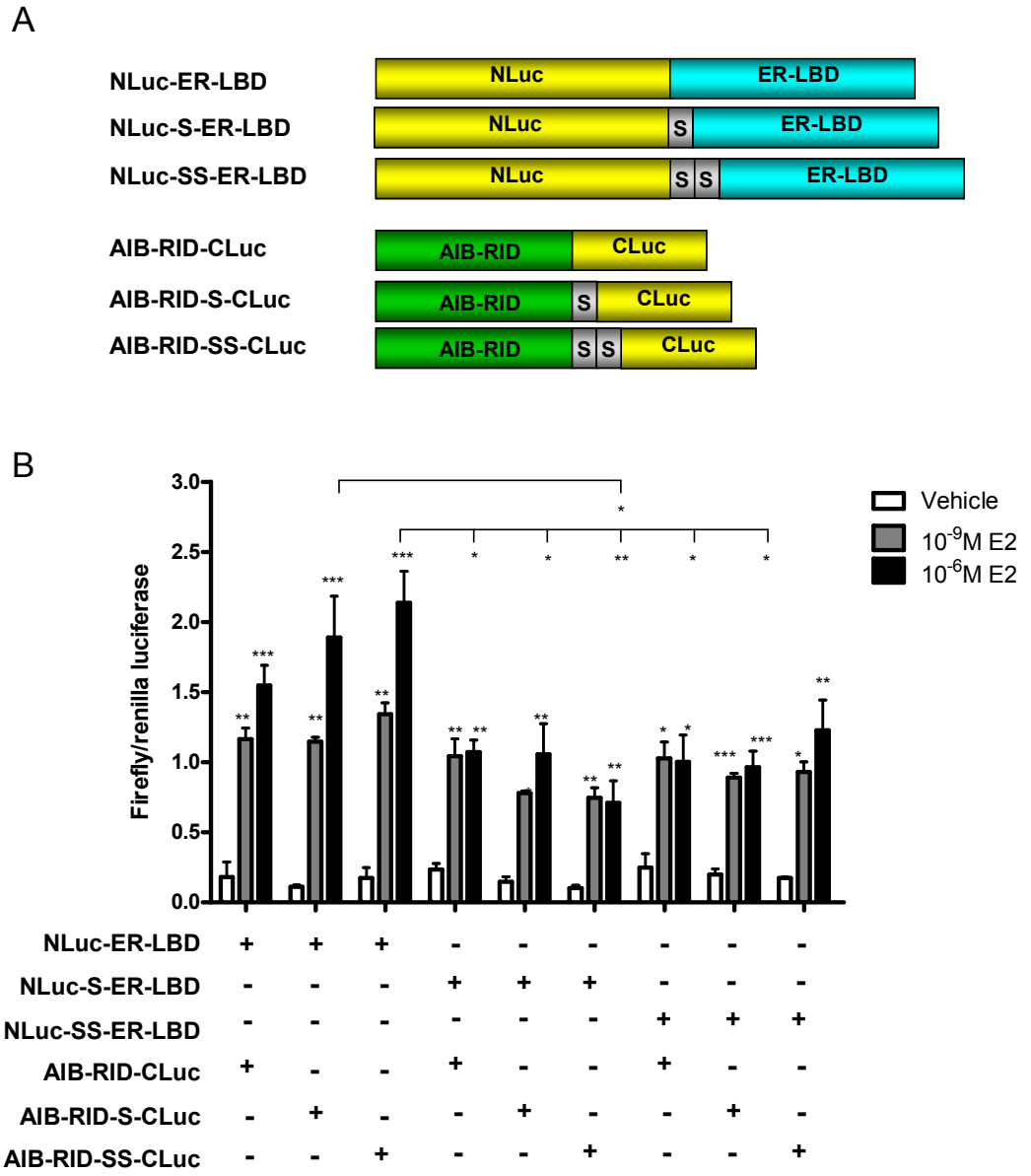

Figure 3.11 - NLuc-ER-LBD/AIB-RID-CLuc complementation and the impact of spacer insertion. NLuc-ER-LBD and AIB-RID-CLuc constructs were produced and modified to contain one (S) or two (SS) copies of a glycine rich flexible spacer (A). (B) $4x10^4$ 293 cells were transfected with 50ng *Renilla* luciferase and 150ng of NLuc-(S/SS)-ER-LBD/AIB-RID-(S/SS)-CLuc as indicated. Cells were treated with vehicle (ethanol; V), 10^{-9}M or 10^{-6}M E2 for 48 hours prior to quantification of luciferase activities. Mean firefly luciferase activities (n = 3) normalized to *Renilla* luciferase activities are shown. Error bars represent the standard errors of the mean (SEM). The ANOVA test was used to determine statistical significance. Asterisks above columns indicate differences +/- E2 are significant, asterisks on horizontal bars indicate that mean of 10^{-6}M E2 treated cells is significantly different (***, $p \leq 0.001$, **, $p \leq 0.01$, *, $p \leq 0.05$).

with 10^{-6}M E2. This effect was only seen with NLuc-ER-LBD; in cotransfections with NLuc-S-ER-LBD or NLuc-SS-ER-LBD, spacer insertion into AIB-RID-CLuc had little impact on the complementation observed.

In order to maximise the sensitivity of the ER-LBD/AIB-RID split-luciferase assay, I selected the construct pair with the greatest fold difference between signal states; NLuc-ER-LBD/AIB-RID-SS-CLuc transfected cells produced the largest fold increase in luciferase activity when treated with E2, more than a 10-fold increase in signal was observed with 10^{-6}M E2 compared to vehicle. However, the relatively low overall signal intensity with this construct pair might be problematic for *in vivo* imaging and for this reason NLuc-SS-ER-LBD/AIB-RID-SS-CLuc were also further characterised, as they represented the construct pair which provided the greatest overall luminescence.

Initially, a more comprehensive E2 titration on NLuc-SS-AIB-RID/ER-LBD-SS-CLuc and NLuc-ER-LBD/AIB-RID-SS-CLuc transfected cells was undertaken (Figure 3.12). Both split-luciferase construct pairs showed a dose dependent increase in luciferase activity with E2 treatment. Near maximal stimulation was observed in the presence of 10^{-8}M E2, with only small increases being observed at higher concentrations. As previously observed, the NLuc-ER-LBD/AIB-RID-SS-CLuc transfected cells appeared to be more sensitive to low concentrations of E2 than the NLuc-SS-AIB-RID/ER-LBD-SS-CLuc transfected cells; a 2-fold induction was observed in presence of 10^{-10}M E2 whereas the NLuc-SS-AIB-RID/ER-LBD-SS-CLuc transfected cells showed no discernable difference in activity at this E2

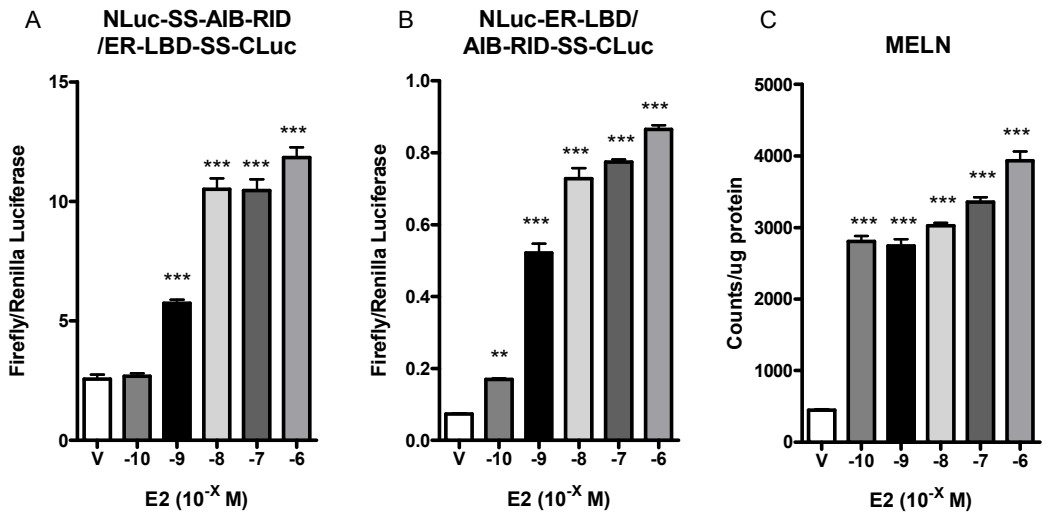

Figure 3.12 - E2 response of ER-LBD/AIB-RID split-luciferase constructs. $4x10^4$ 293 cells were transfected with 50ng *Renilla* luciferase and 150ng of NLuc-SS-AIB-RID, ER-LBD-SS-CLuc, NLuc-ER-LBD and AIB-RID-SS-CLuc, as indicated, in 96 well plates. $1.5x10^4$ MELN cells were seeded into 96 well plates. Cells were treated with vehicle (ethanol; V) or a range of E2 concentrations for 48 hours prior to quantification of luciferase activities. Mean firefly luciferase activity is shown normalised to *Renilla* luciferase activity (A+B) or protein concentration (C). Error bars represent the standard errors of the mean (SEM). The ANOVA test was used to determine statistical significance relative to vehicle treatment (***, $p \leq 0.001$, **, $p \leq 0.01$).

concentration. As a comparison, the MELN cell line also exhibited a dose dependent increase in luciferase activity, but was more sensitive to low concentrations of E2 than either of the split-luciferase construct pairs; the MELN cell line showed more than 70% of maximal activity after incubation with 10^{-10}M E2.

To further validate the ligand-dependent interaction between the ERα LBD and the AIB1 RID, the ERα LBD was mutated to replace the tyrosine residue at position 537 with a serine residue (Y537S) to produce a mutant receptor that is reported to be constitutively active (Weis et al., 1996, White et al., 1997). In a second mutant the leucine residues at positions 539 and 540 were mutated to alanine (L539/40A) to produce a receptor that is incapable of interacting with AIB1 (Danielian et al., 1992, Bai and Giguere, 2003).

Transfection of the mutant constructs with their complementary AIB-RID constructs, produced results consistent with the assay premise that luciferase fragment complementation is driven by the ER-LBD and AIB-RID fragments (Figure 3.13). Transfection of the constitutively active Y537S mutant produced high levels of luciferase activity, in the absence and presence of E2 treatment, consistent with the described constitutive activity of the Y537S mutant and showing sustained interaction with the coactivator AIB1. Mutation of the leucine residues (L539/40A) prevented the interaction of the ER-LBD and AIB-RID, and low luciferase activity was observed in the presence and absence of E2. Western blot of cell lysates confirmed that the observed effects were not attributable to different levels of the proteins in cells.

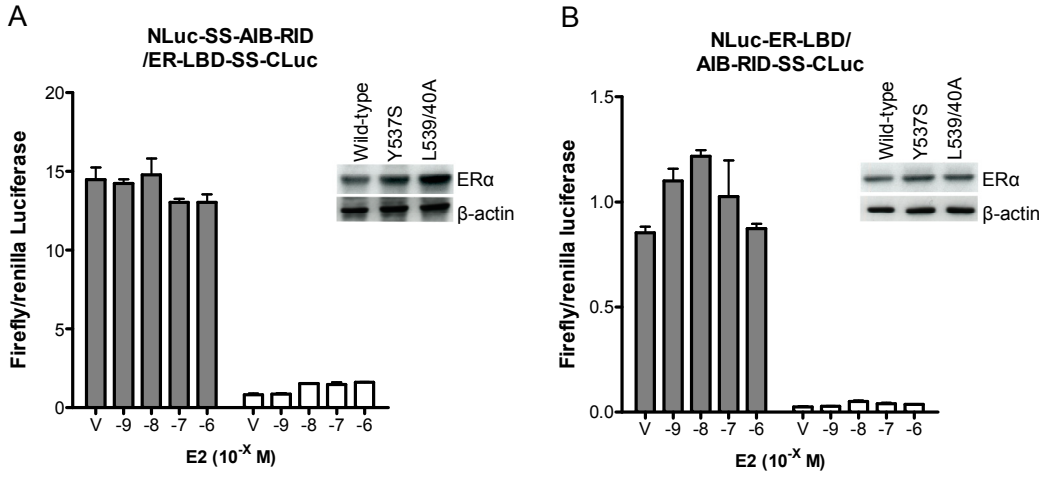

Figure 3.13 - Y537S and L539/40A ER-LBD split-luciferase constructs. $4x10^4$ 293 cells were seeded in 96 wells plates and transfected with 50ng *Renilla* luciferase and 150ng of NLuc-SS-AIB-RID/ER-LBD-SS-CLuc (A) or NLuc-ER-LBD/AIB-RID-SS-CLuc (B). Shown are the activities in the presence of increasing concentrations of E2, or in the absence of ligand (vehicle control; V) for the Y537S (grey bars) or L539A/L540A (white bars) mutants of the ER-LBD. Cells were treated with vehicle (ethanol; V) or E2 for 48 hours prior to quantification of luciferase activities. Mean firefly luciferase activities (n = 3) normalized to *Renilla* luciferase activities are shown. Error bars represent the standard errors of the mean (SEM). Inset shows western blots for ERα and β-actin of cells transfected with wildtype, Y537S or L539A/L540A ER-LBD-SS-CLuc and NLuc-ER-LBD fusion proteins.

Having established the specificity of the E2 induced luciferase fragment complementation, the effect of the antiestrogens OHT and ICI was investigated (Figure 3.14). As expected, both inhibitors produced a dose dependent decrease in luciferase activity. This was very similar to the results obtained for the MELN cell line, which showed luciferase activity below vehicle levels when treated with antiestrogens at concentrations of 10^{-7}M or 10^{-6}M (Figure 3.2).

Western blot analysis of lysates from 293 cells transfected with either NLuc-SS-AIB-RID/ER-LBD-SS-CLuc or NLuc-ER-LBD/AIB-RID-SS-CLuc showed that levels of neither the ER-LBD nor the AIB-RID fusion proteins were significantly altered with ligand treatment (Figure 3.15).

To further characterise the luciferase complementation, a time-course of activity was carried out using 293 cells transfected with NLuc-SS-AIB-RID/ER-LBD-SS-CLuc or NLuc-ER-LBD/AIB-RID-SS-CLuc or MELN cells, which were treated with 10^{-6}M E2 for increasing periods of time, up to a maximum of 48 hours (Figure 3.16). The results show that the split-luciferase transfected cells exhibit a near maximal response to E2 within two hours. The protein fragment complementation-dependent signal from the split-luciferase reporters was observed sooner than the transcription-dependent luciferase signal in the MELN cells in response to E2. However, there were small differences between the two split-luciferase construct pairs; the NLuc-SS-AIB-RID/ER-LBD-SS-CLuc transfected cells produced 60% of maximal activity after 2 hours E2 incubation whereas the NLuc-ER-LBD/AIB-RID-SS-CLuc transfected cells appeared slightly more sensitive to E2 and produced 80% of their maximal activity after 2 hours of E2 incubation.

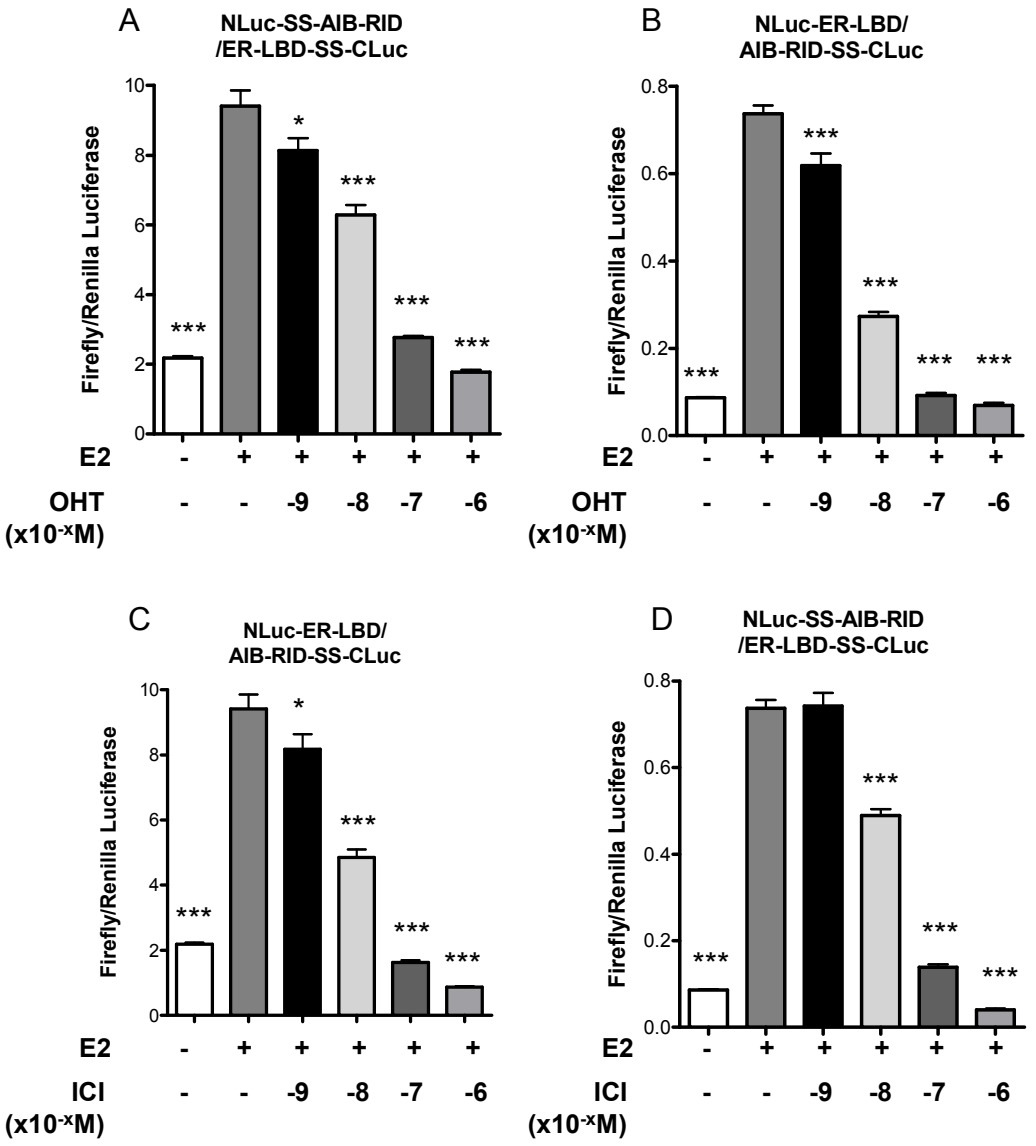

Figure 3.14 - Modulation of ER-LBD/AIB-RID split-luciferase E2 response by OHT and ICI. 4x10^4 293 cells were transfected with 50ng *Renilla* luciferase and 150ng of NLuc-SS-AIB-RID/ER-LBD-SS-CLuc (A+C) or NLuc-ER-LBD/AIB-RID-SS-CLuc (B+D) in 96 well plates. Cells were treated with ethanol, 10^{-9}M E2 or 10^{-9}M E2 and a range of OHT (A+B) or ICI (C+D) concentrations for 48 hours prior to quantification of luciferase activities. Mean firefly luciferase activities (n = 3) normalized to *Renilla* luciferase activities are shown. Error bars represent the standard errors of the mean (SEM). The ANOVA test was used to determine statistical significance relative to E2 treatment (***, $p \leq 0.001$, **, $p \leq 0.01$, *, $p \leq 0.05$).

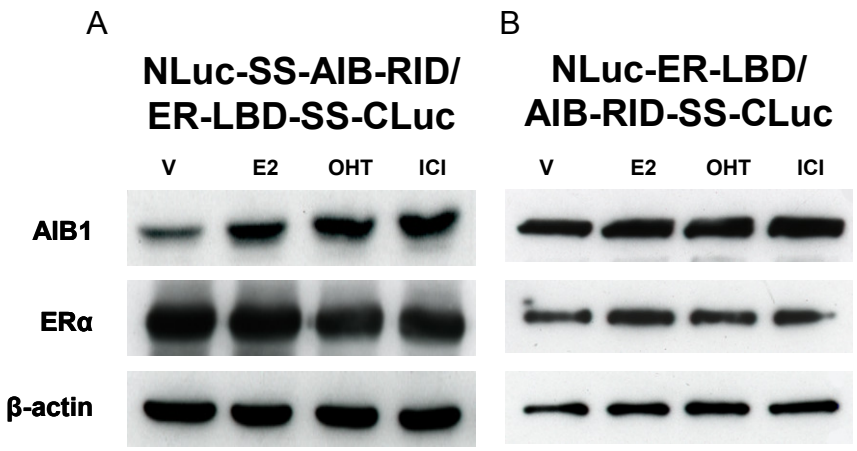

Figure 3.15 - Expression of ER-LBD and AIB-RID fusion proteins in E2, OHT and ICI treated cells. Protein lysates prepared from 293 cells transfected with NLuc-SS-AIB-RID/ER-LBD-SS-CLuc (A) or NLuc-ER-LBD/AIB-RID-SS-CLuc (B) cells treated with vehicle (ethanol; V), 10^{-6}M E2, 10^{-6}M OHT or 10^{-6}M ICI were separated by SDS-PAGE and immunoblotted using AIB1, ERα or β-actin antibodies.

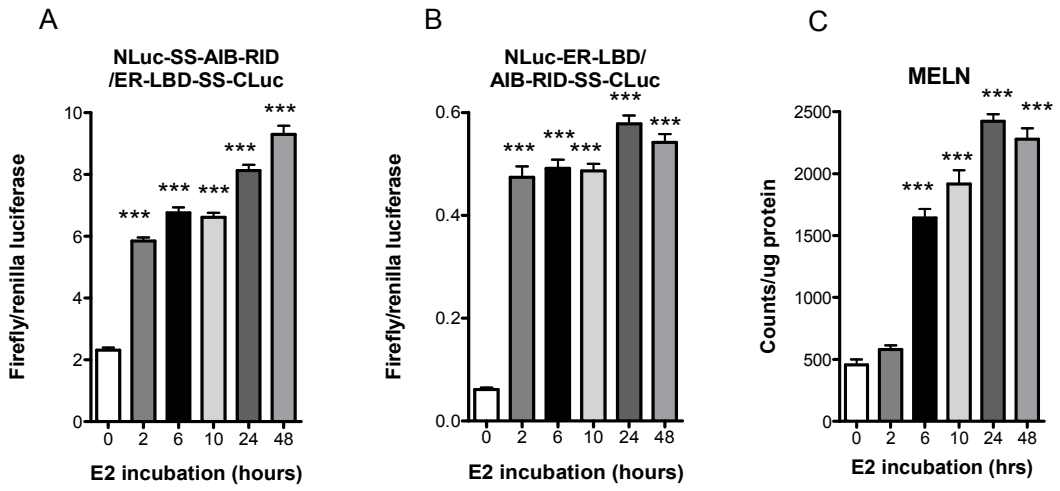

Figure 3.16 - Time-course of E2 response in ER-LBD/AIB-RID split-luciferase transfected and MELN cells. $4x10^4$ 293 cells were transfected with 50ng *Renilla* luciferase and 150ng of NLuc-SS-AIB-RID/ER-LBD-SS-CLuc (A) or NLuc-ER-LBD/AIB-RID-SS-CLuc (B) in 96 well plates. $1.5x10^4$ MELN cells were seeded into 96 well plates (C). At given times, vehicle (ethanol) or E2 was added to wells to a final concentration of 10^{-6}M. Mean luciferase activities (n = 3) are shown, normalized to *Renilla* luciferase activity (A+B) or total protein (C). Error bars represent the standard errors of the mean (SEM). The ANOVA test was used to determine statistical significance relative to vehicle treatment (***, $p \leq 0.001$, **, $p \leq 0.01$, *, $p \leq 0.05$).

A further time-course investigation showed that both split-luciferase construct pairs produced a discernable response to E2 within 15 minutes of ligand addition; a 1.5-fold and 2.4-fold increase in signal was observed for NLuc-SS-AIB-RID/ER-LBD-SS-CLuc and NLuc-ER-LBD/AIB-RID-SS-CLuc transfected cells respectively (Figure 3.17).

To determine whether antiestrogens can inhibit the E2-stimulated ER-LBD-AIB-RID interaction, 293 cells were transfected with the NLuc-SS-AIB-RID/ER-LBD-SS-CLuc or NLuc-ER-LBD/AIB-RID-SS-CLuc and luciferase fragment complementation was stimulated with 10^{-9}M E2 for 24 hours. 10^{-6}M OHT was subsequently added for different durations to determine whether the complemented luciferase activity was affected (Figure 3.18). Both split-luciferase pairs showed a decrease in the E2 signal after 2 hours OHT incubation, although the degree of signal inhibition differed; 20% and 50% signal reduction was observed in NLuc-SS-AIB-RID/ER-LBD-SS-CLuc and NLuc-ER-LBD/AIB-RID-SS-CLuc respectively. After 2 hours, the signal in the NLuc-ER-LBD/AIB-RID-SS-CLuc transfected cells continued to decline rapidly in response to OHT; 4 hours OHT incubation reduced the signal to a little over that observed with vehicle and full signal ablation occurred after just 6 hours.

The signal in the NLuc-SS-AIB-RID/ER-LBD-SS-CLuc transfected cells declined more slowly; a 50% decrease was observed after 4 hours but full signal ablation required between 10 and 24 hours incubation. The MELN luciferase signal was much slower to decline; no difference was seen after 2 hours, a 35% reduction was achieved

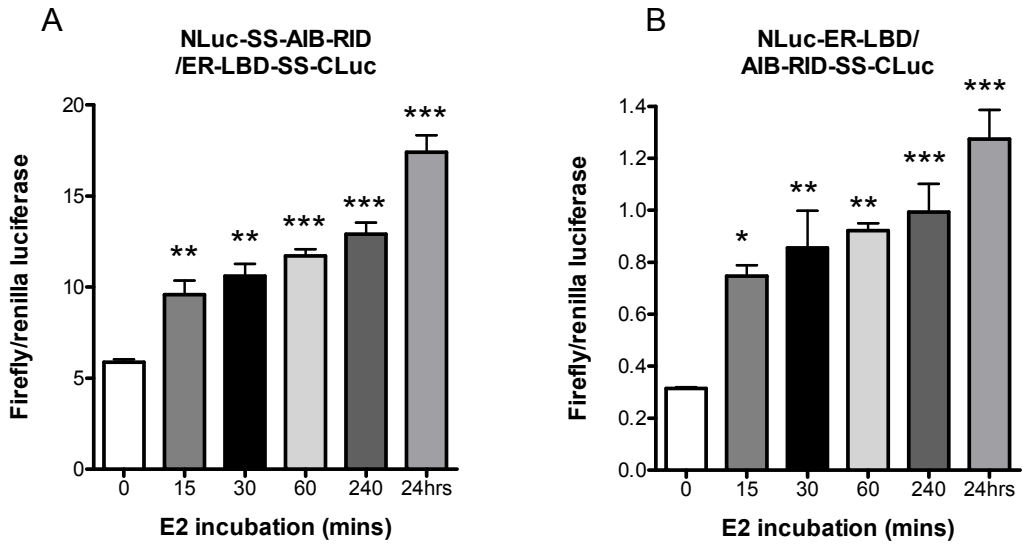

Figure 3.17 - Minute time-course of E2 response in ER-LBD/AIB-RID split-luciferase constructs. $4x10^4$ 293 cells were transfected with 50ng *Renilla* luciferase and 150ng of NLuc-SS-AIB-RID/ER-LBD-SS-CLuc (A) or NLuc-ER-LBD/AIB-RID-SS-CLuc (B) in 96 well plates. At given times, vehicle (ethanol) or 10^{-6}M E2 was added to wells. Mean firefly luciferase activities (n = 3) normalized to *Renilla* luciferase activities are shown. Error bars represent the standard errors of the mean (SEM). The ANOVA test was used to determine statistical significance relative to vehicle treatment (***, $p \leq 0.001$, **, $p \leq 0.01$, *, $p \leq 0.05$).

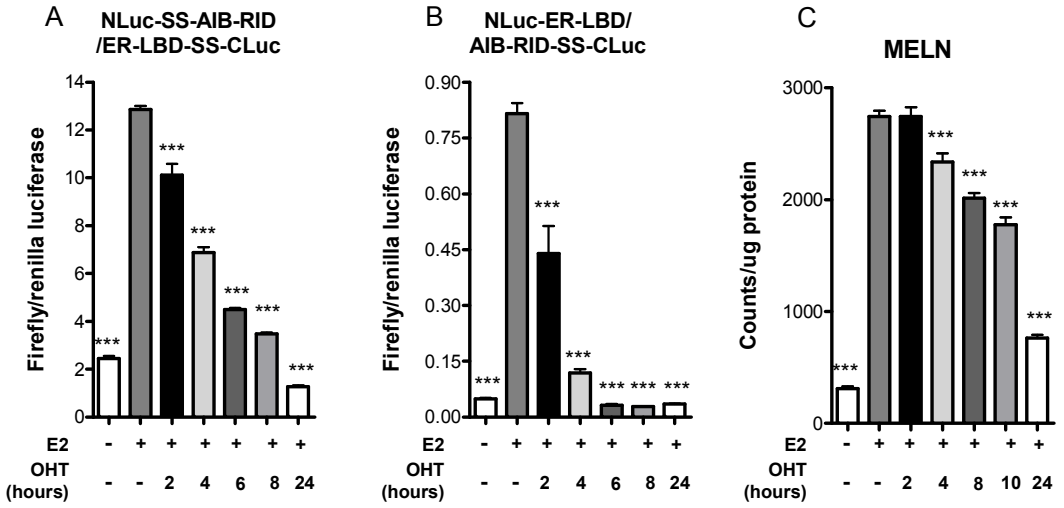

Figure 3.18 - Time-course of E2 signal ablation in ER-LBD/AIB-RID split-luciferase transfected and MELN cells. $4x10^4$ 293 cells were transfected with 50ng *Renilla* luciferase and 150ng of NLuc-SS-AIB-RID/ER-LBD-SS-CLuc (A) or NLuc-ER-LBD/AIB-RID-SS-CLuc (B) in 96 well plates. $1.5x10^4$ MELN cells were seeded into 96 well plates (C). After 24 hours incubation with 10^{-9}M E2, vehicle (ethanol) or 10^{-6}M OHT was added to wells for different periods of time. Mean firefly luciferase activities (n = 3) is shown normalised to *Renilla* luciferase activity (A+B) or protein concentration (C). Error bars represent the standard errors of the mean (SEM). The ANOVA test was used to determine statistical significance relative to E2 treatment (***, $p \leq 0.001$, **).

after 10 hours and after 24 hours OHT incubation the signal still had not reduced to vehicle levels.

I proceeded to perform a minute time-course of signal ablation with the NLuc-SS-AIB-RID/ER-LBD-SS-CLuc and NLuc-ER-LBD/AIB-RID-SS-CLuc transfected cells (Figure 3.19). Results collected from both the split-luciferase constructs indicated a reduction in luciferase fragment complementation within 15 minutes of OHT addition. The NLuc-SS-AIB-RID/ER-LBD-SS-CLuc constructs showed almost 20% signal reduction while the NLuc-ER-LBD/AIB-RID-SS-CLuc transfected cells showed just over 30% signal reduction, although the signal in these cells was greater at the 30 and 60 minute time points.

There were, however, some inconsistencies in the results collected in the 'minute' time-course experiment. The fold induction observed with E2 alone was less than that observed in previous experiments; 2.4-fold and 4-fold for NLuc-SS-AIB-RID/ER-LBD-SS-CLuc and NLuc-ER-LBD/AIB-RID-SS-CLuc transfected cells respectively. Furthermore, the signal reduction observed after 2 and 4 hours in the minute time-course (Figure 3.19) was less than that observed in the hour time-course (Figure 3.18). The NLuc-SS-AIB-RID/ER-LBD-SS-CLuc transfected cells showed 25% signal reduction after 2 hours OHT incubation in the minute time-course, compared to almost 50% reduction in the hour time-course experiment. Similarly, the NLuc-ER-LBD/AIB-RID-SS-CLuc transfected cells showed 35% and 65% signal reduction after 2 and 4 hours OHT incubation in the minute time-course experiment compared to 50% and 85% reduction in the hour time-course experiment.

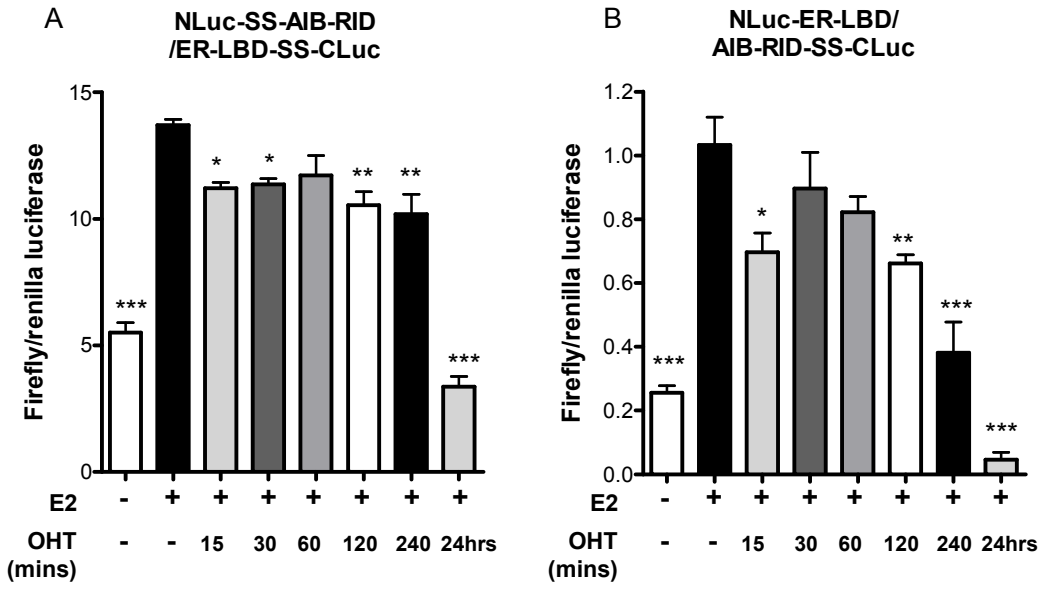

Figure 3.19 - Minute time-course of E2 signal ablation in ER-LBD/AIB-RID split-luciferase constructs. $4x10^4$ 293 cells were transfected with 50ng *Renilla* luciferase and 150ng of NLuc-SS-AIB-RID/ER-LBD-SS-CLuc (A) or NLuc-ER-LBD/AIB-RID-SS-CLuc (B) in 96 well plates. After 24 hours incubation with 10^{-9}M E2, vehicle (ethanol) or 10^{-6}M OHT was added to wells for different periods of time. Mean firefly luciferase activities (n = 3) normalized to *Renilla* luciferase activities are shown. Error bars represent the standard errors of the mean (SEM). The ANOVA test was used to determine statistical significance relative to E2 treatment (***, $p \leq 0.001$, **, $p \leq 0.01$, *, $p \leq 0.05$).

Although I had obtained some unexpected results, the ER-LBD/AIB-RID split-luciferase constructs appeared to be showing much promise as a method for reporting on ER-AIB interaction and ERα activity, and so I chose to examine the ability to modulate their activity *in vivo* in xenograft models. To allow direct comparison of the two split-luciferases *in vivo*, NLuc-SS-AIB-RID/ER-LBD-SS-CLuc and NLuc-ER-LBD/AIB-RID-SS-CLuc transiently transfected 293 cells were implanted into each mouse on opposing flanks (Figure 3.20A). The number of cells implanted was adjusted to minimise differences in signal between the reporters. Mice had E2 or placebo pellets implanted 5 days previously and were treated with ICI or placebo immediately after cell implantation and again 20 hours later. Luciferase activity was quantified 24 hours after cell implantation (Figure 3.20 B and C).

The results show that an E2 induced increase in luciferase activity could be observed with both NLuc-SS-AIB-RID/ER-LBD-SS-CLuc and NLuc-ER-LBD/AIB-RID-SS-CLuc transfected cells *in vivo*. No luciferase activity above background levels was discernable in the double placebo treated mice whereas E2 treatment produced ROI readings of $1.6x10^5$ and $5x10^4$ photons/second in NLuc-SS-AIB-RID/ER-LBD-SS-CLuc and NLuc-ER-LBD/AIB-RID-SS-CLuc cell populations, respectively. The signal in mice treated with E2 and ICI was less in both cell populations, although the degree of reduction differed considerably. The NLuc-ER-LBD/AIB-RID-SS-CLuc transfected cells showed a moderate 20% decrease in signal whereas the NLuc-SS-AIB-RID/ER-LBD-SS-CLuc transfected cells showed 80% decrease in activity. Most unexpectedly, the greatest luciferase activity with both reporters was observed in mice treated with ICI and placebo pellets. This could be a reflection of ICI performing as a

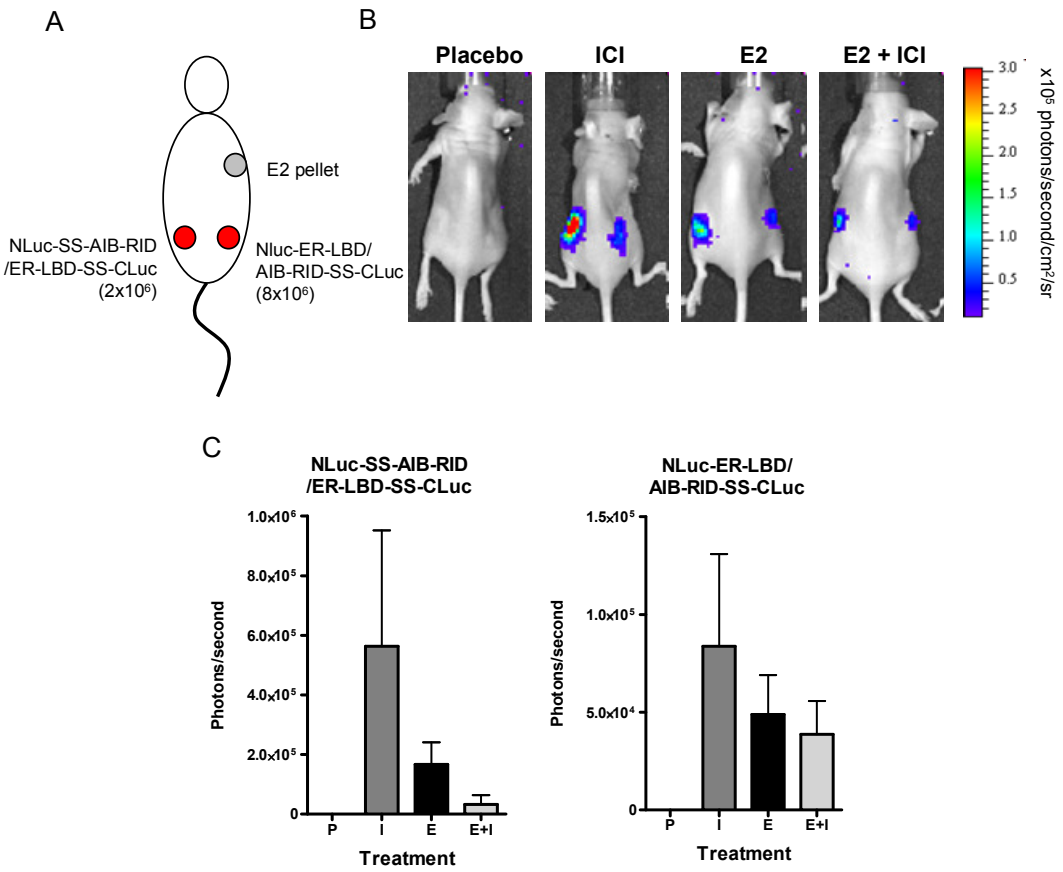

Figure 3.20– *In vivo* modulation of ER-LBD/AIB-RID split-luciferases by E2 and ICI. $2x10^6$ NLuc-SS-AIB-RID/ER-LBD-SS-CLuc and $8x10^6$ NLuc-ER-LBD/AIB-RID-CLuc transfected cells were subcutaneous injected into the left and right flank of nude mice (A) that had 0.72mg/60 day E2 or placebo pellets implanted 5 days previously. Mice were treated with 5mg ICI or peanut oil placebo by subcutaneous injection immediately after cell implantation and again 20 hours later. 24 hours after cell implantation, mice were imaged using the IVIS 100. Representative images (B) and quantified data (C) are shown for each treatment and cell line (n=5; error bars are SEM). P = placebo, I = ICI, E = E2, E+I = E2 and ICI.

E2 agonist, as previously demonstrated in bone and neuronal cells (Sibonga et al., 1998, Zhao et al., 2006).

I proceeded to examine whether I could achieve modulation of the E2 signal by OHT *in vivo*. Once again, NLuc-SS-AIB-RID/ER-LBD-SS-CLuc and NLuc-ER-LBD/AIB-RID-SS-CLuc transfected cells were injected into opposing flanks, but this time MELN cells were also injected into the scruff of the mice (Figure 3.21A). The mice had E2 or placebo and 2x5mg OHT or placebo pellets implanted 5 days previous. Luciferase activity in mice was imaged 24 hours after cell implantation (Figure 3.21B and C).

Though the same quantity of NLuc-SS-AIB-RID/ER-LBD-SS-CLuc and NLuc-ER-LBD/AIB-RID-SS-CLuc transfected cells were injected as in the ICI *in vivo* experiment, in this experiment double placebo treated mice showed luciferase activity well above background levels. However, the signal with E2 treatment was also much higher in this experiment, 60- and 52-fold that observed in the ICI *in vivo* experiment for the NLuc-SS-AIB-RID/ER-LBD-SS-CLuc and NLuc-ER-LBD/AIB-RID-SS-CLuc constructs, respectively.

For both the split-luciferase reporters, approximately a 7-fold increase in luciferase activity was observed with E2 versus placebo treatment *in vivo*, this compares to an average of 4- and 10-fold *in vitro* for the NLuc-SS-AIB-RID/ER-LBD-SS-CLuc and NLuc-ER-LBD/AIB-RID-SS-CLuc constructs. The MELN cells showed more than 20-fold E2 signal induction *in vivo*, which compares to an average of 4-5 fold *in vitro*. The MELN signal in the E2 and OHT treated mice was approximately half that seen

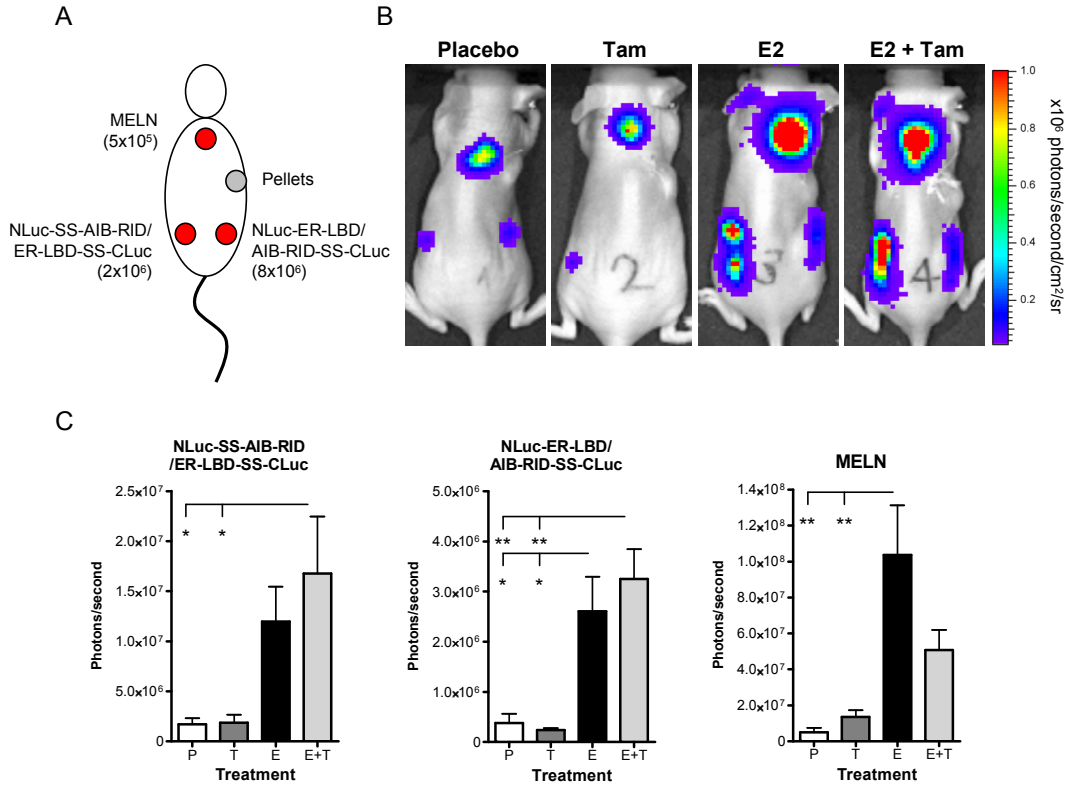

Figure 3.21– *In vivo* modulation of ER-LBD/AIB-RID split-luciferase transfected and MELN cells by E2 and OHT. 5x10^5 MELN, 2x10^6 NLuc-SS-AIB-RID/ER-LBD-SS-CLuc transfected 293 and 8x10^6 NLuc-ER-LBD/AIB-RID-CLuc transfected cells were subcutaneous implanted into nude mice (A). 0.72mg/60 day E2/placebo and/or 2x5mg/60 day OHT/placebo pellets implanted into mice 5 days previously. 24 hours after cell implantation, mice were imaged using the IVIS 100. Representative images (B) and quantified data (C) are shown for each treatment and cell line (n=5). P = placebo, T(am) = Tamoxifen, E(2) = E2, E(2) + T(am) = E2 and Tamoxifen. The ANOVA test was used to determine statistical significance (***, $p \leq 0.001$, **, $p \leq 0.01$, *, $p \leq 0.05$).

in the E2 only mice, indicating that OHT delivery had been successful. However, neither of the split-luciferase reporters showed a decrease in signal intensity with OHT treatment, indeed, both reporters showed greater luciferase activity in the E2 andOHT versus E2 alone treated mice; the NLuc-SS-AIB-RID/ER-LBD-SS-CLuc transfected cells showed a 40% increase whereas the NLuc-ER-LBD/AIB-RID-SS-CLuc transfected cells showed a 25% increase. This is in contrast to the signal in the mice which received OHT but no E2; the signal relative to double placebo mice was approximately equal in the NLuc-SS-AIB-RID/ER-LBD-SS-CLuc cells, was 40% less in the NLuc-ER-LBD/AIB-RID-SS-CLuc cells, but almost 3-fold higher than the double placebo mice in the MELN cells.

3.5 Full length ERα-AIB1 split-luciferase assay

In parallel to the development and characterization of the truncated ER-LBD/AIB-RID split-luciferase constructs, I also chose to produce full length ERα and AIB1 constructs; inclusion of the whole proteins ought to make the split-luciferases more receptive to the intracellular signalling which regulates the activity of the endogenous ERα and AIB1, and thus could produce a better reporter of ERα-coregulator interaction.

Split-luciferase constructs were produced with full length ERα and AIB1 in both orientations (i.e. fused to NLuc and CLuc). Initial transfections of complementary full length constructs produced low luciferase activity. In an effort to optimize the transient transfection, increasing quantities of the larger AIB1 fusion protein construct were used in the transfections (Figure 3.22).

In both orientations, increasing the ratio of the AIB1 fusion construct relative to the ERα fusion construct, increased the difference in signal between vehicle and E2 treated cells. The increase in luciferase activity observed with E2 addition in the NLuc-AIB/ER-CLuc transfected cells increased from 2.3-fold with a 1:1 ratio to 3.5-fold with a 32:1 ratio of AIB to ER fusion protein. In the NLuc-ER/AIB-CLuc transfected cells, the increase in signal observed with E2 went from 1.5-fold with a 1:1 ratio to 2.5-fold with a 16:1 ratio of AIB1 to ER fusion protein. However, with both protein orientations, the higher ratios of AIB1 to ER fusion protein, which produced the greatest fold increase with E2 addition, produced less overall luminescence. This was especially pronounced with the NLuc-ER/AIB-CLuc

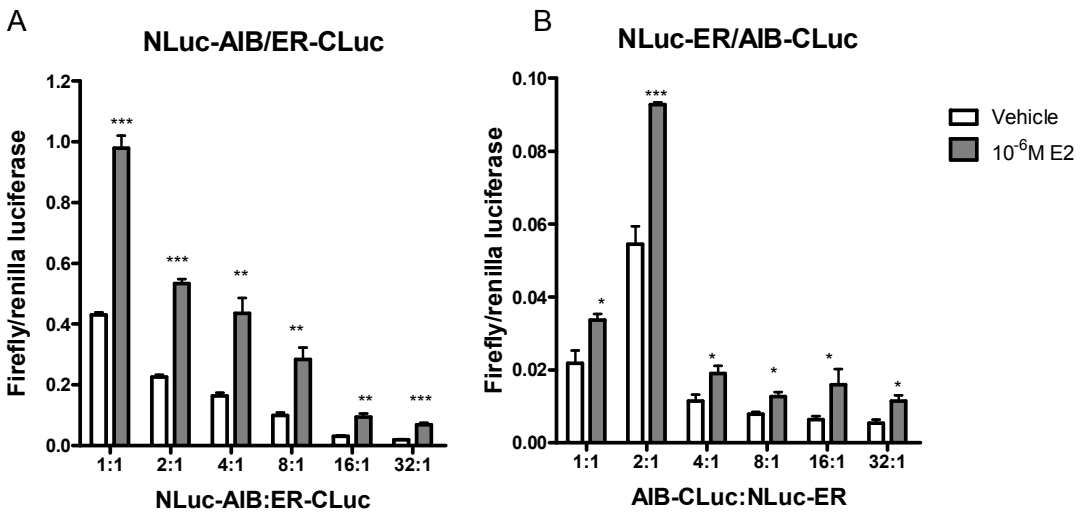

Figure 3.22 - Ratio transfections of full length ER/AIB split-luciferase reporters. $4x10^4$ 293 cells were seeded in 96 well plates and transfected with 50ng *Renilla* luciferase and 150ng of NLuc-AIB/ER-CLuc (A) or NLuc-ER/AIB-CLuc (B) in different ratios. Cells were treated with vehicle (ethanol) or 10^{-6}M E2 for 48 hours prior to quantification of luciferase activities. Mean firefly luciferase activities (n = 3) normalized to *Renilla* luciferase activities are shown. Error bars represent the standard errors of the mean (SEM). A t-test was used to determine statistical significance to between E2 and vehicle treatment (***, $p \leq 0.001$, **, $p \leq 0.01$, *, $p \leq 0.05$).

transfected cells where the signal intensity was only just above background levels.

Immunofluorescence of NLuc-AIB/ER-CLuc and NLuc-ER/AIB-CLuc transfected cells confirmed that all four of the full-length fusion proteins were nuclear in localization (Figure 3.23). The results also indicated that very few cells expressed both of the fusion proteins together.

Given the low luminescence of the full length constructs and our experience with the truncated ER-LBD/AIB-RID split-luciferases, where the stable cell line characteristics were different to transient transfection results (Section 3.6), I decided to produce stable cell lines with the full length ER/AIB1 constructs prior to full characterisation. It had been shown that the constructs complemented in the presence of E2, and so it was felt that it would be more efficient to characterise the constructs once they were stably expressed.

In order to appreciate the agonist/antagonist effects of ERα ligands in the breast, bone and endometrium, efforts were made to produce MCF7, U2OS and Ishikawa cell lines which stably expressed NLuc-SS-AIB/ER-SS-CLuc or NLuc-SS-ER/AIB-SS-CLuc. Initially, transfections were performed with both constructs simultaneously. Colonies were assessed for luminescence in the presence of E2 with the IVIS 100 and more sensitive Topcount luminometer. Expression of the fusion proteins was assessed by western blotting. Though colonies formed which were resistant to the two antibiotics, none screened positive for luciferase activity or dual fusion protein expression. Western blotting indicated that some clones expressed detectable quantities of one of the fusion proteins, and transient transfection of the complementary fusion protein

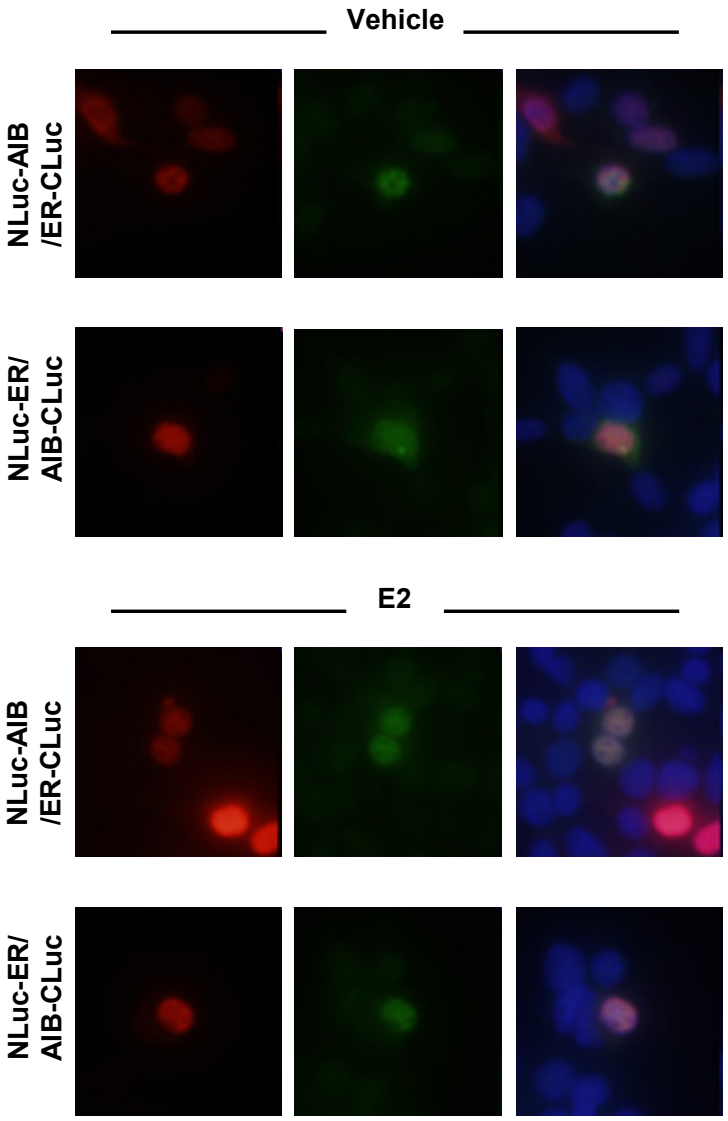

Figure 3.23 - Immunofluorescence of full length ER/AIB split-luciferase reporters. $4x10^4$ 293 cells were seeded into chamber slides prior to transfection with NLuc-AIB/ER-CLuc or NLuc-ER/AIB-CLuc. Cells were treated with vehicle (ethanol) or 10^{-6}M E2 for 24 hours prior to staining with mouse-anti-ERα/Alexa Fluor 594 antibodies and rabbit anti-AIB1/Alexa Fluor 488 antibodies. Slides were mounted with Prolong Gold Antifade with DAPI. Photographs show ERα (red), AIB1 (green) and a merged image with DAPI stained nuclei (blue).

into these cells would produce luciferase activity which would increase in the presence of E2 (Figure 3.24). Attempts were made to establish stable expression of the complementary fusion protein in these cells, however, similar problems of antibiotic resistance without luminescence were encountered.

Due to time constraints, it was not possible to generate cell lines which stably expressed NLuc-SS-AIB and ER-SS-CLuc or NLuc-SS-ER and AIB-SS-CLuc.

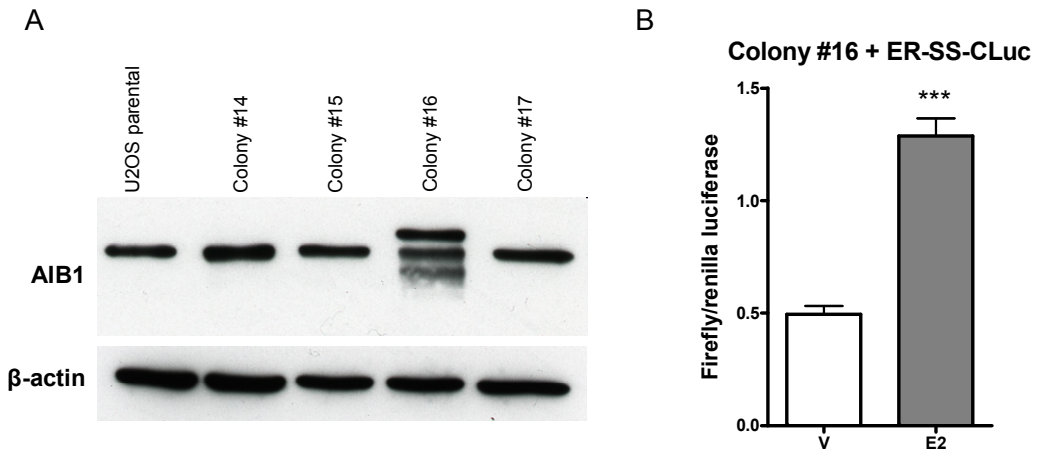

Figure 3.24 - U2OS NLuc-SS-AIB/ER-SS-CLuc stable cell lines. U2OS cell were transfected with NLuc-SS-AIB/ER-SS-CLuc. Western blotting indicated that colony #16 stably expressed NLuc-SS-AIB (A). Colony #16 cells transiently transfected with 50ng *Renilla* luciferase and 150ng of ER-SS-CLuc were treated with vehicle (ethanol) or 10^{-6}M E2 for 48 hours prior to quantification of luciferase activities (B). Mean firefly luciferase activities (n = 4) normalized to *Renilla* luciferase activities are shown. Error bars represent the standard errors of the mean (SEM). A t-test was used to determine statistical significance (***, $p \leq 0.001$).

3.6 Truncated ER-LBD/AIB-RID split-luciferase reporters and the tissue specific actions of ERα ligands

One of the principal aims in developing the ER-AIB1 split-luciferase reporters was to establish a novel method for imaging the tissue specific actions of SERMs. In order to achieve this, it was our intention to stably transform breast (MCF7), bone (U2OS) and endometrial (Ishikawa) cell lines with the split-luciferase reporters to determine whether they complement in a context specific manner when treated with different ligands.

3.6.1 MCF7 stable cell lines

To produce the stable cell line representing breast tissue, MCF7 cells were transfected with NLuc-ER-LBD and AIB-RID-SS-CLuc. These constructs had shown the greatest fold induction in response to E2 and the fastest response to ligand in transient transfections. Both constructs were simultaneously transfected and transformed cells were selected for with antibiotics. Colonies which formed in the presence of selective antibiotics were propagated and screened for luciferase activity using the IVIS 100. The E2 induced complementation of positive clones was examined by incubation with 10^{-9}M and 10^{-6}M E2 (Figure 3.25).

Examination of the luciferase signal in 6 clones showed considerable variation in signal, even though the same constructs had been transfected. The signal intensity ranged from tens to hundreds of photon counts per second. The fold induction observed with E2 addition also varied from 1.6-fold in colony #6 to 3.8-fold in colony #1. In all cases, the fold induction observed with E2 was considerably less than the

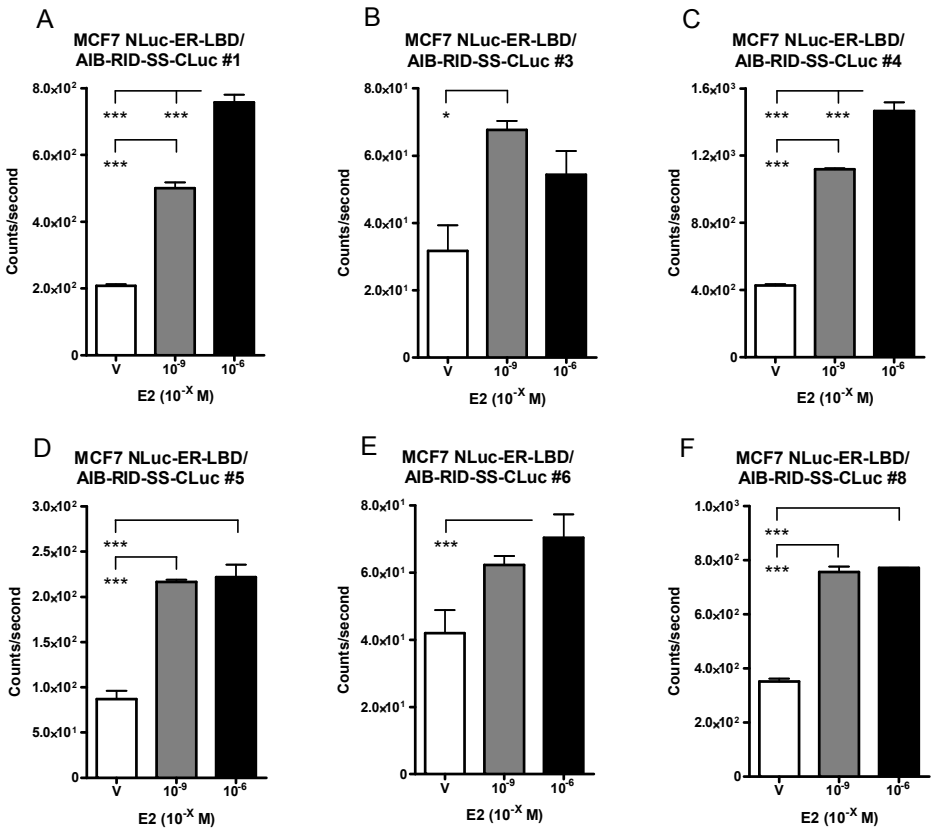

Figure 3.25 - E2 response of MCF7 NLuc-ER-LBD/AIB-RID-SS-CLuc stable cell lines. $1.5x10^4$ cells were seeded in 96 well plates prior to treatment with vehicle (ethanol; V) or 10^{-9}M or 10^{-6}M E2 for 48 hours. Luciferase activity was quantified in live cells after addition of 150µg/ml D-luciferin. Graphs show mean firefly luciferase activities (n = 3). Error bars represent the standard errors of the mean (SEM). SEM (n=3). The ANOVA test was used to determine statistical significance (***, $p \leq 0.001$, **, $p \leq 0.01$, *, $p \leq 0.05$).

average of 10-fold observed with transient transfection of NLuc-ER-LBD and AIB-RID-SS-CLuc into 293 cells.

Based on their signal intensity and fold increase in signal with E2, MCF7 NLuc-ER-LBD/AIB-RID-SS-CLuc #1 and #4 were selected for further characterisation. A more comprehensive titration of E2 showed that cells from colony #1 and #4 reached signal plateau in the presence of 10^{-9}M and 10^{-8}M E2 respectively (Figure 3.26). In transient transfections of NLuc-ER-LBD and AIB-RID-SS-CLuc in 293 cells the maximum signal intensity was observed with 10^{-6}M E2. The maximum stimulation of by E2 was 2.6- and 2-fold vehicle luciferase activity for colony #1 and #4 respectively. By way of comparison, the MELN cells showed a 3.9-fold increase in signal when incubated with 10^{-10}M E2. The E2 titration results also suggested that the split-luciferase reporters expressed in an MCF7 background continue to be less responsive to low levels of E2 when compared to the MELN cells; the MELN cell line showed almost 80% of their maximum signal with 10^{-12}M E2 whereas the split-luciferase reporters showed little, if any, increase above vehicle levels at 10^{-12} M E2.

Incubation of the split-luciferase stable cell lines with OHT and ICI indicated that the E2 response of the split-luciferase stable cell lines was modulated by antiestrogens (Figure 3.27). With both OHT and ICI, the E2 induced increase in signal was ablated to vehicle levels with 10^{-8}M inhibitor and higher concentrations reduced the signal below background levels. In transiently transfected 293 cells 10^{-7}M inhibitor was required to reduce the signal to vehicle levels and in MELN cells the signal was reduced to vehicle levels with inhibitor concentrations between 10^{-8}M and 10^{-7}M.

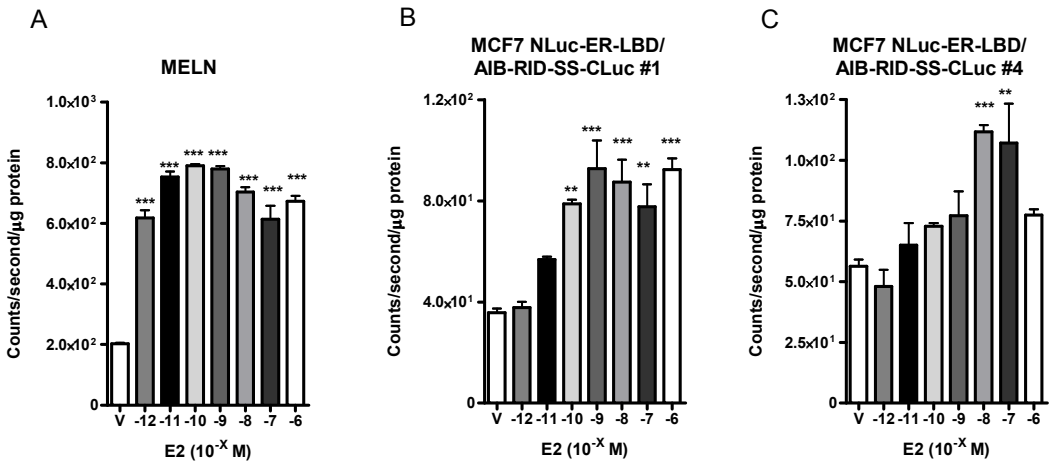

Figure 3.26 - E2 response of MCF7 NLuc-ER-LBD/AIB-RID-SS-CLuc #1 and #4. $1.5x10^4$ MELN (A) or $2x10^4$ MCF7 NLuc-ER-LBD/AIB-RID-SS-CLuc #1 (B) or #4 (C) cells were treated vehicle (ethanol; V) or increasing concentrations of E2 for 48 hours prior to quantification of luciferase activity. Mean firefly luciferase activities (n = 3) normalized to total protein are shown. Error bars represent the standard errors of the mean (SEM). The ANOVA test was used to determine statistical significance relative to vehicle treatment (***, $p \leq 0.001$, **, $p \leq 0.01$, *, $p \leq 0.05$).

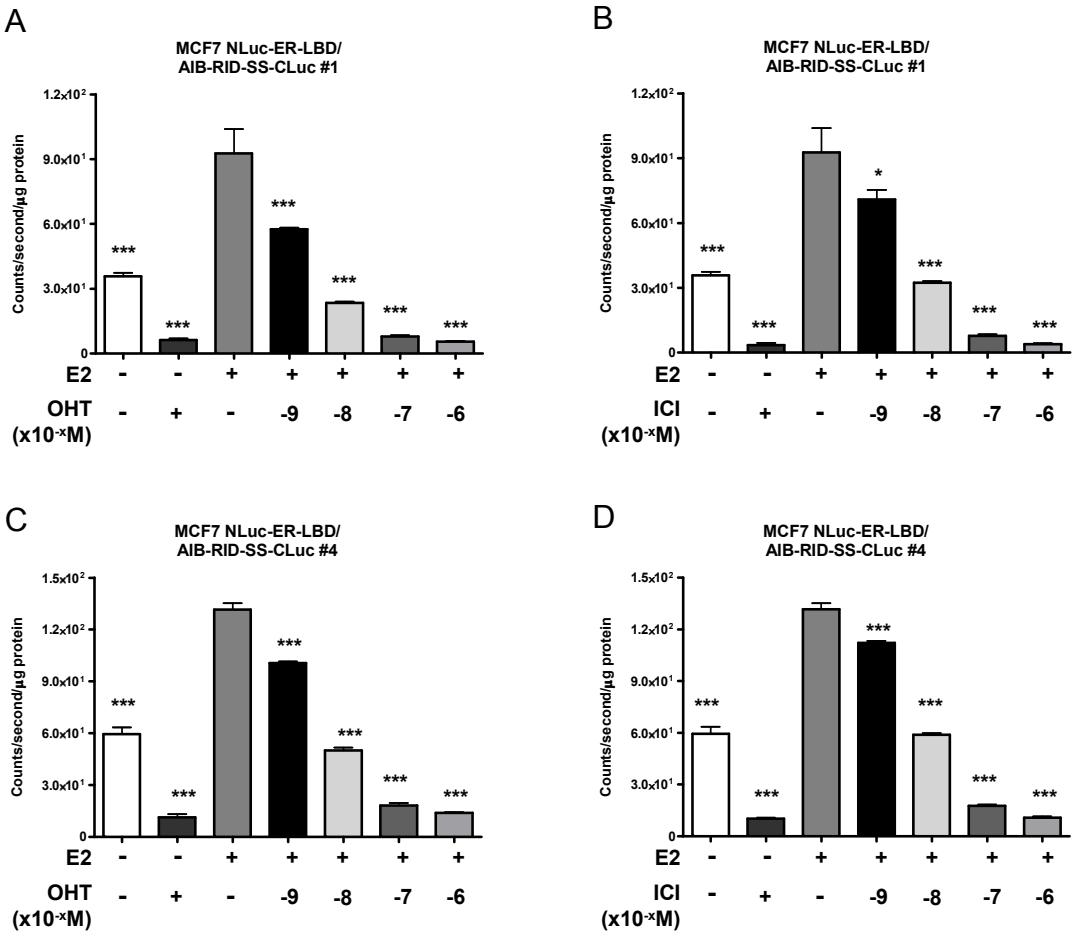

Figure 3.27 – Modulation of MCF7 NLuc-ER-LBD/AIB-RID-SS-CLuc #1 and #4 E2 response by OHT and ICI. $2x10^4$ MCF7 NLuc-ER-LBD/AIB-RID-SS-CLuc #1 (A+B) or #4 (C+D) cells were treated vehicle (ethanol) or 10^{-9}M E2 and different concentrations of OHT (A+C) or ICI (B+D) for 48 hours. Mean firefly luciferase activities (n = 3) normalized to total protein are shown. Error bars represent the standard errors of the mean (SEM). The ANOVA test was used to determine statistical significance relative to E2 treatment (***, $p \leq 0.001$, *, $p \leq 0.05$).

An investigation of the signal dynamics in the stably transfected MCF7 cell lines showed that cells from both colonies produced approximately 65% of their maximum signal after 2 hours incubation with E2 (Figure 3.28A and B). With longer E2 incubations the luciferase signal steadily increased; after 8 hours E2 incubation 95% and 90% of maximum signal had been induced in the MCF7 NLuc-ER-LBD/AIB-RID-SS-CLuc #1 and #4 cells respectively. In 293 cells transiently transfected with NLuc-ER-LBD and AIB-RID-SS-CLuc, 80% of signal was induced with 2 hours E2 incubation (Figure 3.16, Section 3.4).

Investigation of the OHT signal ablation in the MCF7 NLuc-ER-LBD/AIB-RID-SS-CLuc #1 and #4 cells showed that approximately 20% and 15% of the E2 induced signal was lost after 2 hours incubation with OHT (Figure 3.28 C and D). This is in contrast to the transiently transfected 293 cells, where approximately 50% of the signal was lost after 2 hours. However, in common with the transient transfection results, OHT incubation of 4 hours reduced the E2 induced signal to a little more than vehicle levels and 6 hours reduced the signal below vehicle levels.

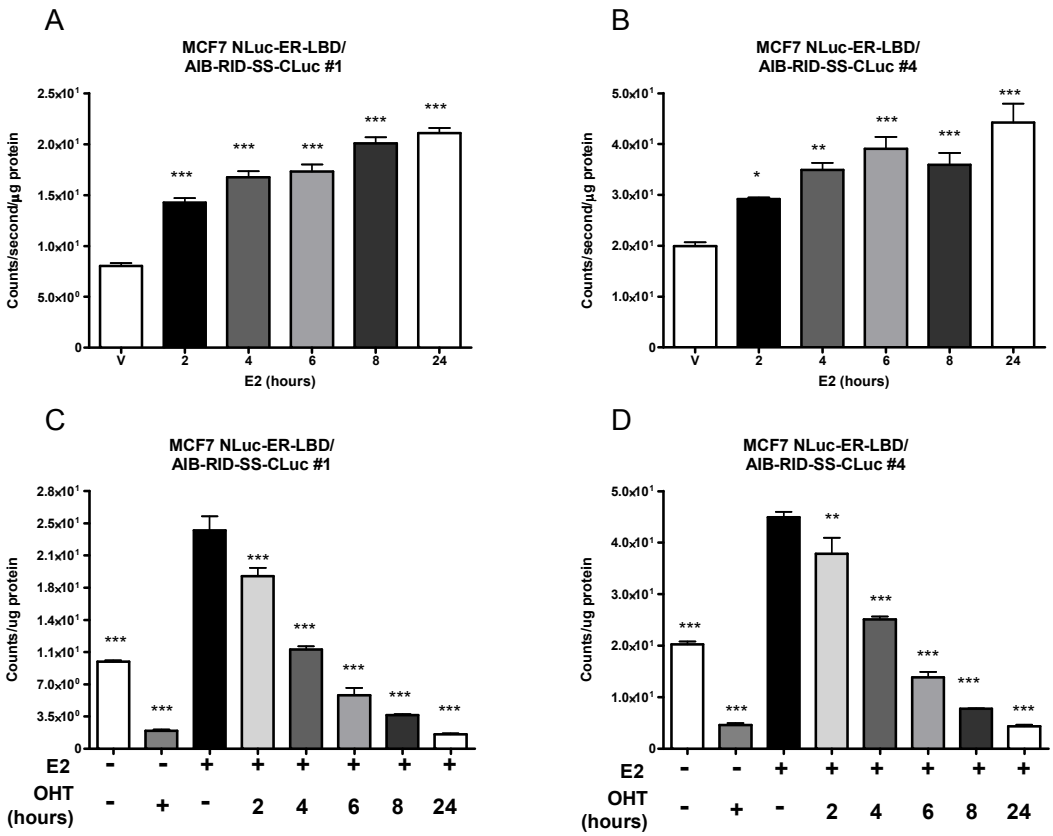

Figure 3.28 - Signal dynamics of MCF7 NLuc-ER-LBD/AIB-RID-SS-CLuc #1 and #4. . $2x10^4$ MCF7 NLuc-ER-LBD/AIB-RID-SS-CLuc #1 (A+C) or #4 (B+D) cells were seeded into 96 well plates. Cells were incubated with 10^{-6}M E2 for increasing periods of time (A+B) or 10^{-9}M E2 for 24 hours prior to addition of 10^{-6}M OHT for increasing periods of time (C+D). Mean firefly luciferase activities (n = 3) normalized to total protein are shown. Error bars represent the standard errors of the mean (SEM). The ANOVA test was used to determine statistical significance relative to E2 treatment (***, $p \leq 0.001$, **, $p \leq 0.01$, *, $p \leq 0.05$).

3.6.2 U2OS stable cell lines

Having observed that results obtained with the MCF7 NLuc-ER-LBD/AIB-RID-SS-CLuc stable cell lines differed from transient transfection results obtained with the same constructs, I decided to produce U2OS stable cell lines with both fusion protein orientations - NLuc-ER-LBD/AIB-RID-SS-CLuc and NLuc-SS-AIB-RID/ER-LBD-SS-CLuc. Using the same selection procedure, five stably transfected U2OS colonies were obtain; one colony was transfected with NLuc-SS-AIB-RID/ER-LBD-SS-CLuc and 4 colonies were transfected with NLuc-ER-LBD/AIB-RID-SS-CLuc. To assess the stable cell lines, their luciferase activity was examined in the presence of vehicle and a range of E2 concentrations (Figure 3.29).

In all five of the U2OS stable cell lines, E2 stimulated a much greater fold increase in luciferase activity than in the MCF7 stable cell lines; the average maximum signal was 8-fold that observed with vehicle. The NLuc-SS-AIB-RID/ER-LBD-SS-CLuc colony produced the greatest fold induction with E2; 12 times the vehicle signal was observed in the presence of 10^{-6}M E2. The NLuc-ER-LBD/AIB-RID-SS-CLuc transfected colonies produced between 7- and 9-fold increases in signal intensity with 10^{-8}M and 10^{-6}M E2. In transient transfection of 293 cells, E2 stimulation was greatest with NLuc-ER-LBD and AIB-RID-SS-CLuc, averaging between 10- and 12-fold the vehicle signal, while lower signal increases of between 5- and 8- fold were observed with NLuc-SS-AIB-RID/ER-LBD-SS-CLuc transfected cells: the opposite scenario to that observed in the U2OS stable cell lines. Western blotting confirmed co-expression of NLuc and CLuc ER and AIB1 fusion proteins of the expected sizes (Figure 3.30).

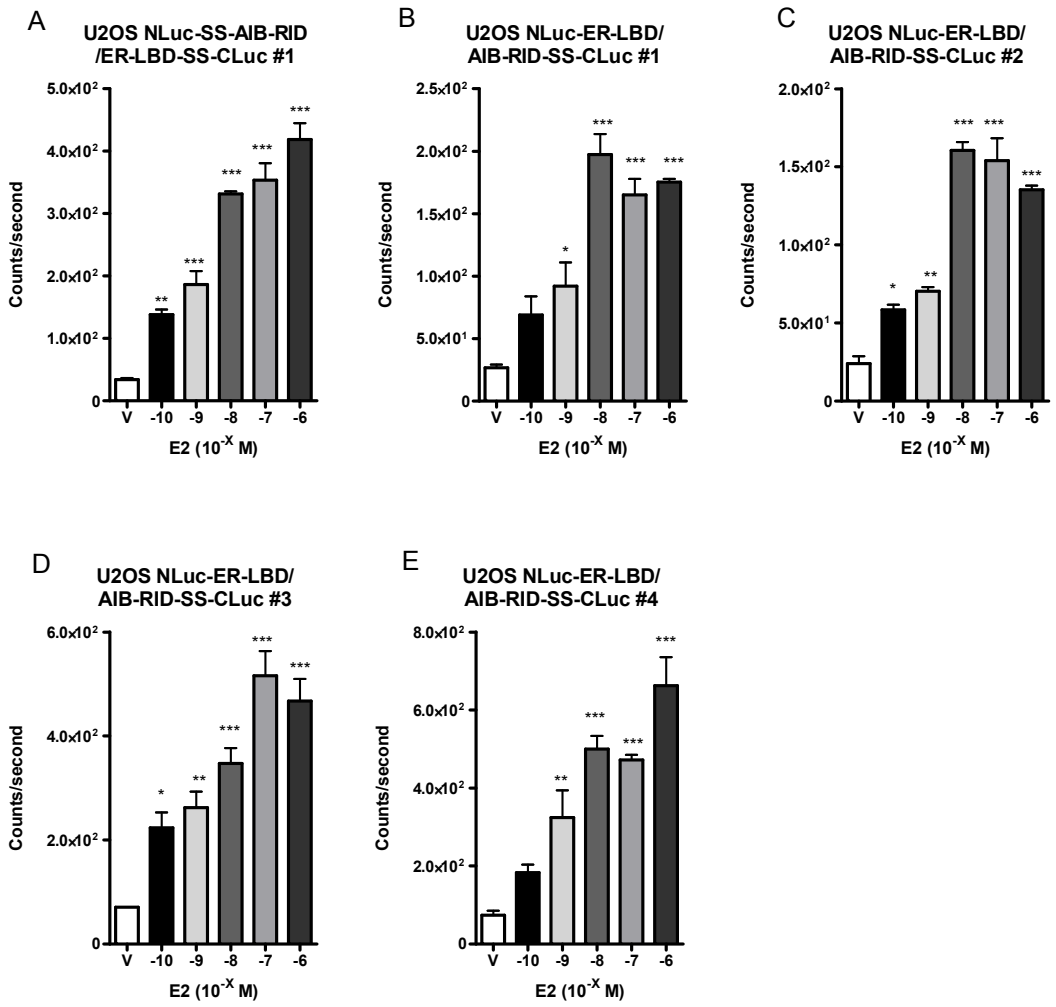

Figure 3.29 - E2 response of U2OS stable cell lines. $6x10^3$ U2OS cells stably transfected with NLuc-SS-AIB-RID/ER-LBD-SS-CLuc (A) or NLuc-ER-LBD/AIB-RID-SS-CLuc (B-E) were treated vehicle (ethanol; V) or increasing concentrations of E2 for 48 hours prior to quantification of luciferase activity. Graphs show mean firefly luciferase activities (n = 3). Error bars represent the standard errors of the mean (SEM). The ANOVA test was used to determine statistical significance relative to vehicle treatment (***, $p \leq 0.001$, **, $p \leq 0.01$, *, $p \leq 0.05$).

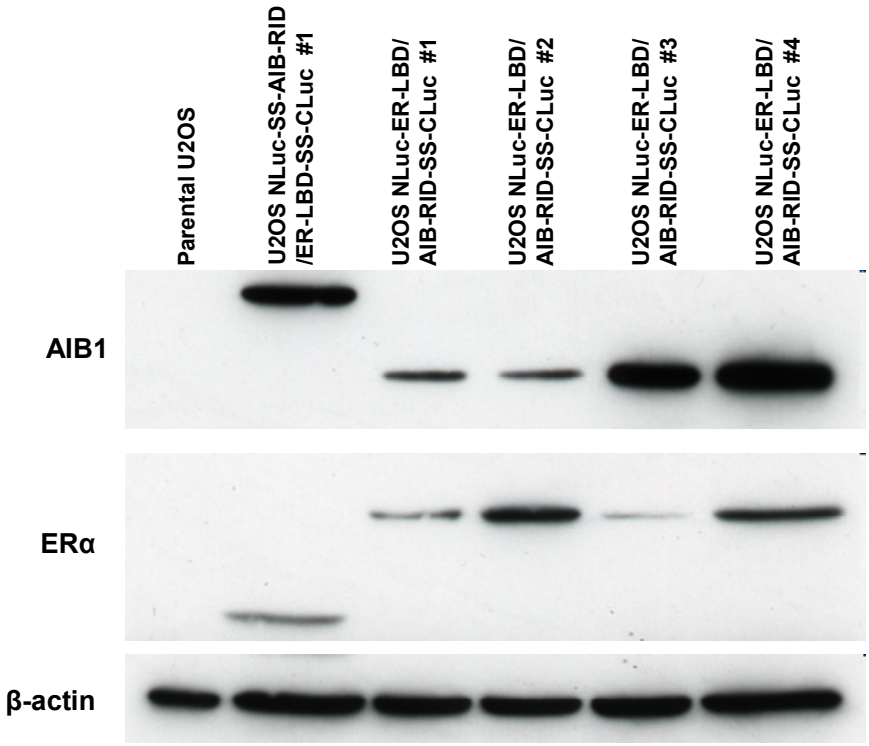

Figure 3.30 - Western blot of fusion proteins in U2OS stable cell lines. 10μg of lysate from U2OS or U2OS cell lines stably transfected with NLuc-SS-AIB-RID/ER-LBD-SS-CLuc or NLuc-ER-LBD/AIB-RID-SS-CLuc were separated by SDS-PAGE and blotted for using rabbit anti-AIB1, mouse anti-ERα or mouse anti-β-actin antibodies.

From the E2 titration experiments, I chose to further characterise NLuc-SS-AIB-RID/ER-LBD-SS-CLuc colony #1 and NLuc-ER-LBD/AIB-RID-SS-CLuc colonies #1 and #4; these colonies showed the greatest induction with E2 and represented both fusion protein orientations. NLuc-ER-LBD/AIB-RID-SS-CLuc colony #1 was further characterised as well as NLuc-ER-LBD/AIB-RID-SS-CLuc colony #4 because it reached a signal maximum at 10^{-8}M E2 whereas NLuc-SS-AIB-RID/ER-LBD-SS-CLuc colony #1 and as NLuc-ER-LBD/AIB-RID-SS-CLuc colony #4 both showed maximum signal intensity with 10^{-6}M E2.

Incubation of U2OS NLuc-SS-AIB-RID/ER-LBD-SS-CLuc colony #1 and NLuc-ER-LBD/AIB-RID-SS-CLuc colonies #1 and #4 with 10^{-9}M E2 and increasing concentrations of OHT or ICI indicated that the luciferase activity of the U2OS stable cell lines was modulated by antiestrogens in a dose dependent manner (Figure 3.31). With both inhibitors, E2 induced luciferase activity was reduced to vehicle levels with inhibitor concentrations of 10^{-7}M or above. Although OHT is thought to be a mild agonist in bone cells, no evidence of this effect was observed; OHT and ICI, a pure antiestrogen, appeared to affect the reporters in a very similar fashion. If any difference was observed, it suggested that OHT was a more potent inhibitor than ICI.

I proceeded to investigate the dynamics of the luciferase signal in the U2OS stable cell lines. Incubation of U2OS NLuc-SS-AIB-RID/ER-LBD-SS-CLuc colony #1 and NLuc-ER-LBD/AIB-RID-SS-CLuc colonies #1 and #4 with 10^{-6}M E2 for increasing periods of time indicated that luciferase activity increased as a function of E2 incubation time (Figure 3.32 A-C).

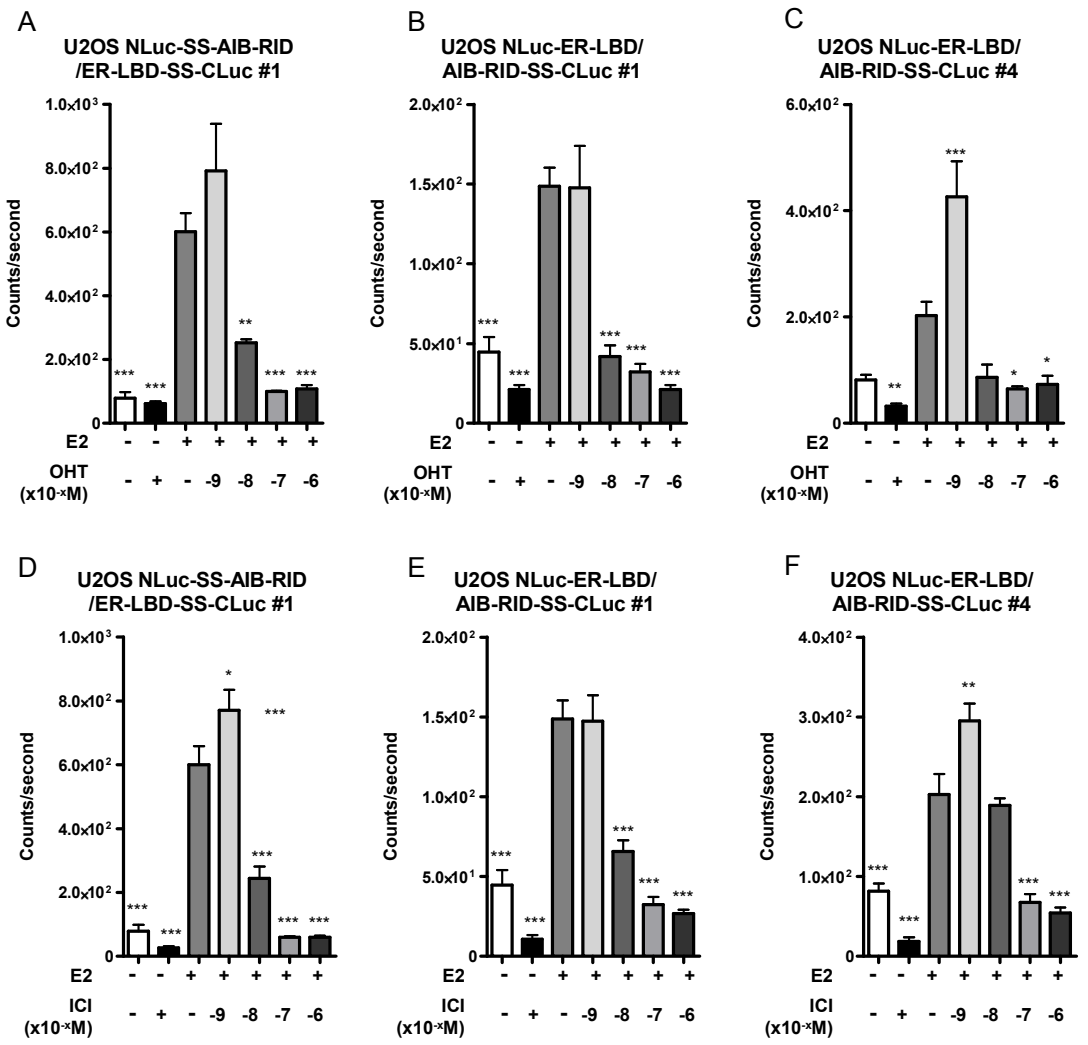

Figure 3.31 - Modulation of E2 response in U2OS stable cell lines by OHT and ICI. $6x10^3$ U2OS NLuc-SS-AIB-RID/ER-LBD-SS-CLuc #1 (A), or U2OS NLuc-ER-LBD/AIB-RID-SS-CLuc #1 (B) or #4 (C) cells were treated vehicle (ethanol) or 10^{-9}M E2 and different concentrations of OHT (A-C) or ICI (D-F) for 48 hours prior to quantification of luciferase activity. Graphs show mean firefly luciferase activities (n = 3). Error bars represent the standard errors of the mean (SEM). The ANOVA test was used to determine statistical significance relative to E2 treatment (***, $p \leq 0.001$, **, $p \leq 0.01$, *, $p \leq 0.05$).

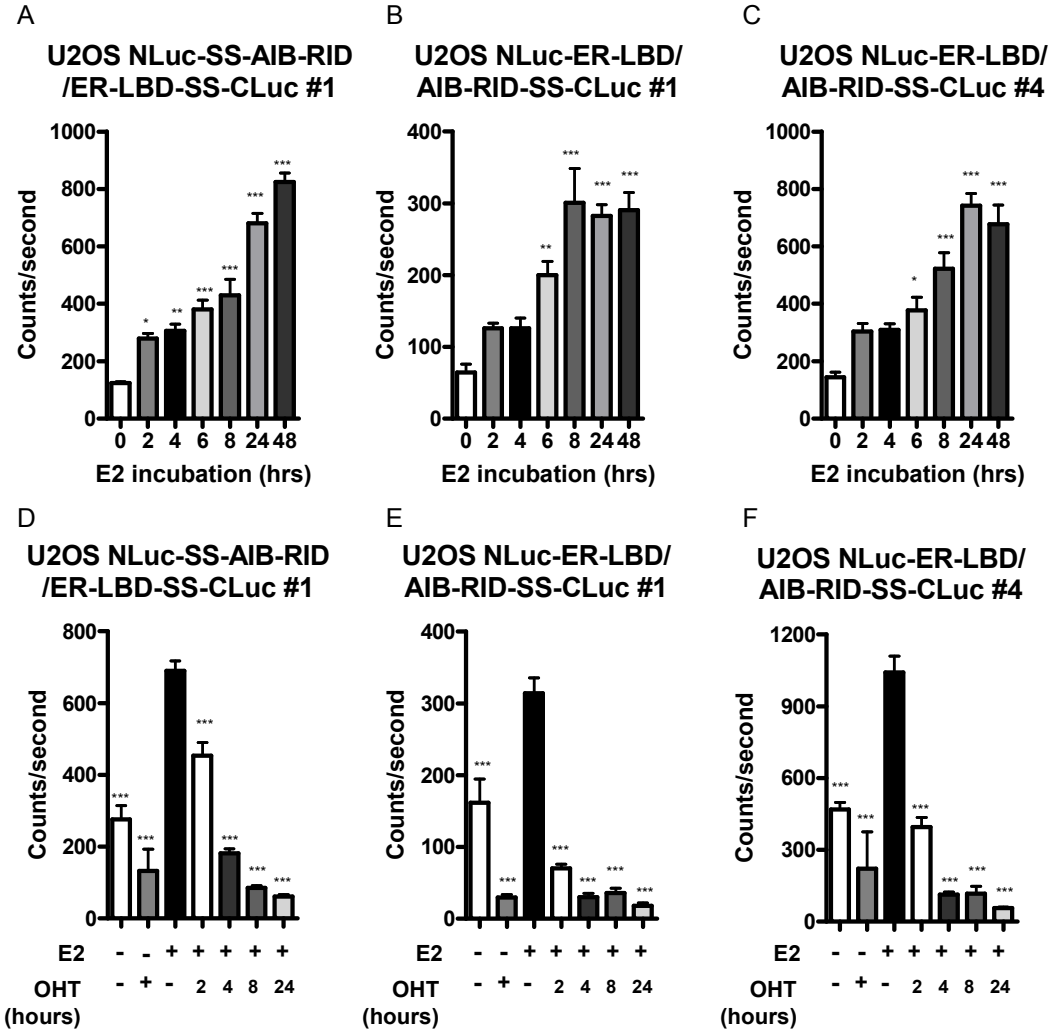

Figure 3.32 – Time-course of luciferase signal in U2OS stable cell lines. $6x10^3$ U2OS NLuc-SS-AIB-RID/ER-LBD-SS-CLuc #1 (A+D), or U2OS NLuc-ER-LBD/AIB-RID-SS-CLuc #1 (B+E) or #4 (C+F) cells were seeded in 96 well plates. Cells were treated with 10^{-6}M E2 for increasing durations (A-C) or 10^{-9}M E2 for 24 hours before addition of concentrated OHT (final concentration 10^{-6}M; D-F) for different durations. Graphs show mean firefly luciferase activities (n = 3). Error bars represent the standard errors of the mean (SEM). SEM (n=3). The ANOVA test was used to determine statistical significance relative to E2 treatment (***, $p \leq 0.001$, **, $p \leq 0.01$, *, $p \leq 0.05$).

The luciferase activity in the entire panel of U2OS stable cell lines increased approximately 2-fold after 2 hours E2 incubation, which represented 35-40% of the maximum luciferase activity observed. The NLuc-SS-AIB-RID/ER-LBD-SS-CLuc #1 cells were the slowest to respond to E2; 8 hours ligand incubation produced 50% of the maximum signal and the signal continued to increase with ligand incubations up to 48 hours. The NLuc-ER-LBD/AIB-RID-SS-CLuc #1 and #4 cells were faster to respond to the E2 signal; 50-60% of maximum signal was achieved after 6 hours E2 incubation and the maximum was reached after 8 and 24 hours for NLuc-ER-LBD/AIB-RID-SS-CLuc #1 and #4 cells, respectively. Although a change in signal was discernable in all the U2OS stable cell lines after 2 hours, in general the E2 stimulated increase in luciferase activity was much slower than in the MCF7 stable and transiently transfected 293 cells, which showed 60-80% of maximum signal after 2 hours E2 incubation.

I next investigated the duration required for OHT to ablate the E2 induced luciferase activity in the U2OS stable cell lines (Figure 3.32 D-F). The results indicate that although the luciferase signal is slow to establish itself in response to E2 in the U2OS stable cell lines, it declines very rapidly in response to OHT. In the NLuc-SS-AIB-RID/ER-LBD-SS-CLuc #1 cells, a 35% reduction in signal intensity was observed after 2 hours OHT incubation and full signal ablation occurred after just 4 hours. In the NLuc-ER-LBD/AIB-RID-SS-CLuc #1 and #4, the signal was reduced below vehicle levels after just 2 hours OHT incubation. In previous experiments, signal ablation required 4-6 hours with the NLuc-ER-LBD/AIB-RID-SS-CLuc constructs in the MCF7 stable and in 293 transient transfections and the NLuc-SS-AIB-RID/ER-

LBD-SS-CLuc constructs required more that 10 hours for full signal ablation in transient transfection experiments.

3.6.3 Reporting of the tissue specific agonist actions of OHT

As previously noted, experiments investigating the antiestrogen modulation of the E2 induced luciferase signal in the U2OS stable cell lines produced results very similar to those seen in MCF7 cells. In order to more closely examine whether I could discern any differences in the actions of the SERM OHT and pure antiestrogen ICI in the U2OS split-luciferase reporters, I titrated both compounds individually without E2 (Figure 3.33).

Incubation of U2OS stable cell lines with increasing concentrations of OHT or ICI appeared to confirm that both inhibitors have the same affect on ER-AIB1 interaction; in all but one instance, addition of the inhibitor reduced luciferase activity below that of vehicle treatment. Treatment of U2OS NLuc-SS-AIB-RID/ER-LBD-SS-CLuc #1 cells with 10^{-10}M OHT did increase luciferase activity above vehicle levels, but this was only seen with a single stable cell line at a single OHT dose and could be due to experimental error. The remaining results appeared to suggest, that if any differences could be discerned between the inhibitors, lower concentrations of OHT were more potent than low concentrations of ICI.

Due to time constraints, I was unable to produce stably transfected Ishikawa cell lines to determine whether the agonist action of OHT in endometrial cells could be observed using the ER-LBD/AIB-RID split-luciferase assay. However, transient

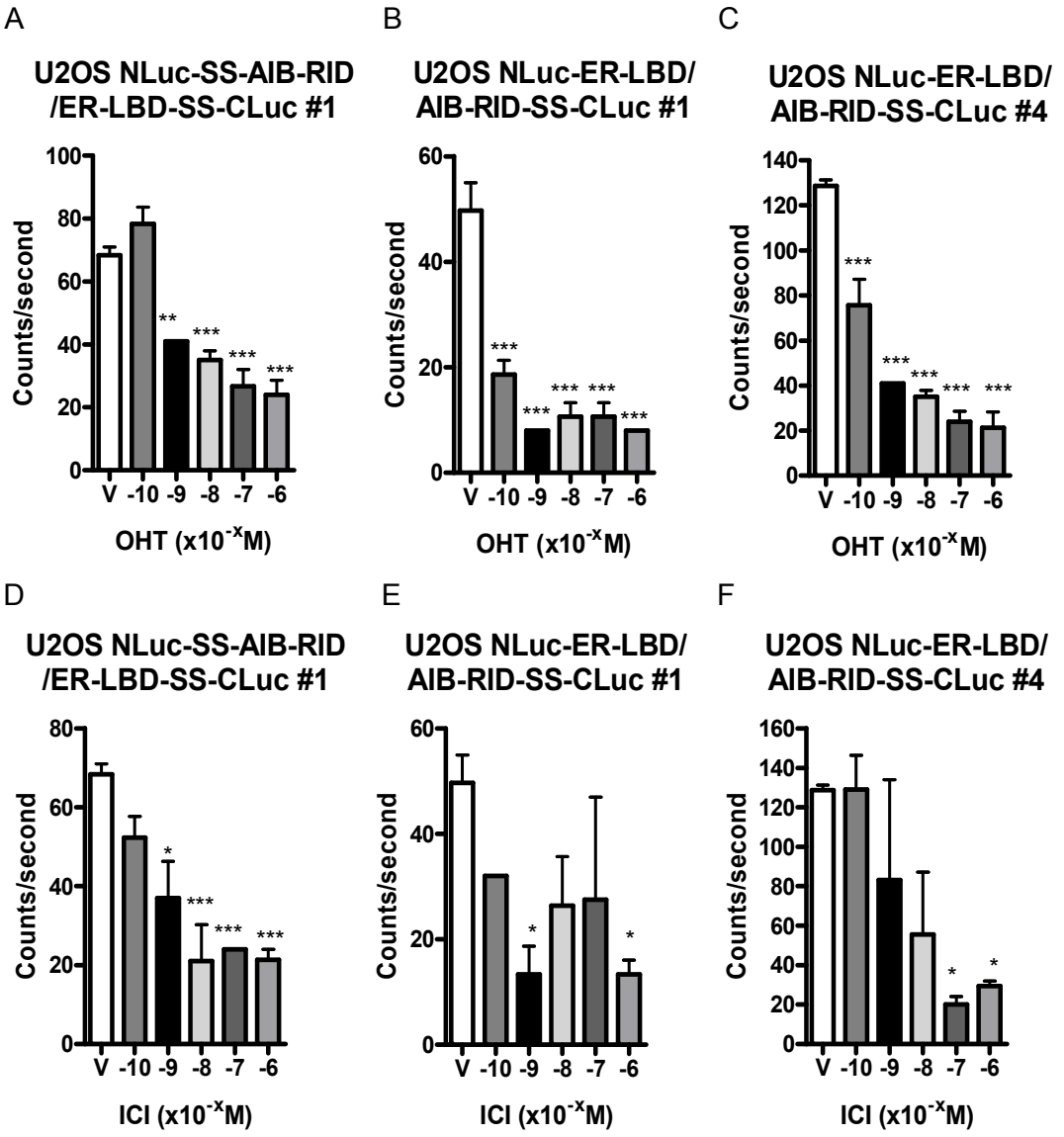

Figure 3.33 - Titration of OHT and ICI on U2OS stable cell lines. $6x10^3$ U2OS NLuc-SS-AIB-RID/ER-LBD-SS-CLuc #1 (A+D), or U2OS NLuc-ER-LBD/AIB-RID-SS-CLuc #1 (B+E) or #4 (C+F) cells were treated with vehicle (ethanol; V) or increasing concentrations of OHT (A-C) or ICI (D-F) for 48 hours prior to quantification of luciferase activity. Graphs show mean firefly luciferase activities (n = 3). Error bars represent the standard errors of the mean (SEM). The ANOVA test was used to determine statistical significance relative to vehicle treatment (***, $p \leq 0.001$, **, $p \leq 0.01$, *, $p \leq 0.05$).

transfection of the constructs into Ishikawa cells suggested that the response to OHT and ICI did not significantly differ and was very similar to that observed in MCF7 cells (Figure 3.34). If any differences could be discerned, they also appeared to suggest that OHT was a more potent inhibitor in the Ishikawa cells than in the MCF7 cells.

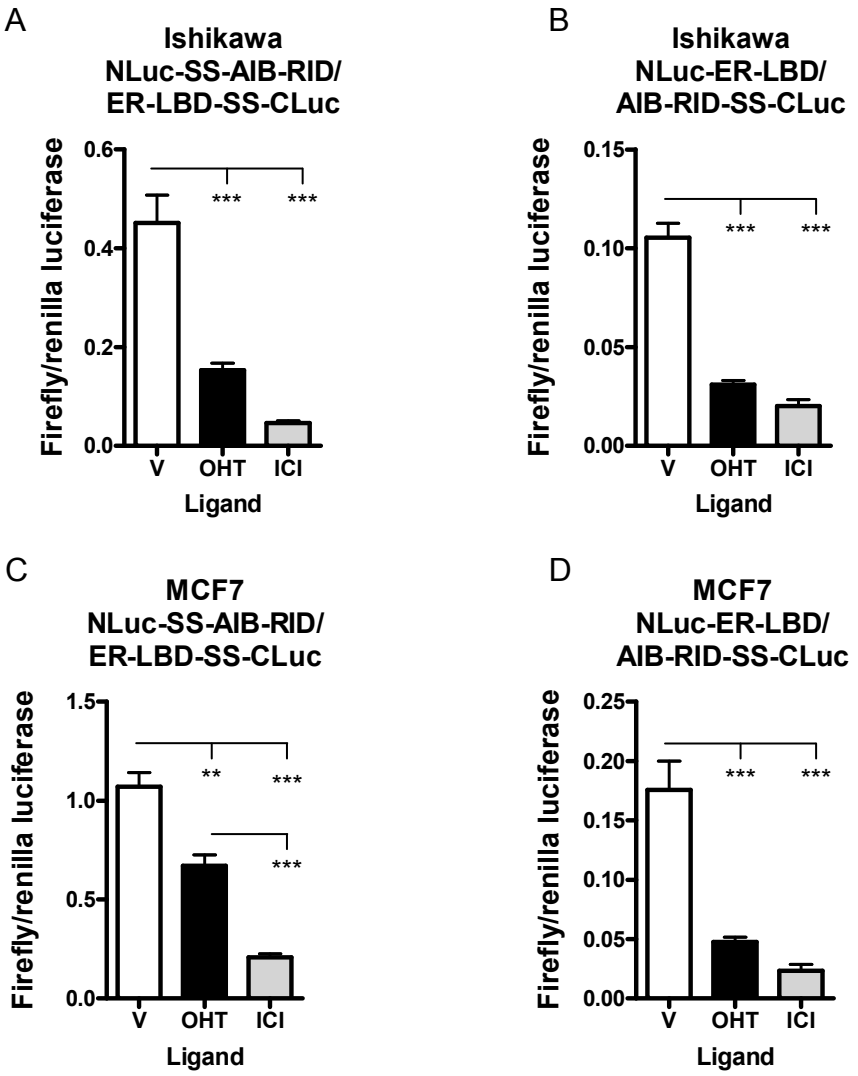

Figure 3.34 - Transient transfection of ER-LBD/AIB-RID split-luciferase constructs into Ishikawa cells. $8x10^3$ Ishikawa (A+B) or $12x10^3$ MCF7 (C+D) cells were transfected with 50ng *Renilla* luciferase and 150ng of NLuc-SS-AIB-RID/ER-LBD-SS-CLuc (A+C) or NLuc-ER-LBD/AIB-RID-SS-CLuc (B+D) in 96 well plates. Cells were treated with vehicle (ethanol; V) or 10^{-6}M OHT or ICI for 48 hours prior to quantification of luciferase activity. Mean firefly luciferase activities (n = 3) normalized to *Renilla* luciferase activities are shown. Error bars represent the standard errors of the mean (SEM). The ANOVA test was used to determine statistical significance (***, $p \leq 0.001$, **, $p \leq 0.01$, *, $p \leq 0.05$).

3.7 SMRT split-luciferase assay

In addition to developing the coactivator based split-luciferase assay to image ERα activation, a corepressor assay was also developed to image the interaction between the ERα and SMRT. It was hoped that this would enable active appreciation of ERα antagonism by antiestrogens.

In order to develop the assay, the SMRT nuclear receptor interaction domain (SMRT-RID) was PCR amplified and cloned into the NLuc and CLuc split-luciferase vectors. Initially, to determine whether the SMRT-RID constructs were expressed and capable of complementation, transfections were performed with the complementary full length ERα and truncated ER-LBD constructs (Figure 3.35).

The initial transfection indicated that both of the SMRT-RID constructs were capable of complementing with both their reciprocal full length and truncated ERα luciferase fusion proteins. All of the construct pairs produced roughly similar levels of luminescence; the brightest construct combination was NLuc-SMRT-RID/ER-LBD-CLuc, which produced approximately twice the luciferase activity of the least bright constructs pairs - the full-length ERα combinations NLuc-SMRT-RID/ER –CLuc and NLuc-ER/SMRT-RID-CLuc.

Transfection of NLuc-SMRT-RID with the reciprocal full length and truncated ERα constructs produced approximately similar results, which were consistent with our expectations; relatively low complementation was observed with vehicle and E2 treatment and high luciferase activity was observed with the antiestrogens OHT

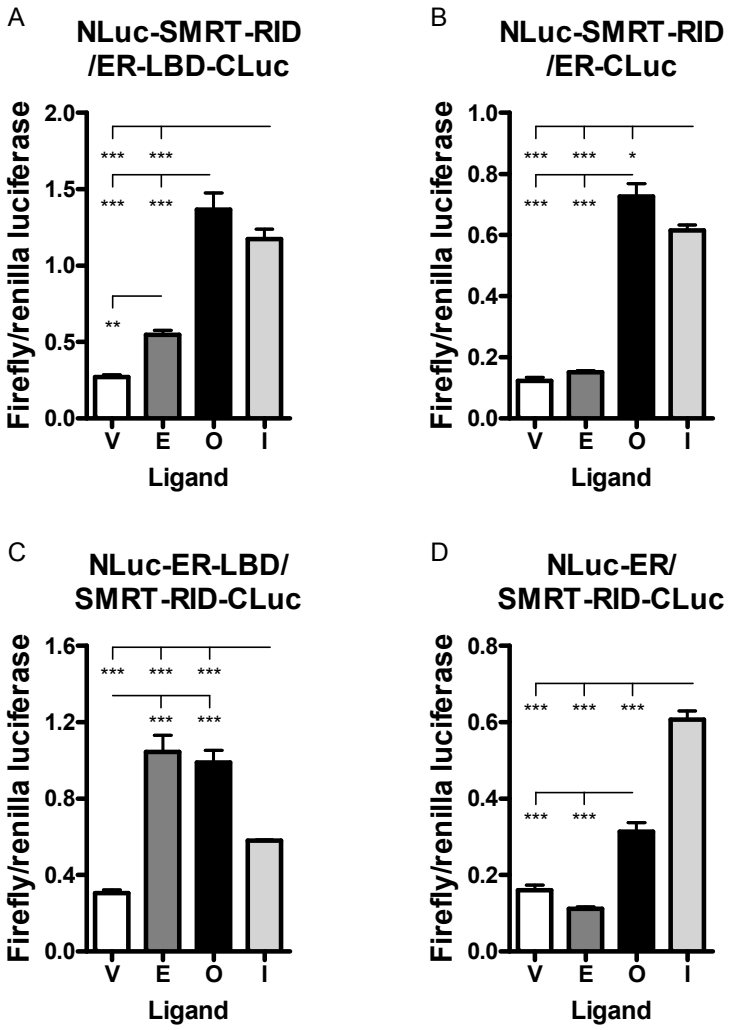

Figure 3.35 - Initial assessment of SMRT-RID constructs. $4x10^4$ 293H cells were transfected with 50ng *Renilla* luciferase and 150ng of NLuc-SMRT-RID with either ER-LBD-CLuc (A) or ER-CLuc (B) or SMRT-RID-CLuc with either NLuc-ER-LBD (C) or NLuc-ER (D). Cells were treated with vehicle (ethanol; V) or 10^{-6}M E2 (E), OHT (O) or ICI (I) for 48 hours prior to quantification of luciferase activities. Mean firefly luciferase activities (n = 3) normalized to *Renilla* luciferase activities are shown. Error bars represent the standard errors of the mean (SEM). The ANOVA test was used to determine statistical significance (***, $p \leq 0.001$, **, $p \leq 0.01$, *, $p \leq 0.05$).

and ICI. With both the full length and truncated ERα fusion protein, NLuc-SMRT-RID complementation was slightly greater with OHT treatment versus ICI. The most notable difference between the transfections of NLuc-SMRT-RID with the full length and truncated ERα fusion proteins was the complementation observed with E2; with full length ERα, only a very slight increase in luciferase activity was observed, whereas with the truncated ER-LBD fusion protein the luciferase activity doubled.

Transfection of the reverse orientation fusion proteins, e.g. SMRT-RID fragment fused to CLuc and the full length or truncated ERα fragment fused to NLuc, produced less consistent results. Cotransfection of NLuc-ER with SMRT-RID-CLuc produced results roughly similar to the NLuc-SMRT-RID/ER-(LBD)-CLuc transfections; higher complementation was observed with antiestrogen treatment compared to vehicle and E2 treated cells. However, in NLuc-ER/SMRT-RID-CLuc transfected cells, complementation was greatest with ICI rather than OHT treatment and E2 treatment resulted in a decrease in luciferase activity relative to vehicle.

Contrary to all the other SMRT-RID transfections, however, the NLuc-ER-LBD/SMRT-RID-CLuc transfected cells produced results inconsistent with our understanding of ERα-corepressor interaction; the greatest complementation was observed with E2 treatment, OHT treatment produced roughly similar luciferase activity and incubation with ICI resulted in intermediate luciferase activity.

In order to ascertain whether the different complementation patterns observed with NLuc-ER-LBD/SMRT-RID-CLuc transfected cells were attributable to protein

localisation, immunofluorescence was performed on cells treated with E2, OHT and ICI (Figure 3.36).

Results from the immunofluorescence broadly agreed with previous experiments which had indicated that the full length ERα fusion proteins are predominantly nuclear in localisation whereas the truncated ERα fusion proteins are predominantly cytoplasmic. Staining for SMRT indicated that SMRT-RID-CLuc was localized within the nucleus and cytoplasm, consistent with its ability to complement with both the truncated and full-length ERα fusion proteins. The NLuc-SMRT-RID fusion protein appeared to be predominantly cytoplasmic in localization, which might account for the higher overall activity observed when co-transfected ER-LBD-CLuc than with ER-CLuc.

No localization patterns were observed which would account for the complementation pattern observed in NLuc-ER-LBD/SMRT-RID-CLuc transfected cells; NLuc-ER-LBD was consistently cytoplasmic and SMRT-RID-CLuc staining was either diffuse over the nucleus and cytoplasm, or in the case of ICI treatment, more intensely cytoplasmic.

ICI treatment had a similar effect on localization in NLuc-ER/SMRT-RID-CLuc transfected cells, where staining for NLuc-ER was more diffuse over the nucleus and cytoplasm in ICI treated cells.

In NLuc-SMRT-RID/ER-LBD-CLuc transfected cells, where both constructs were predominantly cytoplasmic or had a diffuse distribution, ICI treatment resulted in staining for both proteins becoming intensely nuclear in a small proportion of cells.

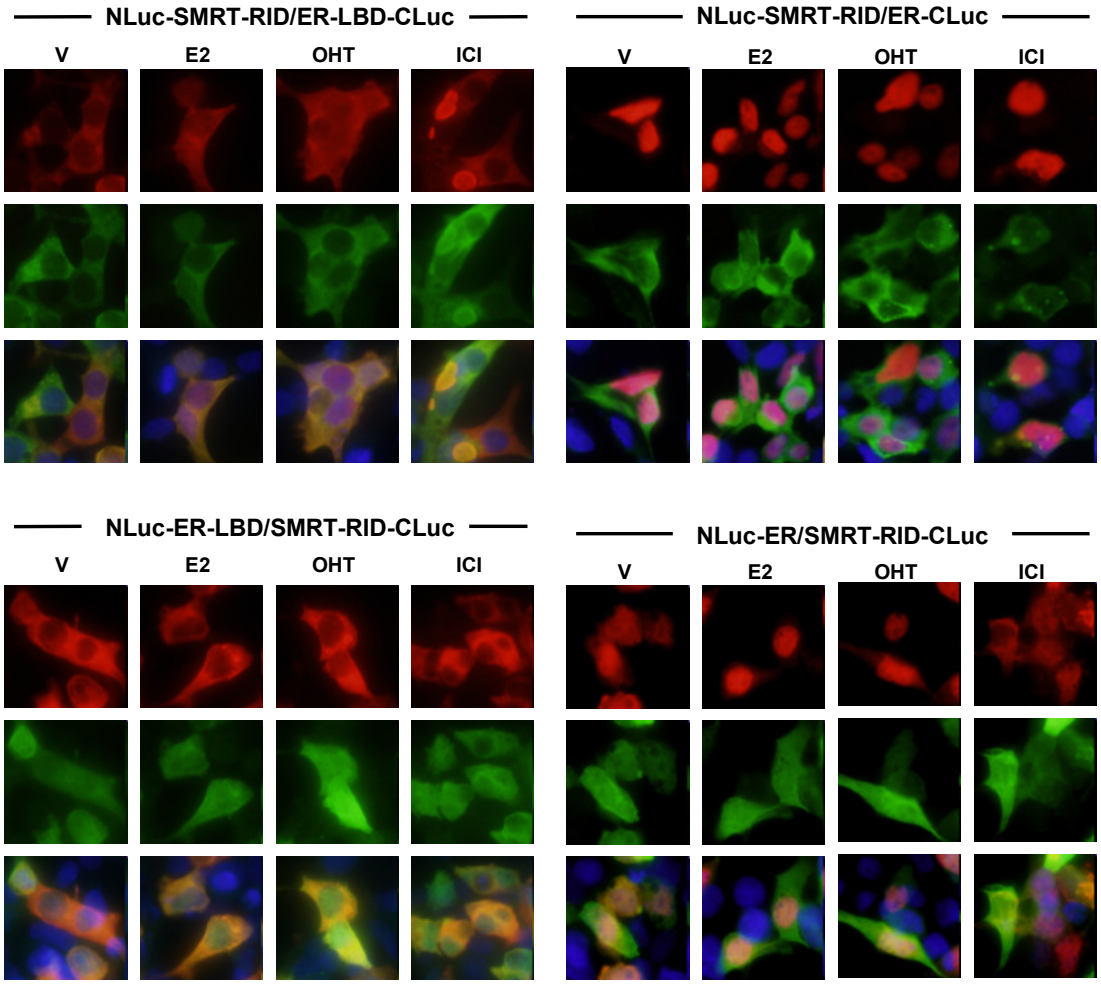

Figure 3.36 - Immunofluorescence of SMRT-RID constructs. $4x10^4$ 293 cells were seeded into chamber slides prior to transfection with NLuc-SMRT-RID/ER-LBD-CLuc, NLuc-SMRT-RID/ER-CLuc, NLuc-ER-LBD/SMRT-RID-CLuc or NLuc-ER/SMRT-RID-CLuc. Cells were treated with vehicle (ethanol; V) or 10^{-6}M E2, OHT or ICI for 24 hours prior to staining with mouse-anti-ERα/Alexa Fluor 594 antibodies and rabbit anti-SMRT/Alexa Fluor 488 antibodies. Slides were mounted with Prolong Gold Antifade with DAPI. Photographs show ERα (red), SMRT (green) and a merged image with DAPI stained nuclei (blue).

This effect was only observed in an estimated 20-30% of the cell population, but where it did occur, the altered localization appeared to affect both proteins.

Although I still did not entirely appreciate the reasons for the different ligand complementation patterns observed with the different fusion protein orientations/combinations in the SMRT-RID split-luciferase assay, a more comprehensive ligand titration was performed (Figure 3.37).

As previously observed, NLuc-SMRT-RID/ER-LBD-CLuc and NLuc-SMRT-RID/ER-CLuc showed approximately similar responses to the ligands tested, particularly the antiestrogens OHT and ICI. OHT produced the greatest increase in signal, 5- and 6-fold vehicle levels when transfected with ER-LBD-CLuc and ER-CLuc, respectively. The increase in signal with OHT incubation was incremental, reaching a maximum at 10^{-6}M OHT. The increased activity observed with ICI was slightly less than that observed with OHT with both ER-LBD-CLuc and ER-CLuc; incubation with 10^{-6}M ICI produced luciferase activity 4- and 5-fold vehicle levels when NLuc-SMRT-RID was transfected with ER-LBD-CLuc and ER-CLuc, respectively. In the presence of increasing quantities of E2, NLuc-SMRT-RID/ER-LBD-CLuc showed incremental increases in activity reaching a maximum 2-fold increase in luciferase activity with 10^{-7}M ligand. NLuc-SMRT-RID/ER-CLuc also showed a similar step-wise increase in activity although the actual increase was only a very modest 1.25-fold vehicle activity.

In NLuc-ER/SMRT-RID-CLuc transfected cells the response to the ligands was roughly similar to those observed with NLuc-SMRT-RID and ER-CLuc, although the

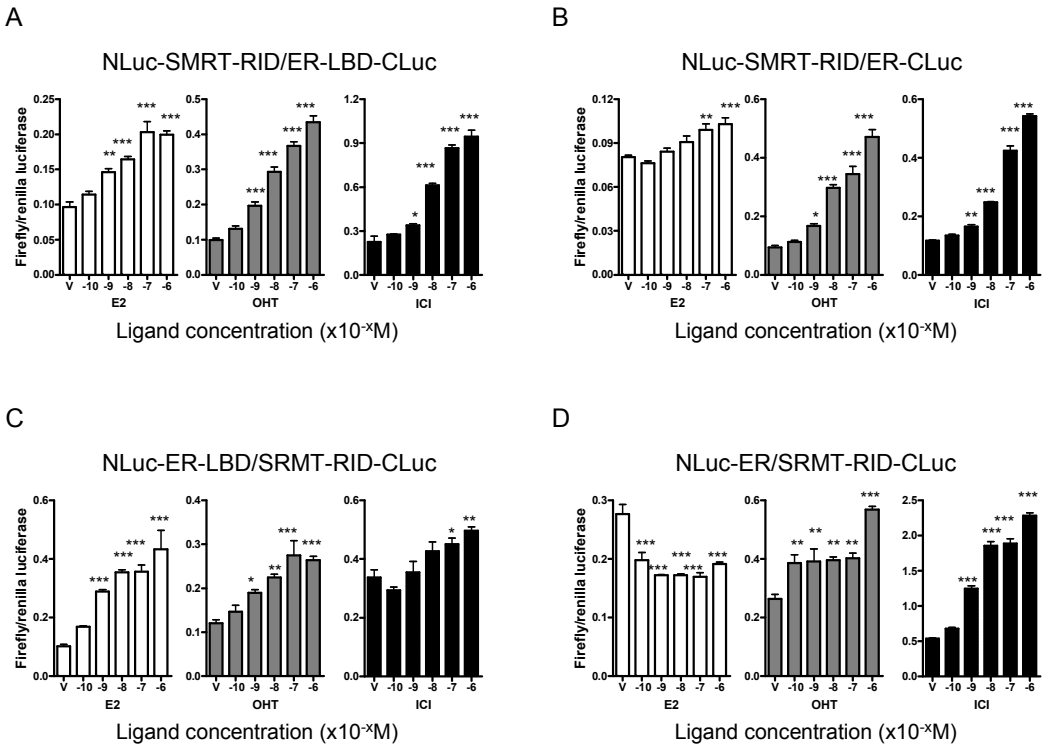

Figure 3.37 - Ligand titration on SMRT-RID constructs. 4x10^4 293H cells were transfected with 50ng *Renilla* luciferase and 150ng of NLuc-SMRT-RID, ER-LBD-CLuc, ER-CLuc, SMRT-RID-CLuc, NLuc-ER-LBD and NLuc-ER as indicated. Cells were treated with vehicle (ethanol; V) or increasing concentrations of E2, OHT or ICI for 48 hours prior to quantification of luciferase activities. Mean firefly luciferase activities (n = 3) normalized to *Renilla* luciferase activities are shown. Error bars represent the standard errors of the mean (SEM). The ANOVA test was used to determine statistical significance relative to vehicle treatment (***, $p \leq 0.001$, **, $p \leq 0.01$, *, $p \leq 0.05$).

potency of the antiestrogens was reversed; a 4-fold increase in signal intensity was observed in the presence of 10^{-6}M ICI and 2-fold the vehicle luciferase activity was observed with 10^{-6}M OHT. In the presence of E2, a 30% decrease in signal intensity was observed. Interestingly, the NLuc-ER/SMRT-RID-CLuc transfected cells appeared to be more responsive to low concentrations of ligand than the NLuc-SMRT-RID/ER(-LBD)-CLuc transfected cells, the maximum change in signal in response to E2 was observed with 10^{-9}M ligand in the NLuc-ER/SMRT-RID-CLuc transfected cells. Similarly, a greater proportion of the overall increase in signal intensity was stimulated by lower levels of the antiestrogens in NLuc-ER/SMRT-RID-CLuc transfected cells, although the signal continued to increase up to 10^{-6}M ligand. For example, in NLuc-ER/SMRT-RID-CLuc transfected cells approximately 40% of the total signal increase was observed with 10^{-10}M OHT and 10^{-9}M ICI compared to 5% and 15% of the respective signal increase in NLuc-SMRT-RID/ER-CLuc transfected cells.

Contrary to expectations, but in agreement with the initial transfection, NLuc-ER-LBD/SMRT-RID-CLuc transfected cells showed the greatest increase in signal with E2 and OHT, 3.5- and 3-fold respectively. In the presence of 10^{-6}M ICI a 2-fold increase was observed. The increases in signal observed with this construct pair were all very incremental, reaching a maximum 10^{-7}M or 10^{-6}M ligand.

Results from the ligand titration experiments on the SMRT-RID split-luciferase constructs produced mixed and contradictory results, which were difficult to interpret without a comparative tool to indicate the endogenous scenario. Efforts were made to establish an immunoprecipitation method to determine how ERα-SMRT interactions

alter with ligand treatment, but were not successful in the time allowed. As such, the SMRT split-luciferase assay was not developed any further.

Chapter 4 Discussion

ERα action requires the recruitment of coregulator proteins that facilitate gene regulation. Estrogen promotes coactivator recruitment while antiestrogens can promote coactivator and corepressor recruitment in a tissue and ligand selective manner. This suggests that it should be possible to visualize the tissue selective action of selective estrogen receptor modulators *in vivo* by imaging ERα coregulator interactions. The work presented here indicates that a split-luciferase assay can be successfully used to image the association of ERα with its coregulators; estrogen stimulation of luciferase fragment complementation could be detected in cells expressing ERα/AIB1 split-luciferase fusion proteins and increased luciferase activity was observed with antiestrogen treatment of cells expressing the SMRT/ER fusion proteins. The experiments conducted show that the split-luciferase assay is suitable for imaging ERα-coregulator interactions *in vitro* and *in vivo*. The primed nature of the split-luciferase assay enabled changes in protein-protein interaction to be detected within 15 minutes of ligand addition and the potential for imaging interaction dynamics using this system was demonstrated.

The ERα-AIB1 coactivator interaction assay was developed as a means of assessing ERα receptor activation. ER-LBD and AIB-RID luciferase fusion protein constructs with each protein cloned in the N-terminal and C-terminal luciferase configurations were produced. As flexible spacers between fusion protein partners have previously been successfully applied, constructs with similar spacer regions were also generated.

In 293 cells transiently transfected with NLuc-SS-AIB-RID/ER-LBD-SS-CLuc and NLuc-ER-LBD/AIB-RID-SS-CLuc, E2 stimulated luciferase fragment complementation occurred with 10^{-9}M and 10^{-10}M E2 and above, respectively. For

both construct pairs maximum stimulation was observed with 10^{-6}M E2 and approximately 50% of maximal activity was observed with 10^{-9}M E2. This is consistent with the dissociation constant (Kd) of E2 bound ERα, which is generally reported to be in the range of 10^{-10} to 10^{-9}M E2 (Anstead et al., 1997). The 50% maximum luciferase fragment complementation observed with 10^{-9}M E2 is also broadly consistent with a study of the binding affinity of E2 bound ERα for peptides encoding the 3 individual nuclear receptor boxes of AIB1. This study found the Kd of nuclear receptor boxes I and II of AIB1 for E2 bound ERα to be in the region of $2x10^{-7}$M (no interaction was detectable for nuclear receptor box III). The authors noted that the affinity of the native coactivator would likely be greater, due to cooperative binding of more than one LXXLL motif (Bramlett et al., 2001). The peak ER-AIB1 interaction observed with 10^{-6}M E2 using the ER-LBD/AIB-RID split-luciferase reporters, is also in agreement with yeast two hybrid and GST-pull down assays investigating ERα-AIB1 interactions; these studies have reported that maximum interaction occurred with E2 concentrations of 10^{-5}M and 10^{-6}M for yeast two hybrid and GST-pull down assays, respectively (Kraichely et al., 2000).

The specificity of the observed split-luciferase complementation to E2 induced interaction between the ER-LBD and AIB-RID fragments was confirmed by antiestrogen modulation of the interaction, mutant ER-LBD constructs and cotransfection of ER-LBD/AIB-RID constructs with the reciprocal FRB/FKBP12 constructs. Contrary to expectations, cotransfection of NLuc-AIB-RID with FKBP12-CLuc resulted in a productive interaction which was modulated by rapamycin. Although this was unexpected, it may represent genuine interaction between FKBP12 and AIB1: FKBP12 is a peptidyl-propyl isomerase (PPI) and other

members of the PPI family have been shown to interact with the AIB-RID (Siekierka et al., 1989, Yi et al., 2005). Peptidyl-propyl isomerase 1 (Pin1) has been shown to interact with amino acids 582-840 of AIB1 (the specific fragment used in this study) in a phosphorylation dependent manner to modulate interactions with p300 and enhance transcription stimulatory activity (Yi et al., 2005). Whether this is a genuine interaction or an artefact of protein fusion and/or overexpression could be determined by cotransfection of NLuc-AIB1-RID with CLuc alone or CLuc fused to another example protein such as Myo or Id (Paulmurugan et al., 2002).

The fold change in luciferase activity that was stimulated with E2 incubation of ER-LBD/AIB-RID transfected cells was consistently less than that observed with rapamycin incubation of NLuc-FRB/FKBP12-CLuc transfected cells. A similar situation was also observed for SMRT-RID/ER(-LBD) complementation . This could be partly attributable to the transient nature of ERα-coregulator interactions and the lower affinity of interaction between ERα-E2 and AIB1 than that of FKBP12-rapamycin and FRB: approximately $2x10^{-7}$M versus $1.2x10^{-8}$M, respectively (Metivier et al., 2003, Shang et al., 2000, Bramlett et al., 2001, Banaszynski et al., 2005). The greater fold induction observed with the FRB/FKBP12 reporters could also be enhanced by the reported absence of interaction between FRB and FKBP12 in rapamycin free conditions (Banaszynski et al., 2005). However, the variability in fold induction observed with the different ER-LBD/AIB-RID fusion proteins in different orientations and in the presence or absence of spacers, indicates that some of the difference in induction observed is attributable to the specific fusion proteins encoded by the split-luciferase constructs. Previous studies have indicated that assisted luciferase fragment complementation can be significantly altered with changes in the

protein orientation and that inclusion of spacers between fusion protein moieties can enhance the function of the fusion partner domains, including their enzymatic activity, presumably by reducing interference between fusion partners (Paulmurugan and Gambhir, 2007, Galarneau et al., 2002, Newton et al., 1996, Arai et al., 2001). From the present studies, it is unclear whether the altered patterns of luciferase fragment complementation observed are attributable to different fusion protein combinations improving ER-LBD/AIB-RID fragment interaction or the efficiency of luciferase fragment complementation. Immunoprecipitation experiments might provide further insight by directly measuring ER-AIB interaction.

Although *in vitro* characterisation indicated that E2 stimulated a greater increase in luciferase activity with NLuc-ER-LBD/AIB-RID-SS-CLuc than NLuc-SS-AIB-RID/ER-LBD-SS-CLuc (10- versus 4-fold, respectively), E2 stimulation *in vivo* produced approximately 7-fold increase in luciferase activity with both constructs pairs. In the same experiment, an approximately 20-fold increase in luciferase activity was observed in the MELN cell line. The reason for the increased fold induction observed with the NLuc-SS-AIB-RID/ER-LBD-SS-CLuc transfected 293 and MELN cells could be attributable to a relatively low background signal in the placebo treated mice, which might, at least in part, be due a reduced influence of estrogen mimics found in tissue culture plastics (Halden, 2010). This effect would be expected to be, and was, most pronounced in the MELN cell line, which is particularly sensitive to low concentrations of E2. A similar increase in fold induction *in vivo* relative to *in vitro* has been observed with a FRB-FKBP12 split-luciferase reporter. In this case, the authors attributed the changes to improved cell permeability *in vivo* allowing a better delivery of rapamycin (Luker et al., 2004). Contrary to the

other reporters, the NLuc-ER-LBD/AIB-RID-SS-CLuc transfected cells showed a reduction in fold induction with E2 treatment *in vivo* (approximately 7-fold versus 10-fold *in vitro*). However this reporter was also the only one to show reduced activity with OHT treatment relative to placebo *in vivo*, suggesting complementation had been stimulated in some manner, possibly prior to implantation.

Although interaction/complementation kinetics were not investigated *in vivo*, in transiently transfected 293 cells, an E2 stimulated increase in luciferase activity could be observed with both split-luciferase reporters after 15 minutes of ligand addition. With longer E2 incubations, the luciferase signal increased and reached a near maximum after 2 hours. This relatively gradual increase in ER-LBD/AIB-RID interaction is in agreement with IP experiments reported in the literature which indicate greater interaction between endogenous ERα and AIB1 after 3.5 versus 0.5 hours E2 incubation (Tikkanen et al., 2000). Most studies of the kinetics of luciferase fragment complementation suggest a plateau in complementation between luciferase fragments is reached 10-15 minutes after addition of the interaction inducer, although some studies report a maximum being reached within 1-2 minutes (Taneoka et al., 2009, Luker et al., 2008, Kim et al., 2007a, Yang et al., 2009). This suggests that the time required to reach a signal plateau in the ER-LBD/AIB-RID assay is a reflection of the interaction kinetics, not a limitation of the time required for the luciferase fragments to complement. Some studies have reported a requirement of several hours to reach a signal maximum, but this has been attributed to the timeframe of changes in receptor conformation or the membrane permeability to ligand, not a requirement of the luciferase fragments to complement (Luker et al., 2004, Luker et al., 2008).

However, it should be noted that none of these studies use the exact luciferase fragments used in the present study.

The ability to image interaction dynamics was investigated by addition of the competitive inhibitor OHT to E2 stimulated cells; in 293 cells transiently transfected with the ER-LBD/AIB-RID split-luciferase constructs, a reduction in luciferase activity was observed within 15 minutes of OHT addition. Although inconsistencies were noted in the "minute" and "hour" time-course studies of signal ablation, depending on the specific construct pair, full ablation of the E2 induced signal was observed after 4-8 hours OHT incubation. The reduced induction observed with E2 and slower decline in signal observed with OHT in the minute time-course studies is most likely a consequence of sub-optimal culture conditions, brought about by removal of the plates from the incubator for ligand addition every 15 minutes. In contrast to fluorescent protein complementation assays, which are generally regarded to be irreversible, luciferase fragment complementation assays are thought to be more reversible; if the interacting proteins of interest cease to interact then the luciferase fragments will dissociate and cease to complement (Hu et al., 2002, Magliery et al., 2005, Nyfeler et al., 2005). Split-luciferase assays using *Renilla*, Gaussia and click beetle luciferases have all been argued to be reversible, although only one report uses an inhibitor of protein translation to fundamentally determine that the loss of luciferase activity observed is independent of protein turnover (Villalobos et al., 2010, Remy and Michnick, 2006, Stefan et al., 2007). In general, these kinetics studies have shown that a reversal of luciferase fragment complementation occurs within 10-30 minutes. However, a study of the association of the androgen receptor with a coactivator LXXLL motif, which claims the interaction of the click beetle fragments

is reversible (although no translation inhibitor is used), indicates that full signal ablation is not observed until 2 hours after ligand removal (Kim et al., 2007b). This is a very similar timeframe to that observed in the present study for the dissociation of the ER-LBD and AIB-RID LXXLL-based interaction, and could suggest that the change in signal observed with OHT addition is reflective of ER-AIB interaction, not a limitation of luciferase fragment dissociation or protein turn-over. The different timeframes required for signal ablation in NLuc-ER-LBD/AIB-RID-SS-CLuc and NLuc-SS-AIB-RID/ER-LBD-SS-CLuc transfected cells could be a reflection of the specific protein moieties hindering ER-LBD/AIB-RID dissociation in the NLuc-SS-AIB-RID/ER-LBD-SS-CLuc cells; in both transiently transfected 293 cells and in U2OS stable cell lines, the NLuc-SS-AIB-RID/ER-LBD-SS-CLuc luciferase signal took longer to ablate than the NLuc-ER-LBD/AIB-RIB-SS-CLuc signal. However, from the experiments performed, one cannot exclude the possibility that this is a reflection of the stability of the different fusion proteins. It is possible that the firefly luciferase fragments in the ER-LBD/AIB-RID complementation assay do irreversibly lock together and that OHT treatment reduces the luciferase activity by blocking the association of newly translated fusion proteins.

Regardless of the mechanism through which changes in the ligand environment are transposed to an alteration in the luciferase signal, the ability to image changes in protein-protein interactions in a timely fashion is advantageous and could be of great use for *in vitro* screening as well as *in vivo* evaluation of the pharmacodynamics of novel ERα targeted therapies.

Experiments conducted to date indicate that the ER-LBD/AIB-RID split-luciferase reporters can be used to image the action of antiestrogens *in vivo*. Administration of the breast cancer drug Faslodex (ICI) to nude mice was able to reduce the increased complementation observed with E2. The degree of signal ablation observed differed between the two reporters, which may be an artefact or may represent subtle differences in the reporter responses *in vivo*. The differences in signal ablation cannot be attributed to variability in the Faslodex doses administered because each mouse gave a measure for both reporters. Most unexpectedly, administration of Faslodex alone (with placebo rather than E2 pellet) stimulated a high level of luciferase fragment complementation. Although there was considerable variability in the individual measurements, this effect was observed with both reporters and so cannot be attributed to irregular cell implantation. ICI is generally regarded as a "pure" antiestrogen: it exerts no ERα agonist properties. This had been thought to be a result of disrupting nucleocytoplasmic shuttling and increasing turnover of ERα but recent evidence suggests it could be a consequence of the receptor conformation ICI induces (Dauvois et al., 1992, Dauvois et al., 1993, Howell et al., 2000, Wardell et al., 2011). However, in tissues other than breast and endometrium, particularly neurons and bone, there is evidence that ICI exhibits a degree of ER agonist activity, particularly at lower clinically relevant levels (Sibonga et al., 1998, Zhao et al., 2006). As such, it is possible that the split-luciferase activity observed in the Faslodex treated mice is a result of this agonist type activity. However, further investigation would be required to determine whether this effect could be observed *in vitro* and whether it is detected using the split-luciferase reporters in an MCF7 background or in the MELN cell line. It is feasible that this could be a temporary effect which would subside with later imaging time points: this could be better investigated better with the stable cell lines.

Using the antiestrogen OHT, I was unable to attenuate the E2 induced signal of the split-luciferase constructs *in vivo*, although a moderate reduction of the E2 induced signal in the MELN cell line was achieved. The modest reduction observed with the MELN cell line suggests that the concentration of OHT achieved was relatively low. Previous studies have indicated that achieving clinically relevant levels of tamoxifen and its major metabolites in nude mice is challenging because metabolism of the drug is different to that in rat and man (Robinson et al., 1991, DeGregorio et al., 1989, DeGregorio et al., 1987, Kisanga et al., 2003). In circumstances such as this, the ER-SMRT split-luciferase reporter could be particularly useful. Use of the corepressor assay would enable direct appreciation of ERα antagonism, without a reliance on inhibition of an E2 induced signal.

In order to study the interaction of ER with the corepressor SMRT, NLuc and CLuc SMRT-RID fusion proteins were produced and transfected with both full length ERα and truncated ER-LBD constructs. Transfection of NLuc-SMRT-RID with either ER-CLuc or ER-LBD-CLuc, and NLuc-ER with SMRT-RID-CLuc produced broadly similar results, which were consistent with the role of SMRT as an ERα corepressor. Increased luciferase fragment complementation was observed with the antiestrogens OHT and ICI and minimal changes were observed with E2. However, between the different construct pairs there were inconsistencies regarding the action of E2 and which antiestrogen produced the greatest luciferase fragment complementation. Whether these difference complementation patterns are a reflection of different ER(-LBD)/SMRT-RID fusion protein interaction or a reflection of the ability of the luciferase fragments to complement within different protein environments would

require further investigation. IP experiments would also be required to determine which construct pair most faithfully reflects the interaction of ERα and SMRT before proceeding with the ER-corepressor assay.

In contrast to the broadly consistent results obtained with the other ER(-LBD)/SMRT-RID constructs, cotransfection of NLuc-ER-LBD with SMRT-RID-CLuc produced the greatest luciferase fragment complementation in the presence of E2 and OHT, but relatively low complementation with ICI. The similar complementation observed with E2 and OHT is very surprising since the ligands are known to produce distinct receptor conformations which promote or occlude ERα-SMRT interaction (Shiau et al., 1998, Shang and Brown, 2002, Webb et al., 2003). Interestingly, Paulmurugan and Gambhir report similar "ligand pharmacology independent" complementation in a *Renilla* luciferase ER-LBD intramolecular folding sensor. Using this reporter, removal of the ERα F domain (amino acids 549-595) enabled E2 and OHT to be distinguished (Paulmurugan and Gambhir, 2006). Whether removing the F domain from NLuc-ER-LBD would enable differential complementation in response to E2 and OHT when co-transfected with SMRT-RID-CLuc remains unclear. Regardless, the ligand induced complementation pattern observed with NLuc-ER-LBD and SMRT-RID-CLuc suggest they would not make a good ER-SMRT interaction reporter.

One of the principal aims in developing the ERα split-luciferase assay was to determine whether the method could be employed to visualise the tissue selective actions of ERα ligands. To this end, the ER-LBD/AIB-RID constructs were stably transformed into MCF7 breast cancer and U2OS osteosarcoma cell lines. A

comparison of the E2 response in the U2OS and MCF7 cells lines indicated that tissue selective patterns of luciferase fragment complementation could be detected. In U2OS cell lines stably expressing NLuc-ER-LBD and AIB-RID-SS-CLuc, the kinetics and fold induction of E2 stimulated luciferase activity was consistently more rapid and of greater magnitude than in MCF7 cells expressing the same fusion proteins. Similarly, the signal ablation observed with OHT addition to E2 stimulated cells was also much more rapid in the U2OS compared to MCF7 stable cell lines. Although the influence of fusion protein stability on these patterns of complementation would need to be confirmed, the results obtained indicate that the split-luciferase assay is sensitive to the specific cellular context and therefore offers the potential to image tissue specific interactions between ERα and AIB1. The tissue specific complementation patterns observed with the ER-LBD/AIB-RID split-luciferase reporters in U2OS and MCF7 cells is supported by previous ChIP and ERE-luciferase transgenic mice studies which have shown that the transcriptional response to E2 is cell type specific and that different tissues show a different time-course and amplitude of signal in response to E2 (Della Torre et al., 2011, Rando et al., 2010, Frasor et al., 2003, Krum et al., 2008).

Though some tissue specific patterns of complementation could be observed with the ER-LBD/AIB-RID split-luciferase constructs, I was unable to detect the agonist actions of OHT in bone or endometrial cell lines. OHT produced a similar ERα antagonist response in the ER-LBD/AIB-RID split-luciferase reporters in breast, bone and endometrial cell lines, which made it indistinguishable from the pure antiestrogen ICI. This is perhaps somewhat unsurprising given that the antagonist actions of OHT have been attributed to the N terminal AF1 region, which is absent from the ER-LBD

fusion proteins (Berry et al., 1990). In order to most accurately reflect endogenous ERα-AIB1 interaction, luciferase fusion proteins with full-length ERα and AIB1 would be required. Full length proteins would be receptive to the alterations in cell signalling and protein-protein interactions which regulate the interaction of ERα and AIB1. During the course of the project, extensive efforts were made to produce full length ERα and AIB1 fusion proteins. After initial cloning difficulties, NLuc and CLuc full length fusion proteins were produced and transient transfection of constructs indicated that E2 stimulated an increase in luciferase activity. However, because the luminescent signal was very low, stable cell line generation was initiated prior to characterization. Unfortunately, time constraints prevented completion of the work to generate such lines and therefore it was not possible to determine the impact of full length proteins on the split-luciferase assay.

4.1 Conclusions and Future Directions

Luciferase imaging is a powerful tool for non-invasive preclinical imaging. It offers the potential for relatively cheap, sensitive and high throughput imaging of tumour biology in modified cells or organisms. The present study has shown that using ER-LBD, AIB-RID and SMRT-RID luciferase fragment fusion proteins, the interaction of ERα with its coactivator and corepressor can be imaged. Although the assay requires further validation, the split-luciferase method offers distinct advantages over previously used fluorescence based techniques for imaging ERα-coregulator interaction: namely, that the luciferase method can be applied to *in vivo* imaging of protein-protein interactions. This would allow the modulation of interactions in a native tumour environment to be appreciated. Previous *in vivo* studies of ERα activity have focused on transcriptional reporters, which although undoubtedly a valuable

technique, are limited in their potential to image the dynamics of ERα activation because of the lag associated with signal accumulation and ablation. Furthermore, imaging ERα-coregulator interactions, which are assumed to be common to all E2 regulated genes and are a prerequisite for transcription of estrogen-regulated genes, could be considered broader and more indicative of the global ERα signalling than transcriptional reporters, which focus on the activity of ERα and ERβ at a select number of promoters or genes.

In the stable cell line format, the present assay offers a fast, easy and potentially high throughput method for assessing alterations in E2 induced ER-AIB1 interaction and could be applied to the screening of novel compounds. The assay could be particularly useful for novel compounds which aim to block the ERα-LXXLL interaction, rather than targeting the ligand binding pocket (Galande et al., 2005, Geistlinger et al., 2004, Gunther et al., 2008, Rodriguez et al., 2004). Although less developed, the ER-LBD-SMRT-RID offers similar potential for screening novel antiestrogens which induce a conformation that promotes corepressor binding. The capacity to screen compounds in an appropriate cellular background offers advantages over other high throughput cell free systems. And the ability to transfer the split-luciferase method from a high throughput screening tool to an *in vivo* method for studying the pharmacodynamics of newly identified compounds is also beneficial.

Using the current ER-LBD/AIB-RID assay, the potential for imaging tissue specific ERα-AIB1 interactions was alluded to. However, in order to maximise the sensitivity of the assay to the detection of tissue specific endogenous interactions, the assay would be best performed using full-length receptor/coregulator fusion proteins. Using

such proteins, the impact of post-translational modification, interactions with other proteins and native protein regulation, could be appreciated on the interaction of ERα with its coregulators. Similar to the ERE-luciferase mice, transgenic mice expressing the full length ERα/coregulator fusion proteins could be generated to visualise the impact of E2 signalling in different tissues at different stages of the estrus cycle and in response to different ER ligands. However, because of the potential transformative effects of over-expressing ERα and AIB1, transgenic knock-in mice would need to be established. This would ensure appropriate expression levels of both proteins in tissues and would ensure that overexpression of the proteins was not altering the native signalling in different cell types. However, with a native expression system difficulties could be encountered in imaging ERα-AIB1 interaction in tissues with relatively low expression levels or in deep tissues. In order to overcome this, the luciferase fragments could be changed to split thymidine kinase fragments, to enable PET imaging of protein-protein interactions or to a genetically encoded BRET system for optical imaging (Dragulescu-Andrasi et al., 2011, Massoud et al., 2010). Switching to a PET system would enable very sensitive, highly resolved, 3D, deep tissue imaging. However, a potential hindrance for the split-luciferase assay is the idiosyncratic nature of assisted complementation between luciferase fragment fusion proteins; it is difficult to know whether results are specific to the interaction between the proteins of interest or related to the ability of the luciferase fragments to complement in a given protein environment or receptor conformation. Changing to a BRET based system could overcome this issue because a BRET signal is produced through the transfer of energy, which is subject to less interference from the protein environment than the complementary folding of protein fragments. A recent study reported successful deep tissue imaging of protein-protein interactions using a novel

BRET system with an emission spectrum of 640nm (Dragulescu-Andrasi et al., 2011). The immediate nature of energy transfer in the BRET system could also improve the potential for imaging interaction kinetics.

In the future, the current split-luciferase based assay could also be developed to image the interaction of ER-LBD with AIB-RID and SMRT-RID in the same cell by using red and green click beetle luciferases, as recently demonstrated (Villalobos et al., 2010). Additionally, the assay could be expanded to investigate the differences between ligand induced ERα and ERβ coregulator recruitment. It has been suggested that some of the tissue specific actions of certain ligands could be attributable to differential activity with ERα and ERβ and there is some interest in developing ERβ specific agonists (Gustafsson, 2003, Meyers et al., 2001). Alternatively, the interaction of ERα and ERβ with a single coregulator could be investigated using the dual colour click beetle system, although the ability of ERα and ERβ to heterodimerise might complicate this (Pace et al., 1997).

Nuclear receptors have been shown to be involved in a number of different human diseases and their ligand dependent transcriptional regulation have made them attractive targets for drug development (Sladek, 2003). The interaction of nuclear receptors with coregulators, and the meaning this has for receptor activity, also makes nuclear receptor-coregulator interactions highly applicable to luciferase fragment complementation assays as a means of gauging receptor activity. As such, the approach detailed in this report could be applied to a number of different nuclear receptor-coregulator protein pairs with the aim of screening novel compounds *in vitro* and confirming and further characterising identified compounds *in vivo*.

Chapter 5 References

ALI, S., METZGER, D., BORNERT, J. M. & CHAMBON, P. 1993. Modulation of transcriptional activation by ligand-dependent phosphorylation of the human oestrogen receptor A/B region. *Embo J,* 12**,** 1153-60.

ANDERSON, E. 2002. Progesterone receptors - animal models and cell signaling in breast cancer: The role of oestrogen and progesterone receptors in human mammary development and tumorigenesis. *Breast Cancer Res,* 4**,** 197 - 201.

ANSTEAD, G. M., CARLSON, K. E. & KATZENELLENBOGEN, J. A. 1997. The estradiol pharmacophore: ligand structure-estrogen receptor binding affinity relationships and a model for the receptor binding site. *Steroids,* 62**,** 268-303.

ANZICK, S. L., KONONEN, J., WALKER, R. L., AZORSA, D. O., TANNER, M. M., GUAN, X. Y., SAUTER, G., KALLIONIEMI, O. P., TRENT, J. M. & MELTZER, P. S. 1997. AIB1, a steroid receptor coactivator amplified in breast and ovarian cancer. *Science,* 277**,** 965-8.

ARAI, R., UEDA, H., KITAYAMA, A., KAMIYA, N. & NAGAMUNE, T. 2001. Design of the linkers which effectively separate domains of a bifunctional fusion protein. *Protein Eng,* 14**,** 529-32.

ARAI, R., WRIGGERS, W., NISHIKAWA, Y., NAGAMUNE, T. & FUJISAWA, T. 2004. Conformations of variably linked chimeric proteins evaluated by synchrotron X-ray small-angle scattering. *Proteins,* 57**,** 829-38.

AWAIS, M., SATO, M. & UMEZAWA, Y. 2007. A fluorescent indicator to visualize ligand-induced receptor/coactivator interactions for screening of peroxisome proliferator-activated receptor gamma ligands in living cells. *Biosens Bioelectron,* 22**,** 2564-9.

BAI, Y. & GIGUERE, V. 2003. Isoform-selective interactions between estrogen receptors and steroid receptor coactivators promoted by estradiol and ErbB-2 signaling in living cells. *Mol Endocrinol,* 17**,** 589-99.

BALAGUER, P., BOUSSIOUX, A. M., DEMIRPENCE, E. & NICOLAS, J. C. 2001. Reporter cell lines are useful tools for monitoring biological activity of nuclear receptor ligands. *Luminescence,* 16**,** 153-8.

BANASZYNSKI, L. A., LIU, C. W. & WANDLESS, T. J. 2005. Characterization of the FKBP.rapamycin.FRB ternary complex. *J Am Chem Soc,* 127**,** 4715-21.

BERGGARD, T., LINSE, S. & JAMES, P. 2007. Methods for the detection and analysis of protein-protein interactions. *Proteomics,* 7**,** 2833-42.

BERRY, M., METZGER, D. & CHAMBON, P. 1990. Role of the two activating domains of the oestrogen receptor in the cell-type and promoter-context dependent agonistic activity of the anti-oestrogen 4-hydroxytamoxifen. *Embo J,* 9**,** 2811-8.

BHAUMIK, S. & GAMBHIR, S. S. 2002. Optical imaging of Renilla luciferase reporter gene expression in living mice. *Proceedings of the National Academy of Sciences,* 99**,** 377-382.

BOURAS, T., SOUTHEY, M. C. & VENTER, D. J. 2001. Overexpression of the Steroid Receptor Coactivator AIB1 in Breast Cancer Correlates with the Absence of Estrogen and Progesterone Receptors and Positivity for p53 and HER2/neu. *Cancer Res,* 61**,** 903-907.

BRAMLETT, K. S., WU, Y. & BURRIS, T. P. 2001. Ligands specify coactivator nuclear receptor (NR) box affinity for estrogen receptor subtypes. *Mol Endocrinol,* 15**,** 909-22.

BRZOZOWSKI, A. M., PIKE, A. C., DAUTER, Z., HUBBARD, R. E., BONN, T., ENGSTROM, O., OHMAN, L., GREENE, G. L., GUSTAFSSON, J. A. & CARLQUIST, M. 1997. Molecular basis of agonism and antagonism in the oestrogen receptor. *Nature,* 389**,** 753-8.

CACERES, G., ZANKINA, R., ZHU, X., JIAO, J. A., WONG, H., ALLER, A. & ANDREOTTI, P. 2003. Determination of chemotherapeutic activity in vivo by luminescent imaging of luciferase-transfected human tumors. *Anticancer Drugs,* 14**,** 569-74.

CENNI, B. & PICARD, D. 1999. Ligand-independent Activation of Steroid Receptors: New Roles for Old Players. *Trends Endocrinol Metab,* 10**,** 41-46.

CHANG, C., NORRIS, J. D., GRON, H., PAIGE, L. A., HAMILTON, P. T., KENAN, D. J., FOWLKES, D. & MCDONNELL, D. P. 1999. Dissection of the LXXLL nuclear receptor-coactivator interaction motif using combinatorial peptide libraries: discovery of peptide antagonists of estrogen receptors alpha and beta. *Mol Cell Biol,* 19**,** 8226-39.

CHEN, D., WASHBROOK, E., SARWAR, N., BATES, G. J., PACE, P. E., THIRUNUVAKKARASU, V., TAYLOR, J., EPSTEIN, R. J., FULLER-PACE, F. V., EGLY, J. M., COOMBES, R. C. & ALI, S. 2002. Phosphorylation of human estrogen receptor alpha at serine 118 by two distinct signal transduction pathways revealed by phosphorylation-specific antisera. *Oncogene,* 21**,** 4921-31.

CHEN, H., LIN, R. J., SCHILTZ, R. L., CHAKRAVARTI, D., NASH, A., NAGY, L., PRIVALSKY, M. L., NAKATANI, Y. & EVANS, R. M. 1997. Nuclear receptor coactivator ACTR is a novel histone acetyltransferase and forms a multimeric activation complex with P/CAF and CBP/p300. *Cell,* 90**,** 569-80.

CHEN, H., ZOU, Y., SHANG, Y., LIN, H., WANG, Y., CAI, R., TANG, X. & ZHOU, J.-M. 2008. Firefly Luciferase Complementation Imaging Assay for Protein-Protein Interactions in Plants. *Plant Physiol.,* 146**,** 368-376.

CHEN, J. D. & EVANS, R. M. 1995. A transcriptional co-repressor that interacts with nuclear hormone receptors. *Nature,* 377**,** 454-7.

CHEN, J. D., UMESONO, K. & EVANS, R. M. 1996. SMRT isoforms mediate repression and anti-repression of nuclear receptor heterodimers. *Proc Natl Acad Sci U S A,* 93**,** 7567-71.

CIANA, P., DI LUCCIO, G., BELCREDITO, S., POLLIO, G., VEGETO, E., TATANGELO, L., TIVERON, C. & MAGGI, A. 2001. Engineering of a mouse for the in vivo profiling of estrogen receptor activity. *Mol Endocrinol,* 15**,** 1104-13.

CIANA, P., RAVISCIONI, M., MUSSI, P., VEGETO, E., QUE, I., PARKER, M. G., LOWIK, C. & MAGGI, A. 2003. In vivo imaging of transcriptionally active estrogen receptors. *Nat Med,* 9**,** 82-6.

CLARK, G. M., OSBORNE, C. K. & MCGUIRE, W. L. 1984. Correlations between estrogen receptor, progesterone receptor, and patient characteristics in human breast cancer. *J Clin Oncol,* 2**,** 1102-9.

CLEMONS, M. & GOSS, P. 2001. Estrogen and the risk of breast cancer. *N Engl J Med,* 344**,** 276-85.

CONTI, E., FRANKS, N. P. & BRICK, P. 1996. Crystal structure of firefly luciferase throws light on a superfamily of adenylate-forming enzymes. *Structure,* 4**,** 287-98.

COPPOLA, J. M., ROSS, B. D. & REHEMTULLA, A. 2008. Noninvasive Imaging of Apoptosis and Its Application in Cancer Therapeutics. *Clin Cancer Res,* 14**,** 2492-2501.

COSTANTINO, J. P., KULLER, L. H., IVES, D. G., FISHER, B. & DIGNAM, J. 1997. Coronary heart disease mortality and adjuvant tamoxifen therapy. *J Natl Cancer Inst,* 89**,** 776-82.

CRUK. 2011a. Available: http://info.cancerresearchuk.org/cancerstats/types/breast/incidence/uk-breast-cancer-incidence-statistics

CRUK. 2011b. Available: http://info.cancerresearchuk.org/cancerstats/types/breast/riskfactors/breast-cancer-risk-factors.

CRUK. 2011c. Available: http://info.cancerresearchuk.org/cancerstats/types/breast/survival/breast-cancer-survival-statistics.

CUZICK, J., POWLES, T., VERONESI, U., FORBES, J., EDWARDS, R., ASHLEY, S. & BOYLE, P. 2003. Overview of the main outcomes in breast-cancer prevention trials. *Lancet,* 361**,** 296-300.

DANIELIAN, P. S., WHITE, R., LEES, J. A. & PARKER, M. G. 1992. Identification of a conserved region required for hormone dependent transcriptional activation by steroid hormone receptors. *Embo J,* 11**,** 1025-33.

DAUVOIS, S., DANIELIAN, P. S., WHITE, R. & PARKER, M. G. 1992. Antiestrogen ICI 164,384 reduces cellular estrogen receptor content by increasing its turnover. *Proc Natl Acad Sci U S A,* 89**,** 4037-41.

DAUVOIS, S., WHITE, R. & PARKER, M. G. 1993. The antiestrogen ICI 182780 disrupts estrogen receptor nucleocytoplasmic shuttling. *J Cell Sci,* 106 (Pt 4)**,** 1377-88.

DAY, R. N., PERIASAMY, A. & SCHAUFELE, F. 2001. Fluorescence Resonance Energy Transfer Microscopy of Localized Protein Interactions in the Living Cell Nucleus. *Methods,* 25**,** 4-18.

DE, A. & GAMBHIR, S. S. 2005. Noninvasive imaging of protein-protein interactions from live cells and living subjects using bioluminescence resonance energy transfer. *FASEB J,* 19**,** 2017-9.

DE, A., RAY, P., LOENING, A. M. & GAMBHIR, S. S. 2009. BRET3: a red-shifted bioluminescence resonance energy transfer (BRET)-based integrated platform for imaging protein-protein interactions from single live cells and living animals. *FASEB J,* 23**,** 2702-9.

DE WET, J. R., WOOD, K. V., DELUCA, M., HELINSKI, D. R. & SUBRAMANI, S. 1987. Firefly luciferase gene: structure and expression in mammalian cells. *Mol Cell Biol,* 7**,** 725-37.

DE WET, J. R., WOOD, K. V., HELINSKI, D. R. & DELUCA, M. 1985. Cloning of firefly luciferase cDNA and the expression of active luciferase in Escherichia coli. *Proc Natl Acad Sci U S A,* 82**,** 7870-3.

DEGREGORIO, M. W., CORONADO, E. & KENT OSBORNE, C. 1989. Tumor and serum tamoxifen concentrations in the athymic nude mouse. *Cancer Chemotherapy and Pharmacology,* 23**,** 68-70.

DEGREGORIO, M. W., WILBUR, B. J., CORONADO, E. & OSBORNE, C. K. 1987. Serum tamoxifen concentrations in the athymic nude mouse after three methods of administration. *Cancer Chemotherapy and Pharmacology,* 20**,** 316-318.

DELLA TORRE, S., BISERNI, A., RANDO, G., MONTELEONE, G., CIANA, P., KOMM, B. & MAGGI, A. 2011. The conundrum of estrogen receptor oscillatory activity in the search for an appropriate hormone replacement therapy. *Endocrinology,* 152**,** 2256-65.

DEMARCO, I. A., PERIASAMY, A., BOOKER, C. F. & DAY, R. N. 2006. Monitoring dynamic protein interactions with photoquenching FRET. *Nat Methods,* 3**,** 519-24.

DONG, J., TSAI-MORRIS, C. H. & DUFAU, M. L. 2006. A novel estradiol/estrogen receptor alpha-dependent transcriptional mechanism controls expression of the human prolactin receptor. *J Biol Chem,* 281**,** 18825-36.

DRAGULESCU-ANDRASI, A., CHAN, C. T., DE, A., MASSOUD, T. F. & GAMBHIR, S. S. 2011. Bioluminescence resonance energy transfer (BRET) imaging of protein–protein interactions within deep tissues of living subjects. *Proceedings of the National Academy of Sciences,* 108**,** 12060-12065.

EBCTCG 1992. Systemic treatment of early breast cancer by hormonal, cytotoxic, or immune therapy. 133 randomised trials involving 31,000 recurrences and 24,000 deaths among 75,000 women. Early Breast Cancer Trialists' Collaborative Group. *Lancet,* 339**,** 71-85.

EBCTCG 1998. Tamoxifen for early breast cancer: an overview of the randomised trials. Early Breast Cancer Trialists' Collaborative Group. *Lancet,* 351**,** 1451-67.

EL-TANANI, M. K. & GREEN, C. D. 1997. Two separate mechanisms for ligand-independent activation of the estrogen receptor. *Mol Endocrinol,* 11**,** 928-37.

ENMARK, E. & GUSTAFSSON, J. A. 1999. Oestrogen receptors - an overview. *J Intern Med,* 246**,** 133-8.

ENMARK, E., PELTO-HUIKKO, M., GRANDIEN, K., LAGERCRANTZ, S., LAGERCRANTZ, J., FRIED, G., NORDENSKJÖLD, M. & GUSTAFSSON, J.-Å. 1997. Human Estrogen Receptor β-Gene Structure, Chromosomal Localization, and Expression Pattern. *Journal of Clinical Endocrinology & Metabolism,* 82**,** 4258-4265.

FERLAY J, S. H., BRAY F, FORMAN D, MATHERS C, PARKIN DM. 2010. *GLOBOCAN 2008, Cancer Incidence and Mortality Worldwide: IARC CancerBase No. 10 [Internet]* [Online]. Lyon, France: International Agency for Research on Cancer; 2010. Available: Available from: http://globocan.iarc.fr.

FERNANDEZ, S. M. & BERLIN, R. D. 1976. Cell surface distribution of lectin receptors determined by resonance energy transfer. *Nature,* 264**,** 411-415.

FISHER, B., COSTANTINO, J. P., REDMOND, C. K., FISHER, E. R., WICKERHAM, D. L. & CRONIN, W. M. 1994. Endometrial cancer in tamoxifen-treated breast cancer patients: findings from the National Surgical Adjuvant Breast and Bowel Project (NSABP) B-14. *J Natl Cancer Inst,* 86**,** 527-37.

FISHER, B., COSTANTINO, J. P., WICKERHAM, D. L., CECCHINI, R. S., CRONIN, W. M., ROBIDOUX, A., BEVERS, T. B., KAVANAH, M. T., ATKINS, J. N., MARGOLESE, R. G., RUNOWICZ, C. D., JAMES, J. M., FORD, L. G. & WOLMARK, N. 2005. Tamoxifen for the prevention of breast cancer: current status of the National Surgical Adjuvant Breast and Bowel Project P-1 study. *J Natl Cancer Inst,* 97**,** 1652-62.

FISHER, B., COSTANTINO, J. P., WICKERHAM, D. L., REDMOND, C. K., KAVANAH, M., CRONIN, W. M., VOGEL, V., ROBIDOUX, A.,

DIMITROV, N., ATKINS, J., DALY, M., WIEAND, S., TAN-CHIU, E., FORD, L. & WOLMARK, N. 1998. Tamoxifen for prevention of breast cancer: report of the National Surgical Adjuvant Breast and Bowel Project P-1 Study. *J Natl Cancer Inst,* 90**,** 1371-88.

FONT DE MORA, J. & BROWN, M. 2000. AIB1 is a conduit for kinase-mediated growth factor signaling to the estrogen receptor. *Mol Cell Biol,* 20**,** 5041-7.

FORNANDER, T., RUTQVIST, L. E., CEDERMARK, B., GLAS, U., MATTSSON, A., SILFVERSWARD, C., SKOOG, L., SOMELL, A., THEVE, T., WILKING, N. & ET AL. 1989. Adjuvant tamoxifen in early breast cancer: occurrence of new primary cancers. *Lancet,* 1**,** 117-20.

FRASOR, J., DANES, J. M., KOMM, B., CHANG, K. C. N., LYTTLE, C. R. & KATZENELLENBOGEN, B. S. 2003. Profiling of Estrogen Up- and Down-Regulated Gene Expression in Human Breast Cancer Cells: Insights into Gene Networks and Pathways Underlying Estrogenic Control of Proliferation and Cell Phenotype. *Endocrinology,* 144**,** 4562-4574.

GALANDE, A. K., BRAMLETT, K. S., TRENT, J. O., BURRIS, T. P., WITTLIFF, J. L. & SPATOLA, A. F. 2005. Potent inhibitors of LXXLL-based protein-protein interactions. *Chembiochem,* 6**,** 1991-8.

GALARNEAU, A., PRIMEAU, M., TRUDEAU, L. E. & MICHNICK, S. W. 2002. Beta-lactamase protein fragment complementation assays as in vivo and in vitro sensors of protein protein interactions. *Nat Biotechnol,* 20**,** 619-22.

GEISTLINGER, T. R., MCREYNOLDS, A. C. & GUY, R. K. 2004. Ligand-selective inhibition of the interaction of steroid receptor coactivators and estrogen receptor isoforms. *Chem Biol,* 11**,** 273-81.

GLASS, C. K. & ROSENFELD, M. G. 2000. The coregulator exchange in transcriptional functions of nuclear receptors. *Genes Dev,* 14**,** 121-41.

GOJIS, O., RUDRARAJU, B., GUDI, M., HOGBEN, K., SOUSHA, S., COOMBES, R. C., CLEATOR, S. & PALMIERI, C. 2010. The role of SRC-3 in human breast cancer. *Nat Rev Clin Oncol,* 7**,** 83-9.

GREEN, K. A. & CARROLL, J. S. 2007. Oestrogen-receptor-mediated transcription and the influence of co-factors and chromatin state. *Nat Rev Cancer,* 7**,** 713-722.

GUNTHER, J. R., MOORE, T. W., COLLINS, M. L. & KATZENELLENBOGEN, J. A. 2008. Amphipathic benzenes are designed inhibitors of the estrogen receptor alpha/steroid receptor coactivator interaction. *ACS Chem Biol,* 3**,** 282-6.

GUSTAFSSON, J. A. 2003. What pharmacologists can learn from recent advances in estrogen signalling. *Trends Pharmacol Sci,* 24**,** 479-85.

HALDEN, R. U. 2010. Plastics and health risks. *Annu Rev Public Health,* 31**,** 179-94.

HAN, S. J., O'MALLEY, B. W. & DEMAYO, F. J. 2009. An estrogen receptor alpha activity indicator model in mice. *Genesis,* 47**,** 815-24.

HARTMAN, J., STRÖM, A. & GUSTAFSSON, J.-Å. 2009. Estrogen receptor beta in breast cancer--Diagnostic and therapeutic implications. *Steroids,* 74**,** 635-641.

HASTINGS, J. W. 1983. Biological diversity, chemical mechanisms, and the evolutionary origins of bioluminescent systems. *Journal of Molecular Evolution,* 19**,** 309-321.

HASTINGS, J. W. 1996. Chemistries and colors of bioluminescent reactions: a review. *Gene,* 173**,** 5-11.

HEERY, D. M., KALKHOVEN, E., HOARE, S. & PARKER, M. G. 1997. A signature motif in transcriptional co-activators mediates binding to nuclear receptors. *Nature,* 387**,** 733-6.

HELDRING, N., PIKE, A., ANDERSSON, S., MATTHEWS, J., CHENG, G., HARTMAN, J., TUJAGUE, M., STROM, A., TREUTER, E., WARNER, M. & GUSTAFSSON, J. A. 2007. Estrogen receptors: how do they signal and what are their targets. *Physiol Rev,* 87**,** 905-31.

HENDERSON, B. E. & FEIGELSON, H. S. 2000. Hormonal carcinogenesis. *Carcinogenesis,* 21**,** 427-33.

HENDERSON, B. E., ROSS, R. K., PIKE, M. C. & CASAGRANDE, J. T. 1982. Endogenous hormones as a major factor in human cancer. *Cancer Res,* 42**,** 3232-9.

HERMANSON, O., JEPSEN, K. & ROSENFELD, M. G. 2002. N-CoR controls differentiation of neural stem cells into astrocytes. *Nature,* 419**,** 934-939.

HERY, C., FERLAY, J., BONIOL, M. & AUTIER, P. 2008. Changes in breast cancer incidence and mortality in middle-aged and elderly women in 28 countries with Caucasian majority populations. *Ann Oncol,* 19**,** 1009-18.

HICKSON, J., ACKLER, S., KLAUBERT, D., BOUSKA, J., ELLIS, P., FOSTER, K., OLEKSIJEW, A., RODRIGUEZ, L., SCHLESSINGER, S., WANG, B. & FROST, D. 2010. Noninvasive molecular imaging of apoptosis in vivo using a modified firefly luciferase substrate, Z-DEVD-aminoluciferin. *Cell Death Differ,* 17**,** 1003-10.

HORLEIN, A. J., NAAR, A. M., HEINZEL, T., TORCHIA, J., GLOSS, B., KUROKAWA, R., RYAN, A., KAMEI, Y., SODERSTROM, M., GLASS, C. K. & ROSENFELD, M. G. 1995. Ligand-independent repression by the thyroid hormone receptor mediated by a nuclear receptor co-repressor. *Nature,* 377**,** 397-404.

HOWELL, A., OSBORNE, C. K., MORRIS, C. & WAKELING, A. E. 2000. ICI 182,780 (Faslodex): development of a novel, "pure" antiestrogen. *Cancer,* 89**,** 817-25.

HU, C. D., CHINENOV, Y. & KERPPOLA, T. K. 2002. Visualization of interactions among bZIP and Rel family proteins in living cells using bimolecular fluorescence complementation. *Mol Cell,* 9**,** 789-98.

HU, X. & LAZAR, M. A. 1999. The CoRNR motif controls the recruitment of corepressors by nuclear hormone receptors. *Nature,* 402**,** 93-6.

HUANG, A. & KALEY, G. 2004. Gender-specific regulation of cardiovascular function: estrogen as key player. *Microcirculation,* 11**,** 9-38.

HULTMAN, M. L., KRASNOPEROVA, N. V., LI, S., DU, S., XIA, C., DIETZ, J. D., LALA, D. S., WELSCH, D. J. & HU, X. 2005. The ligand-dependent interaction of mineralocorticoid receptor with coactivator and corepressor peptides suggests multiple activation mechanisms. *Mol Endocrinol,* 19**,** 1460-73.

IANNONE, M. A., SIMMONS, C. A., KADWELL, S. H., SVOBODA, D. L., VANDERWALL, D. E., DENG, S. J., CONSLER, T. G., SHEARIN, J., GRAY, J. G. & PEARCE, K. H. 2004. Correlation between in vitro peptide binding profiles and cellular activities for estrogen receptor-modulating compounds. *Mol Endocrinol,* 18**,** 1064-81.

IWASE, H., OMOTO, Y., TOYAMA, T., YAMASHITA, H., HARA, Y., SUGIURA, H. & ZHANG, Z. 2003. Clinical significance of AIB1 expression in human breast cancer. *Breast Cancer Res Treat,* 80**,** 339-45.

JANKEVICS, H., PRUMMER, M., IZEWSKA, P., PICK, H., LEUFGEN, K. & VOGEL, H. 2005. Diffusion-time distribution analysis reveals characteristic ligand-dependent interaction patterns of nuclear receptors in living cells. *Biochemistry,* 44**,** 11676-83.

JENSEN, E. V. & JORDAN, V. C. 2003. The estrogen receptor: a model for molecular medicine. *Clin Cancer Res,* 9**,** 1980-9.

JEPSEN, K. & ROSENFELD, M. G. 2002. Biological roles and mechanistic actions of co-repressor complexes. *Journal of Cell Science,* 115**,** 689-698.

JOHNSSON, N. & VARSHAVSKY, A. 1994. Split ubiquitin as a sensor of protein interactions in vivo. *Proc Natl Acad Sci U S A,* 91**,** 10340-4.

JONAS, B. A. & PRIVALSKY, M. L. 2004. SMRT and N-CoR corepressors are regulated by distinct kinase signaling pathways. *J Biol Chem,* 279**,** 54676-86.

JORDAN, V. C., PHELPS, E. & LINDGREN, J. U. 1987. Effects of anti-estrogens on bone in castrated and intact female rats. *Breast Cancer Res Treat,* 10**,** 31-5.

KATZENELLENBOGEN, B. S., CHOI, I., DELAGE-MOURROUX, R., EDIGER, T. R., MARTINI, P. G. V., MONTANO, M., SUN, J., WEIS, K. & KATZENELLENBOGEN, J. A. 2000. Molecular mechanisms of estrogen action: selective ligands and receptor pharmacology. *The Journal of Steroid Biochemistry and Molecular Biology,* 74**,** 279-285.

KEETON, E. K. & BROWN, M. 2005. Cell cycle progression stimulated by tamoxifen-bound estrogen receptor-alpha and promoter-specific effects in breast cancer cells deficient in N-CoR and SMRT. *Mol Endocrinol,* 19**,** 1543-54.

KELLOFF, G. J., HOFFMAN, J. M., JOHNSON, B., SCHER, H. I., SIEGEL, B. A., CHENG, E. Y., CHESON, B. D., O'SHAUGHNESSY, J., GUYTON, K. Z., MANKOFF, D. A., SHANKAR, L., LARSON, S. M., SIGMAN, C. C., SCHILSKY, R. L. & SULLIVAN, D. C. 2005. Progress and Promise of FDG-PET Imaging for Cancer Patient Management and Oncologic Drug Development. *Clinical Cancer Research,* 11**,** 2785-2808.

KIM, S. B., KANNO, A., OZAWA, T., TAO, H. & UMEZAWA, Y. 2007a. Nongenomic Activity of Ligands in the Association of Androgen Receptor with Src. *ACS Chem. Biol.,* 2**,** 484-492.

KIM, S. B., OTANI, Y., UMEZAWA, Y. & TAO, H. 2007b. Bioluminescent Indicator for Determining Protein-Protein Interactions Using Intramolecular Complementation of Split Click Beetle Luciferase. *Anal. Chem.,* 79**,** 4820-4826.

KIRKEGAARD, T., MCGLYNN, L. M., CAMPBELL, F. M., MULLER, S., TOVEY, S. M., DUNNE, B., NIELSEN, K. V., COOKE, T. G. & BARTLETT, J. M. 2007. Amplified in breast cancer 1 in human epidermal growth factor receptor - positive tumors of tamoxifen-treated breast cancer patients. *Clin Cancer Res,* 13**,** 1405-11.

KISANGA, E. R., GJERDE, J., SCHJOTT, J., MELLGREN, G. & LIEN, E. A. 2003. Tamoxifen administration and metabolism in nude mice and nude rats. *J Steroid Biochem Mol Biol,* 84**,** 361-7.

KLEIN-HITPASS, L., SCHORPP, M., WAGNER, U. & RYFFEL, G. U. 1986. An estrogen-responsive element derived from the 5' flanking region of the Xenopus vitellogenin A2 gene functions in transfected human cells. *Cell,* 46**,** 1053-61.

KLINGE, C. M. 2000. Estrogen receptor interaction with co-activators and co-repressors. *Steroids,* 65**,** 227-51.

KRAICHELY, D. M., SUN, J., KATZENELLENBOGEN, J. A. & KATZENELLENBOGEN, B. S. 2000. Conformational changes and coactivator recruitment by novel ligands for estrogen receptor-alpha and estrogen receptor-beta: correlations with biological character and distinct differences among SRC coactivator family members. *Endocrinology,* 141**,** 3534-45.

KRISTENSEN, B., EJLERTSEN, B., DALGAARD, P., LARSEN, L., HOLMEGAARD, S. N., TRANSBOL, I. & MOURIDSEN, H. T. 1994. Tamoxifen and bone metabolism in postmenopausal low-risk breast cancer patients: a randomized study. *J Clin Oncol,* 12**,** 992-7.

KRUM, S. A., MIRANDA-CARBONI, G. A., LUPIEN, M., EECKHOUTE, J., CARROLL, J. S. & BROWN, M. 2008. Unique ER{alpha} Cistromes Control Cell Type-Specific Gene Regulation. *Mol Endocrinol,* 22**,** 2393-2406.

KUIPER, G. G., CARLSSON, B., GRANDIEN, K., ENMARK, E., HAGGBLAD, J., NILSSON, S. & GUSTAFSSON, J. A. 1997. Comparison of the ligand binding specificity and transcript tissue distribution of estrogen receptors alpha and beta. *Endocrinology,* 138**,** 863-70.

KUMAR, V. & CHAMBON, P. 1988. The estrogen receptor binds tightly to its responsive element as a ligand-induced homodimer. *Cell,* 55**,** 145-56.

KUMAR, V., GREEN, S., STACK, G., BERRY, M., JIN, J. R. & CHAMBON, P. 1987. Functional domains of the human estrogen receptor. *Cell,* 51**,** 941-51.

KUSHNER, P. J., AGARD, D. A., GREENE, G. L., SCANLAN, T. S., SHIAU, A. K., UHT, R. M. & WEBB, P. 2000. Estrogen receptor pathways to AP-1. *J Steroid Biochem Mol Biol,* 74**,** 311-7.

LAGUETTE, M. J., ABRAHAMS, Y., PRINCE, S. & COLLINS, M. 2011. Sequence variants within the 3'-UTR of the COL5A1 gene alters mRNA stability: Implications for musculoskeletal soft tissue injuries. *Matrix Biol*.

LAVINSKY, R. M., JEPSEN, K., HEINZEL, T., TORCHIA, J., MULLEN, T. M., SCHIFF, R., DEL-RIO, A. L., RICOTE, M., NGO, S., GEMSCH, J., HILSENBECK, S. G., OSBORNE, C. K., GLASS, C. K., ROSENFELD, M. G. & ROSE, D. W. 1998. Diverse signaling pathways modulate nuclear receptor recruitment of N-CoR and SMRT complexes. *Proc Natl Acad Sci U S A,* 95**,** 2920-5.

LE ROMANCER, M., POULARD, C., COHEN, P., SENTIS, S., RENOIR, J.-M. & CORBO, L. 2011. Cracking the Estrogen Receptor's Posttranslational Code in Breast Tumors. *Endocrine Reviews*.

LEES, J. A., FAWELL, S. E. & PARKER, M. G. 1989. Identification of two transactivation domains in the mouse oestrogen receptor. *Nucleic Acids Res,* 17**,** 5477-88.

LEMMEN, J. G., ARENDS, R. J., VAN BOXTEL, A. L., VAN DER SAAG, P. T. & VAN DER BURG, B. 2004. Tissue- and time-dependent estrogen receptor activation in estrogen reporter mice. *J Mol Endocrinol,* 32**,** 689-701.

LEVY, N., TATOMER, D., HERBER, C. B., ZHAO, X., TANG, H., SARGEANT, T., BALL, L. J., SUMMERS, J., SPEED, T. P. & LEITMAN, D. C. 2008. Differential Regulation of Native Estrogen Receptor-Regulatory Elements by Estradiol, Tamoxifen, and Raloxifene. *Molecular Endocrinology,* 22**,** 287-303.

LEWIS, J. S. & JORDAN, V. C. 2005. Selective estrogen receptor modulators (SERMs): mechanisms of anticarcinogenesis and drug resistance. *Mutat Res,* 591**,** 247-263.

LI, H., GOMES, P. J. & CHEN, J. D. 1997. RAC3, a steroid/nuclear receptor-associated coactivator that is related to SRC-1 and TIF2. *Proceedings of the National Academy of Sciences,* 94**,** 8479-8484.

LI, W., LI, F., HUANG, Q., FREDERICK, B., BAO, S. & LI, C.-Y. 2008. Noninvasive Imaging and Quantification of Epidermal Growth Factor Receptor Kinase Activation In vivo. *Cancer Res,* 68**,** 4990-4997.

LINTERMANS, A., NEVEN, P. & PARIDAENS, R. 2011. Drug safety evaluation of exemestane. *Expert Opinion on Drug Safety,* 10**,** 473-487.

LIST, H.-J., LAURITSEN, K. J., REITER, R., POWERS, C., WELLSTEIN, A. & RIEGEL, A. T. 2001. Ribozyme Targeting Demonstrates That the Nuclear Receptor Coactivator AIB1 Is a Rate-limiting Factor for Estrogen-dependent Growth of Human MCF-7 Breast Cancer Cells. *Journal of Biological Chemistry,* 276**,** 23763-23768.

LIU, J., KNAPPENBERGER, K. S., KACK, H., ANDERSSON, G., NILSSON, E., DARTSCH, C. & SCOTT, C. W. 2003. A homogeneous in vitro functional assay for estrogen receptors: coactivator recruitment. *Mol Endocrinol,* 17**,** 346-55.

LIU, M. M., ALBANESE, C., ANDERSON, C. M., HILTY, K., WEBB, P., UHT, R. M., PRICE, R. H., JR., PESTELL, R. G. & KUSHNER, P. J. 2002. Opposing action of estrogen receptors alpha and beta on cyclin D1 gene expression. *J Biol Chem,* 277**,** 24353-60.

LLOPIS, J., WESTIN, S., RICOTE, M., WANG, Z., CHO, C. Y., KUROKAWA, R., MULLEN, T. M., ROSE, D. W., ROSENFELD, M. G., TSIEN, R. Y. & GLASS, C. K. 2000. Ligand-dependent interactions of coactivators steroid receptor coactivator-1 and peroxisome proliferator-activated receptor binding protein with nuclear hormone receptors can be imaged in live cells and are required for transcription. *Proc Natl Acad Sci U S A,* 97**,** 4363-8.

LOVE, R. R., MAZESS, R. B., BARDEN, H. S., EPSTEIN, S., NEWCOMB, P. A., JORDAN, V. C., CARBONE, P. P. & DEMETS, D. L. 1992. Effects of tamoxifen on bone mineral density in postmenopausal women with breast cancer. *N Engl J Med,* 326**,** 852-6.

LUKER, G. D. & LUKER, K. E. 2008. Optical Imaging: Current Applications and Future Directions. *J Nucl Med,* 49**,** 1-4.

LUKER, K. E., GUPTA, M. & LUKER, G. D. 2008. Imaging CXCR4 Signaling with Firefly Luciferase Complementation. *Anal. Chem.,* 80**,** 5565-5573.

LUKER, K. E., GUPTA, M. & LUKER, G. D. 2009. Imaging chemokine receptor dimerization with firefly luciferase complementation. *The FASEB Journal,* 23**,** 823-834.

LUKER, K. E., SMITH, M. C., LUKER, G. D., GAMMON, S. T., PIWNICA-WORMS, H. & PIWNICA-WORMS, D. 2004. Kinetics of regulated protein-protein interactions revealed with firefly luciferase complementation imaging in cells and living animals. *Proc Natl Acad Sci U S A,* 101**,** 12288-93.

MAGLIERY, T. J., WILSON, C. G., PAN, W., MISHLER, D., GHOSH, I., HAMILTON, A. D. & REGAN, L. 2005. Detecting protein-protein interactions with a green fluorescent protein fragment reassembly trap: scope and mechanism. *J Am Chem Soc,* 127**,** 146-57.

MANGELSDORF, D. J., THUMMEL, C., BEATO, M., HERRLICH, P., SCHUTZ, G., UMESONO, K., BLUMBERG, B., KASTNER, P., MARK, M., CHAMBON, P. & EVANS, R. M. 1995. The nuclear receptor superfamily: the second decade. *Cell,* 83**,** 835-9.

MANKOFF, D. 2007. A definition of molecular imaging. *Journal of nuclear medicine*, 18N-21N.

MASSARWEH, S., OSBORNE, C. K., CREIGHTON, C. J., QIN, L., TSIMELZON, A., HUANG, S., WEISS, H., RIMAWI, M. & SCHIFF, R. 2008. Tamoxifen resistance in breast tumors is driven by growth factor receptor signaling with repression of classic estrogen receptor genomic function. *Cancer Res,* 68**,** 826-33.

MASSOUD, T. F. & GAMBHIR, S. S. 2003. Molecular imaging in living subjects: seeing fundamental biological processes in a new light. *Genes & Development,* 17**,** 545-580.

MASSOUD, T. F., PAULMURUGAN, R. & GAMBHIR, S. S. 2010. A molecularly engineered split reporter for imaging protein-protein interactions with positron emission tomography. *Nat Med,* 16**,** 921-6.

METIVIER, R., PENOT, G., HUBNER, M. R., REID, G., BRAND, H., KOS, M. & GANNON, F. 2003. Estrogen receptor-alpha directs ordered, cyclical, and combinatorial recruitment of cofactors on a natural target promoter. *Cell,* 115**,** 751-63.

MEYERS, M. J., SUN, J., CARLSON, K. E., MARRINER, G. A., KATZENELLENBOGEN, B. S. & KATZENELLENBOGEN, J. A. 2001. Estrogen Receptor-β Potency-Selective Ligands: Structure−Activity Relationship Studies of Diarylpropionitriles and Their Acetylene and Polar Analogues. *Journal of Medicinal Chemistry,* 44**,** 4230-4251.

MOSSELMAN, S., POLMAN, J. & DIJKEMA, R. 1996. ER[beta]: Identification and characterization of a novel human estrogen receptor. *FEBS Letters,* 392**,** 49-53.

MURPHY, L. C., SIMON, S. L., PARKES, A., LEYGUE, E., DOTZLAW, H., SNELL, L., TROUP, S., ADEYINKA, A. & WATSON, P. H. 2000. Altered expression of estrogen receptor coregulators during human breast tumorigenesis. *Cancer Res,* 60**,** 6266-71.

NAGEL, S. C., HAGELBARGER, J. L. & MCDONNELL, D. P. 2001. Development of an ER action indicator mouse for the study of estrogens, selective ER modulators (SERMs), and Xenobiotics. *Endocrinology,* 142**,** 4721-8.

NAGY, L., KAO, H. Y., LOVE, J. D., LI, C., BANAYO, E., GOOCH, J. T., KRISHNA, V., CHATTERJEE, K., EVANS, R. M. & SCHWABE, J. W. 1999. Mechanism of corepressor binding and release from nuclear hormone receptors. *Genes Dev,* 13**,** 3209-16.

NEUFELD, H. A., TOWNER, R. D. & PACE, J. 1975. A rapid method for determining ATP by the firefly luciferin-luciferase system. *Cellular and Molecular Life Sciences,* 31**,** 391-392.

NEWTON, D. L., XUE, Y., OLSON, K. A., FETT, J. W. & RYBAK, S. M. 1996. Angiogenin single-chain immunofusions: influence of peptide linkers and spacers between fusion protein domains. *Biochemistry,* 35**,** 545-53.

NYFELER, B., MICHNICK, S. W. & HAURI, H. P. 2005. Capturing protein interactions in the secretory pathway of living cells. *Proc Natl Acad Sci U S A,* 102**,** 6350-5.

ORDENTLICH, P., DOWNES, M., XIE, W., GENIN, A., SPINNER, N. B. & EVANS, R. M. 1999. Unique forms of human and mouse nuclear receptor corepressor SMRT. *Proc Natl Acad Sci U S A,* 96**,** 2639-44.

OSBORNE, C. K. 1998. Tamoxifen in the treatment of breast cancer. *N Engl J Med,* 339**,** 1609-18.

OSBORNE, C. K., BARDOU, V., HOPP, T. A., CHAMNESS, G. C., HILSENBECK, S. G., FUQUA, S. A. W., WONG, J., ALLRED, D. C., CLARK, G. M. & SCHIFF, R. 2003. Role of the estrogen receptor coactivator AIB1 (SRC-3) and HER-2/neu in tamoxifen resistance in breast cancer. *J Natl Cancer Inst,* 95**,** 353-361.

OSBORNE, C. K., NEVEN, P., DIRIX, L. Y., MACKEY, J. R., ROBERT, J., UNDERHILL, C., SCHIFF, R., GUTIERREZ, C., MIGLIACCIO, I., ANAGNOSTOU, V. K., RIMM, D. L., MAGILL, P. & SELLERS, M. 2011. Gefitinib or placebo in combination with tamoxifen in patients with hormone receptor-positive metastatic breast cancer: a randomized phase II study. *Clin Cancer Res,* 17**,** 1147-59.

OZERS, M. S., ERVIN, K. M., STEFFEN, C. L., FRONCZAK, J. A., LEBAKKEN, C. S., CARNAHAN, K. A., LOWERY, R. G. & BURKE, T. J. 2005. Analysis of ligand-dependent recruitment of coactivator peptides to estrogen receptor using fluorescence polarization. *Mol Endocrinol,* 19**,** 25-34.

PACE, P., TAYLOR, J., SUNTHARALINGAM, S., COOMBES, R. C. & ALI, S. 1997. Human estrogen receptor beta binds DNA in a manner similar to and dimerizes with estrogen receptor alpha. *J Biol Chem,* 272**,** 25832-8.

PAPOUTSI, Z., KASSI, E., FOKIALAKIS, N., MITAKOU, S., LAMBRINIDIS, G., MIKROS, E. & MOUTSATSOU, P. 2007. Deoxybenzoins are novel potent selective estrogen receptor modulators. *Steroids,* 72**,** 693-704.

PAULMURUGAN, R. & GAMBHIR, S. S. 2003. Monitoring protein-protein interactions using split synthetic renilla luciferase protein-fragment-assisted complementation. *Anal Chem,* 75**,** 1584-9.

PAULMURUGAN, R. & GAMBHIR, S. S. 2006. An intramolecular folding sensor for imaging estrogen receptor-ligand interactions. *Proc Natl Acad Sci U S A,* 103**,** 15883-8.

PAULMURUGAN, R. & GAMBHIR, S. S. 2007. Combinatorial library screening for developing an improved split-firefly luciferase fragment-assisted complementation system for studying protein-protein interactions. *Anal Chem,* 79**,** 2346-53.

PAULMURUGAN, R., MASSOUD, T. F., HUANG, J. & GAMBHIR, S. S. 2004. Molecular imaging of drug-modulated protein-protein interactions in living subjects. *Cancer Res,* 64**,** 2113-9.

PAULMURUGAN, R., UMEZAWA, Y. & GAMBHIR, S. S. 2002. Noninvasive imaging of protein-protein interactions in living subjects by using reporter protein complementation and reconstitution strategies. *Proceedings of the National Academy of Sciences of the United States of America,* 99**,** 15608-15613.

PEARCE, S. T. & JORDAN, V. C. 2004. The biological role of estrogen receptors alpha and beta in cancer. *Crit Rev Oncol Hematol,* 50**,** 3-22.

PELLETIER, J. N., CAMPBELL-VALOIS, F. X. & MICHNICK, S. W. 1998. Oligomerization domain-directed reassembly of active dihydrofolate reductase from rationally designed fragments. *Proc Natl Acad Sci U S A,* 95**,** 12141-6.

PRASHER, D. C., ECKENRODE, V. K., WARD, W. W., PRENDERGAST, F. G. & CORMIER, M. J. 1992. Primary structure of the Aequorea victoria green-fluorescent protein. *Gene,* 111**,** 229-33.

PRIVALSKY, M. L. 2004. The role of corepressors in transcriptional regulation by nuclear hormone receptors. *Annu Rev Physiol,* 66**,** 315-60.

RANDO, G., HORNER, D., BISERNI, A., RAMACHANDRAN, B., CARUSO, D., CIANA, P., KOMM, B. & MAGGI, A. 2010. An innovative method to classify SERMs based on the dynamics of estrogen receptor transcriptional activity in living animals. *Mol Endocrinol,* 24**,** 735-44.

RAZANDI, M., PEDRAM, A., PARK, S. T. & LEVIN, E. R. 2003. Proximal events in signaling by plasma membrane estrogen receptors. *J Biol Chem,* 278**,** 2701-12.

REMY, I. & MICHNICK, S. W. 2006. A highly sensitive protein-protein interaction assay based on Gaussia luciferase. *Nat Methods,* 3**,** 977-9.

RIGGS, B. L., KHOSLA, S. & MELTON, L. J., 3RD 2002. Sex steroids and the construction and conservation of the adult skeleton. *Endocr Rev,* 23**,** 279-302.

ROBINSON, S. P., LANGAN-FAHEY, S. M., JOHNSON, D. A. & JORDAN, V. C. 1991. Metabolites, pharmacodynamics, and pharmacokinetics of tamoxifen in rats and mice compared to the breast cancer patient. *Drug Metabolism and Disposition,* 19**,** 36-43.

RODRIGUEZ, A. L., TAMRAZI, A., COLLINS, M. L. & KATZENELLENBOGEN, J. A. 2004. Design, synthesis, and in vitro biological evaluation of small molecule inhibitors of estrogen receptor alpha coactivator binding. *J Med Chem,* 47**,** 600-11.

ROSSI, F., CHARLTON, C. A. & BLAU, H. M. 1997. Monitoring protein-protein interactions in intact eukaryotic cells by beta-galactosidase complementation. *Proc Natl Acad Sci U S A,* 94**,** 8405-10.

RUSSO, J., FERNANDEZ, S. V., RUSSO, P. A., FERNBAUGH, R., SHERIFF, F. S., LAREEF, H. M., GARBER, J. & RUSSO, I. H. 2006. 17-Beta-estradiol induces transformation and tumorigenesis in human breast epithelial cells. *FASEB J,* 20**,** 1622-34.

RUTQVIST, L. E. & MATTSSON, A. 1993. Cardiac and thromboembolic morbidity among postmenopausal women with early-stage breast cancer in a randomized trial of adjuvant tamoxifen. The Stockholm Breast Cancer Study Group. *J Natl Cancer Inst,* 85**,** 1398-406.

SAVILLE, B., WORMKE, M., WANG, F., NGUYEN, T., ENMARK, E., KUIPER, G., GUSTAFSSON, J. A. & SAFE, S. 2000. Ligand-, cell-, and estrogen receptor subtype (alpha/beta)-dependent activation at GC-rich (Sp1) promoter elements. *J Biol Chem,* 275**,** 5379-87.

SCHIFF, R., MASSARWEH, S., SHOU, J. & OSBORNE, C. K. 2003. Breast cancer endocrine resistance: how growth factor signaling and estrogen receptor coregulators modulate response. *Clin Cancer Res,* 9**,** 447S-54S.

SCOTT, S. M., BROWN, M. & COME, S. E. 2011. Emerging data on the efficacy and safety of fulvestrant, a unique antiestrogen therapy for advanced breast cancer. *Expert Opinion on Drug Safety***,** 1-8.

SHANG, Y. & BROWN, M. 2002. Molecular determinants for the tissue specificity of SERMs. *Science,* 295**,** 2465-2468.

SHANG, Y., HU, X., DIRENZO, J., LAZAR, M. A. & BROWN, M. 2000. Cofactor dynamics and sufficiency in estrogen receptor-regulated transcription. *Cell,* 103**,** 843-52.

SHIAU, A. K., BARSTAD, D., LORIA, P. M., CHENG, L., KUSHNER, P. J., AGARD, D. A. & GREENE, G. L. 1998. The structural basis of estrogen receptor/coactivator recognition and the antagonism of this interaction by tamoxifen. *Cell,* 95**,** 927-37.

SHIMOMURA, O., JOHNSON, F. H. & SAIGA, Y. 1962. Extraction, purification and properties of aequorin, a bioluminescent protein from the luminous hydromedusan, Aequorea. *J Cell Comp Physiol,* 59**,** 223-39.

SHOU, J., MASSARWEH, S., OSBORNE, C. K., WAKELING, A. E., ALI, S., WEISS, H. & SCHIFF, R. 2004. Mechanisms of tamoxifen resistance: increased estrogen receptor-HER2/neu cross-talk in ER/HER2-positive breast cancer. *J Natl Cancer Inst,* 96**,** 926-35.

SIBONGA, J. D., DOBNIG, H., HARDEN, R. M. & TURNER, R. T. 1998. Effect of the high-affinity estrogen receptor ligand ICI 182,780 on the rat tibia. *Endocrinology,* 139**,** 3736-42.

SIEKIERKA, J. J., HUNG, S. H. Y., POE, M., LIN, C. S. & SIGAL, N. H. 1989. A cytosolic binding protein for the immunosuppressant FK506 has peptidyl-prolyl isomerase activity but is distinct from cyclophilin. *Nature,* 341**,** 755-757.

SLADEK, F. M. 2003. Nuclear Receptors as Drug Targets: New Developments in Coregulators, Orphan Receptors and Major Therapeutic Areas. *Expert Opinion on Therapeutic Targets,* 7**,** 679-684.

SMITH, C. L., NAWAZ, Z. & O'MALLEY, B. W. 1997. Coactivator and corepressor regulation of the agonist/antagonist activity of the mixed antiestrogen, 4-hydroxytamoxifen. *Mol Endocrinol,* 11**,** 657-66.

SONG, R. X., MCPHERSON, R. A., ADAM, L., BAO, Y., SHUPNIK, M., KUMAR, R. & SANTEN, R. J. 2002. Linkage of rapid estrogen action to MAPK activation by ERalpha-Shc association and Shc pathway activation. *Mol Endocrinol,* 16**,** 116-27.

SONG, R. X. D., FAN, P., YUE, W., CHEN, Y. & SANTEN, R. J. 2006. Role of receptor complexes in the extranuclear actions of estrogen receptor {alpha} in breast cancer. *Endocr Relat Cancer,* 13**,** S3-13.

SONG, R. X. D., ZHANG, Z., CHEN, Y., BAO, Y. & SANTEN, R. J. 2007. Estrogen Signaling via a Linear Pathway Involving Insulin-Like Growth Factor I Receptor, Matrix Metalloproteinases, and Epidermal Growth Factor Receptor to Activate Mitogen-Activated Protein Kinase in MCF-7 Breast Cancer Cells. *Endocrinology,* 148**,** 4091-4101.

SPENCER, T. E., JENSTER, G., BURCIN, M. M., ALLIS, C. D., ZHOU, J., MIZZEN, C. A., MCKENNA, N. J., ONATE, S. A., TSAI, S. Y., TSAI, M. J. & O'MALLEY, B. W. 1997. Steroid receptor coactivator-1 is a histone acetyltransferase. *Nature,* 389**,** 194-8.

STAFSLIEN, D. K., VEDVIK, K. L., DE ROSIER, T. & OZERS, M. S. 2007. Analysis of ligand-dependent recruitment of coactivator peptides to RXRbeta in a time-resolved fluorescence resonance energy transfer assay. *Mol Cell Endocrinol,* 264**,** 82-9.

STEFAN, E., AQUIN, S., BERGER, N., LANDRY, C. R., NYFELER, B., BOUVIER, M. & MICHNICK, S. W. 2007. Quantification of dynamic protein complexes using Renilla luciferase fragment complementation applied to protein kinase A activities in vivo. *Proceedings of the National Academy of Sciences,* 104**,** 16916-16921.

STRYER, L. & HAUGLAND, R. P. 1967. Energy transfer: a spectroscopic ruler. *Proc Natl Acad Sci U S A,* 58**,** 719-26.

SUN, Y., WALLRABE, H., SEO, S. A. & PERIASAMY, A. 2011. FRET microscopy in 2010: the legacy of Theodor Forster on the 100th anniversary of his birth. *Chemphyschem,* 12**,** 462-74.

TANEOKA, A., SAKAGUCHI-MIKAMI, A., YAMAZAKI, T., TSUGAWA, W. & SODE, K. 2009. The construction of a glucose-sensing luciferase. *Biosens Bioelectron,* 25**,** 76-81.

THOMAS, R. S., SARWAR, N., PHOENIX, F., COOMBES, R. C. & ALI, S. 2008. Phosphorylation at serines 104 and 106 by Erk1/2 MAPK is important for estrogen receptor-alpha activity. *J Mol Endocrinol,* 40**,** 173-84.

TIKKANEN, M. K., CARTER, D. J., HARRIS, A. M., LE, H. M., AZORSA, D. O., MELTZER, P. S. & MURDOCH, F. E. 2000. Endogenously expressed estrogen receptor and coactivator AIB1 interact in MCF-7 human breast cancer cells. *Proceedings of the National Academy of Sciences of the United States of America,* 97**,** 12536-12540.

TODA, K., OKADA, Y., ZUBAIR, M., MOROHASHI, K., SAIBARA, T. & OKADA, T. 2004. Aromatase-knockout mouse carrying an estrogen-inducible enhanced green fluorescent protein gene facilitates detection of estrogen actions in vivo. *Endocrinology,* 145**,** 1880-8.

TOMAYKO, M. M. & REYNOLDS, C. P. 1989. Determination of subcutaneous tumor size in athymic (nude) mice. *Cancer Chemother Pharmacol,* 24**,** 148-54.

TORA, L., MULLICK, A., METZGER, D., PONGLIKITMONGKOL, M., PARK, I. & CHAMBON, P. 1989a. The cloned human oestrogen receptor contains a mutation which alters its hormone binding properties. *Embo J,* 8**,** 1981-6.

TORA, L., WHITE, J., BROU, C., TASSET, D., WEBSTER, N., SCHEER, E. & CHAMBON, P. 1989b. The human estrogen receptor has two independent nonacidic transcriptional activation functions. *Cell,* 59**,** 477-87.

TORCHIA, J., ROSE, D. W., INOSTROZA, J., KAMEI, Y., WESTIN, S., GLASS, C. K. & ROSENFELD, M. G. 1997. The transcriptional co-activator p/CIP binds CBP and mediates nuclear-receptor function. *Nature,* 387**,** 677-84.

TORRES-ARZAYUS, M. I., FONT DE MORA, J., YUAN, J., VAZQUEZ, F., BRONSON, R., RUE, M., SELLERS, W. R. & BROWN, M. 2004. High tumor incidence and activation of the PI3K/AKT pathway in transgenic mice define AIB1 as an oncogene. *Cancer Cell,* 6**,** 263-74.

TROY, T., JEKIC-MCMULLEN, D., SAMBUCETTI, L. & RICE, B. 2004. Quantitative comparison of the sensitivity of detection of fluorescent and bioluminescent reporters in animal models. *Mol Imaging,* 3**,** 9-23.

TURNER, R. T., WAKLEY, G. K., HANNON, K. S. & BELL, N. H. 1987. Tamoxifen prevents the skeletal effects of ovarian hormone deficiency in rats. *J Bone Miner Res,* 2**,** 449-56.

TZUKERMAN, M. T., ESTY, A., SANTISO-MERE, D., DANIELIAN, P., PARKER, M. G., STEIN, R. B., PIKE, J. W. & MCDONNELL, D. P. 1994. Human estrogen receptor transactivational capacity is determined by both cellular and promoter context and mediated by two functionally distinct intramolecular regions. *Mol Endocrinol,* 8**,** 21-30.

VILLALOBOS, V., NAIK, S., BRUINSMA, M., DOTHAGER, R. S., PAN, M. H., SAMRAKANDI, M., MOSS, B., ELHAMMALI, A. & PIWNICA-WORMS, D. 2010. Dual-color click beetle luciferase heteroprotein fragment complementation assays. *Chem Biol,* 17**,** 1018-29.

VOGEL, V. G., COSTANTINO, J. P., WICKERHAM, D. L., CRONIN, W. M., CECCHINI, R. S., ATKINS, J. N., BEVERS, T. B., FEHRENBACHER, L., PAJON, E. R., JR., WADE, J. L., 3RD, ROBIDOUX, A., MARGOLESE, R. G., JAMES, J., LIPPMAN, S. M., RUNOWICZ, C. D., GANZ, P. A., REIS,

S. E., MCCASKILL-STEVENS, W., FORD, L. G., JORDAN, V. C. & WOLMARK, N. 2006. Effects of tamoxifen vs raloxifene on the risk of developing invasive breast cancer and other disease outcomes: the NSABP Study of Tamoxifen and Raloxifene (STAR) P-2 trial. *JAMA,* 295**,** 2727-41.

VON MERING, C., KRAUSE, R., SNEL, B., CORNELL, M., OLIVER, S. G., FIELDS, S. & BORK, P. 2002. Comparative assessment of large-scale data sets of protein-protein interactions. *Nature,* 417**,** 399-403.

WARDELL, S. E., MARKS, J. R. & MCDONNELL, D. P. 2011. The turnover of estrogen receptor alpha by the selective estrogen receptor degrader (SERD) fulvestrant is a saturable process that is not required for antagonist efficacy. *Biochem Pharmacol,* 82**,** 122-30.

WEATHERMAN, R. V., CHANG, C. Y., CLEGG, N. J., CARROLL, D. C., DAY, R. N., BAXTER, J. D., MCDONNELL, D. P., SCANLAN, T. S. & SCHAUFELE, F. 2002. Ligand-selective interactions of ER detected in living cells by fluorescence resonance energy transfer. *Mol Endocrinol,* 16**,** 487-96.

WEBB, P., ANDERSON, C. M., VALENTINE, C., NGUYEN, P., MARIMUTHU, A., WEST, B. L., BAXTER, J. D. & KUSHNER, P. J. 2000. The nuclear receptor corepressor (N-CoR) contains three isoleucine motifs (I/LXXII) that serve as receptor interaction domains (IDs). *Mol Endocrinol,* 14**,** 1976-85.

WEBB, P., NGUYEN, P. & KUSHNER, P. J. 2003. Differential SERM effects on corepressor binding dictate ERalpha activity in vivo. *J Biol Chem,* 278**,** 6912-20.

WEBB, P., NGUYEN, P., SHINSAKO, J., ANDERSON, C., FENG, W., NGUYEN, M. P., CHEN, D., HUANG, S. M., SUBRAMANIAN, S., MCKINERNEY, E., KATZENELLENBOGEN, B. S., STALLCUP, M. R. & KUSHNER, P. J. 1998. Estrogen receptor activation function 1 works by binding p160 coactivator proteins. *Mol Endocrinol,* 12**,** 1605-18.

WEIS, K. E., EKENA, K., THOMAS, J. A., LAZENNEC, G. & KATZENELLENBOGEN, B. S. 1996. Constitutively active human estrogen receptors containing amino acid substitutions for tyrosine 537 in the receptor protein. *Mol Endocrinol,* 10**,** 1388-98.

WEISSLEDER, R. & NTZIACHRISTOS, V. 2003. Shedding light onto live molecular targets. *Nat Med,* 9**,** 123-8.

WHITE, R., SJOBERG, M., KALKHOVEN, E. & PARKER, M. G. 1997. Ligand-independent activation of the oestrogen receptor by mutation of a conserved tyrosine. *Embo J,* 16**,** 1427-35.

WU, R. C., FENG, Q., LONARD, D. M. & O'MALLEY, B. W. 2007. SRC-3 coactivator functional lifetime is regulated by a phospho-dependent ubiquitin time clock. *Cell,* 129**,** 1125-40.

WU, R. C., QIN, J., YI, P., WONG, J., TSAI, S. Y., TSAI, M. J. & O'MALLEY, B. W. 2004. Selective phosphorylations of the SRC-3/AIB1 coactivator integrate genomic reponses to multiple cellular signaling pathways. *Mol Cell,* 15**,** 937-49.

WU, R. C., SMITH, C. L. & O'MALLEY, B. W. 2005. Transcriptional regulation by steroid receptor coactivator phosphorylation. *Endocr Rev,* 26**,** 393-9.

YADAV, Y., MACLEAN, E. D., BHATTACHARYYA, A., PARMAR, V. S., BALZARINI, J., BARDEN, C. J., TOO, C. K. & JHA, A. 2011. Design, synthesis and bioevaluation of novel candidate selective estrogen receptor modulators. *Eur J Med Chem*.

YANG, K. S., ILAGAN, M. X., PIWNICA-WORMS, D. & PIKE, L. J. 2009. Luciferase fragment complementation imaging of conformational changes in the epidermal growth factor receptor. *J Biol Chem,* 284**,** 7474-82.

YI, P., WU, R. C., SANDQUIST, J., WONG, J., TSAI, S. Y., TSAI, M. J., MEANS, A. R. & O'MALLEY, B. W. 2005. Peptidyl-prolyl isomerase 1 (Pin1) serves as a coactivator of steroid receptor by regulating the activity of phosphorylated steroid receptor coactivator 3 (SRC-3/AIB1). *Mol Cell Biol,* 25**,** 9687-99.

ZHANG, L., LEE, K. C., BHOJANI, M. S., KHAN, A. P., SHILMAN, A., HOLLAND, E. C., ROSS, B. D. & REHEMTULLA, A. 2007. Molecular imaging of Akt kinase activity. *Nat Med,* 13**,** 1114-1119.

ZHANG, X., JEYAKUMAR, M., PETUKHOV, S. & BAGCHI, M. K. 1998. A nuclear receptor corepressor modulates transcriptional activity of antagonist-occupied steroid hormone receptor. *Mol Endocrinol,* 12**,** 513-24.

ZHAO, H., DOYLE, T. C., COQUOZ, O., KALISH, F., RICE, B. W. & CONTAG, C. H. 2005. Emission spectra of bioluminescent reporters and interaction with mammalian tissue determine the sensitivity of detection in vivo. *J Biomed Opt,* 10**,** 41210.

ZHAO, L., O'NEILL, K. & BRINTON, R. D. 2006. Estrogenic agonist activity of ICI 182,780 (Faslodex) in hippocampal neurons: implications for basic science understanding of estrogen signaling and development of estrogen modulators with a dual therapeutic profile. *J Pharmacol Exp Ther,* 319**,** 1124-32.

ZHOU, G., CUMMINGS, R., LI, Y., MITRA, S., WILKINSON, H. A., ELBRECHT, A., HERMES, J. D., SCHAEFFER, J. M., SMITH, R. G. & MOLLER, D. E. 1998. Nuclear Receptors Have Distinct Affinities for Coactivators: Characterization by Fluorescence Resonance Energy Transfer. *Mol Endocrinol,* 12**,** 1594-1604.

ZIEGLER, R. G., HOOVER, R. N., PIKE, M. C., HILDESHEIM, A., NOMURA, A. M., WEST, D. W., WU-WILLIAMS, A. H., KOLONEL, L. N., HORN-ROSS, P. L., ROSENTHAL, J. F. & HYER, M. B. 1993. Migration patterns and breast cancer risk in Asian-American women. *J Natl Cancer Inst,* 85**,** 1819-27.